



AUTOMOTIVE MASS BENCHMARKING

February, 2017

Prepared by
A2Mac1 Automotive Benchmarking

Donald Malen
Bharaht Nagaraj
Benoit Singher

Executive summary

The purpose of this study was to investigate mass efficiency for several vehicle subsystems:

Closures	Front door
	Hood
	Hatchback
	Decklid
	Liftgate
Body systems	Front & rear bumper beam
	Instrument panel beam
	Front seat frame
	Body structure with and without sub frame
Chassis	Lower control arm - McPherson, SLA
	Wheels
	Front & rear suspensions

The mass data used in this study was taken from the *A2Mac1* tear-down database and includes model year 2002 to 2015 vehicles disassembled to a component level. A detailed analysis of 2011 to 2015 vehicles was performed. This sample includes approximately 250 vehicles. By focusing on a five year period, comparisons may be made with the previous study to confirm the statistical models and to detect any trends.

For each of the above subsystems, the objective of this work was to:

- 1) Quantify mass statistics for each subsystem. (*Results at beginning of each report section.*)
These statistics included the mean and standard deviation unadjusted for vehicle type or subsystem attributes.
- 2) Gain insight into mass drivers for each subsystem. (*Results summarized in Appendix A*)
Mass drivers are defined as attributes of the vehicle and subsystem which, to some degree, determine the subsystem mass. Mass drivers for each subsystem had been identified in the two previous studies. In this study, the mass drivers were either validated, or eliminated to achieve a more concise equation.
- 3) Create predictive models for expected subsystem mass. (*Results summarized in Appendix A*)
Regression was used to fit a model which estimates the subsystem average mass based on the significant mass drivers.
In addition to the usual linear additive model, a power model was estimated of the form

$$\hat{m} = \beta_0 (attribute_1)^{\beta_1} (attribute_2)^{\beta_2} \dots$$

where

\hat{m} =The estimated subsystem mass

β_i =Coefficients estimated by regression

$attribute_i$ =The value for a mass driver. For example, the gross mass for the vehicle.

- 4) Identify those subsystems with exceptional mass efficiency, and identify the effect of material on these mass efficient subsystems.

By comparing actual subsystem mass to the estimated mass using the equations identified in the above step, those subsystems with lower mass than expected are defined to be mass efficient. This set of mass efficient subsystems may then be compared to understand the true effects of material selection on subsystem mass.

Table of Contents

1.0 Introduction.....	1
1.1 Study background and scope.....	2
1.2 Mass benchmarking methodology.....	3
2.0 Automotive Mass Benchmarking – Detailed results.....	6
2.1 Closures.....	6
2.1.1 Front side door.....	8
2.1.2 Hood.....	15
2.1.3 Hatchback.....	21
2.1.4 Decklid.....	28
2.1.5 Liftgate.....	35
2.2 Body Subsystems.....	42
2.2.1 Front bumper.....	42
2.2.2 Rear bumper.....	47
2.2.3 Instrument panel beam.....	52
2.2.4 Front seat frame.....	57
2.2.5 Body structure.....	61
2.3 Chassis.....	67
2.3.1 Lower control arm.....	67
2.3.2 Wheels.....	75
2.3.3 Front suspension.....	80
2.3.4 Rear suspension.....	85
3.0 Observations.....	90
References.....	93
Appendix A – Model equations.....	94
– Values for r , n_{ALUM} , and n_{STEEL}	96
– R Square and Adjusted R Square	97
Appendix B – Body structure less sub frame.....	98
Appendix C – 2014 study vehicle types.....	101

1.0 Introduction

This is the third benchmarking study commissioned by WorldAutoSteel which uses statistical analysis to assess material effects on automotive components.

In the first of these studies, conducted by the University of Michigan [1], an objective methodology was established to compare component mass for a large sample of vehicles. Rather than considering a single vehicle or a small set of vehicles, this method looks at a very large sample of vehicles over a range of sizes and segments. From this larger population, assumptions on mass drivers and their influence on real vehicles may be tested via statistical methods. An automotive designer can then look at subsystems which are much lighter than the 'average' vehicle, and therefore set subsystem targets on a more accurate basis than that which is being accomplished in the industry today.

In the second study, conducted by EDAG [2], the number of vehicles was significantly increased allowing a broader range of conclusions to be drawn.

The major conclusions included [3],

1. When comparing steel components of the same size and function, there is a considerable range of mass. Thus, there is an opportunity in current production vehicles for mass reduction, even with the technology and materials already in use.
2. When compared to an efficient steel design, the mass savings gap with aluminum significantly reduces and in some cases reverses.
3. Mass saving achieved at the component level due to material substitution is often not realized at the system level.

With the two previous studies establishing methodology and general conclusions, the purpose of this third study was to investigate the robustness of these earlier conclusions and to begin to track changes over time.

1.1 Study Background and Scope

Figure 1.1-1 provides a timeline for WorldAutoSteel sponsored mass benchmarking studies. The EDAG study, shown with a red outline, comprehended all vehicles used in the earlier University of Michigan study, blue outline, with approximately 100 additional vehicles up to model year 2012.

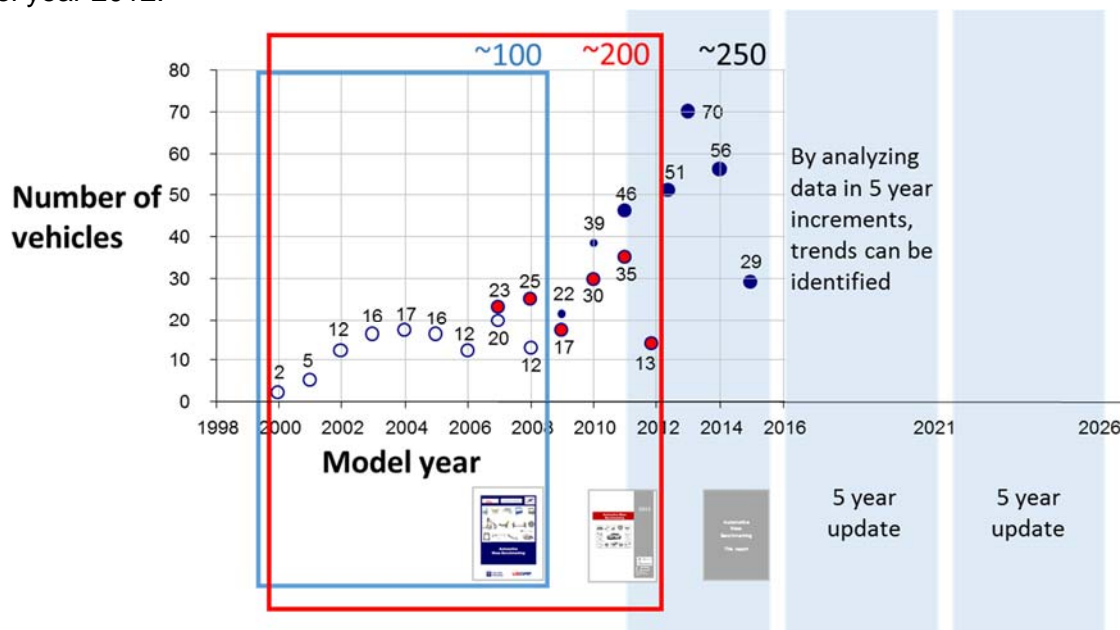


Figure 1.1-1 Timeline of studies

Rather than including all prior vehicles in this study, it was decided to focus on vehicles not previously analyzed. There were approximately 250 vehicles available for the 2011-2015 model years. This allows comparisons over time to test both the robustness of the statistical models, and to detect any time dependent trends which may be present. This methodology is recommended for future studies as well.

The vehicle mix for this study is illustrated in Figures 1.1-2 to 1.1-5. Appendix C contains similar data for the EDAG study for comparison.

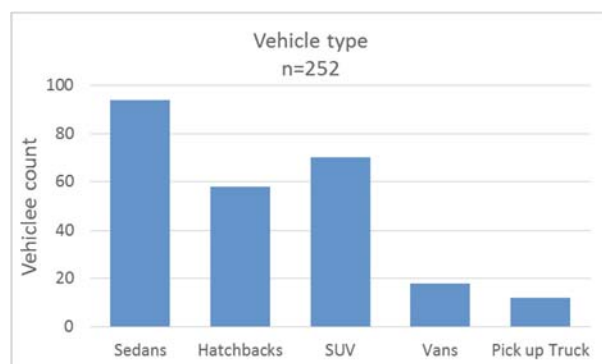


Figure 1.1-2 Vehicle count by type

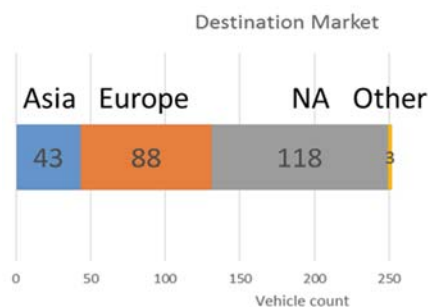


Figure 1.1-3 Vehicle count by destination market

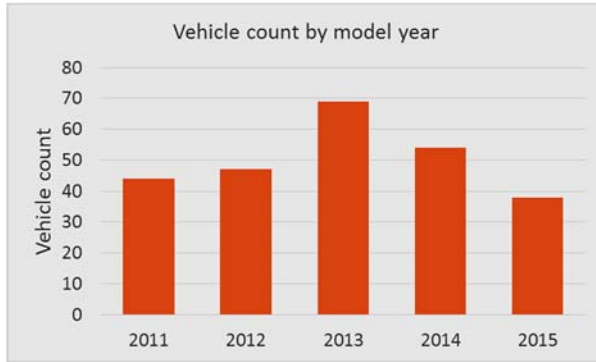


Figure 1.1-4 Vehicle count by model year

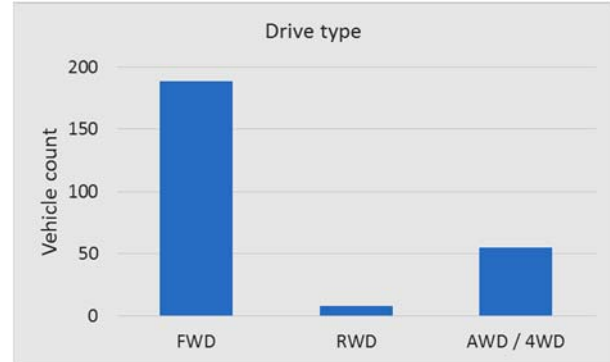


Figure 1.1-5 Vehicle count by drive type

As in prior studies, the subsystems of interest are those with significant material options, Table 1.1-1.

Table 1.1-1 Subsystems studied

Closures	Front door
	Hood
	Hatchback
	Decklid
	Liftgate
Body systems	Front & rear bumper beam
	Instrument panel beam
	Front seat frame
	Body structure
Chassis	Lower control arm
	Wheels

1.2 Mass Benchmarking Methodology

The methodology followed in this study is consistent with the automotive mass benchmarking conducted by the University of Michigan in 2010, and applied by EDAG in 2014. A brief summary of the steps is provided here, Figure 1.2-1.

- 1) The parts comprising each subsystem to be studied were carefully defined to allow comparisons across vehicles. Mass drivers for each subsystem had been identified in the two previous studies. Mass drivers are attributes which, to some degree, determine the subsystem mass. For this study, the mass drivers were either validated, or eliminated to achieve a more parsimonious equation.
- 2) Data for subsystem mass and mass drivers were then downloaded from the A2Mac1 database [4] and formatted in an Excel workbook.
- 3) Mass statistics for each subsystem were determined. These include mean and standard deviation unadjusted for mass drivers other than material. Scatter plots were constructed to gain insight into mass driver correlation with subsystem mass, and these were used to guide the multiple regression process.

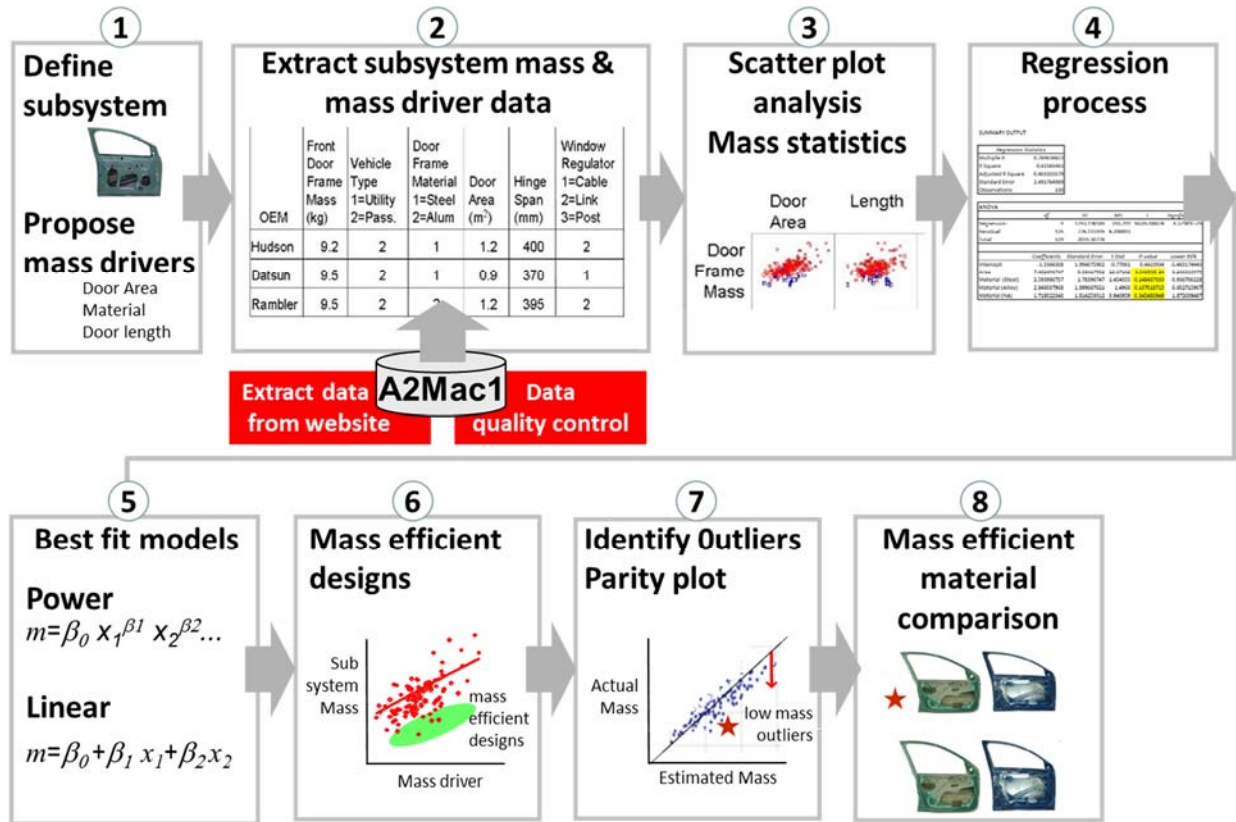


Figure 1.2-1 Summary of statistical benchmarking methodology

- 4) The standard multiple regression process was used to fit a model estimating subsystem average mass based on the significant mass drivers.
- 5) Regression was used to fit a linear equation and a power equation. The linear model was first determined retaining the statistically significant attributes, and then the same retained attributes were used for the power model. Linear models were of the form,

$$\hat{m} = \beta_0 + \beta_1(\text{attribute}_1) + \beta_2(\text{attribute}_2) + \dots$$

Where \hat{m} is the subsystem nominal mass for the full set of vehicles considered. Some of the attributes were continuous variables (gross vehicle weight, for example), some were categorical attributes (construction A, construction B, or construction C), and others were a binary attribute (Steel, Aluminum).

After determining mass drivers using the linear model, a power model was fit of the form,

$$\hat{m}_{EFF} = \beta_0 (\text{attribute}_1)^{\beta_1} (\text{attribute}_2)^{\beta_2} \dots$$

This form was used for comparing mass of competitive materials.

- 6) Mass efficient designs were identified using the power model equation modified by varying the number of standard errors below the mean, keeping at least three data points below the mass efficient curve,

$$\hat{m}_{EFF} = \frac{\beta_0(attribute_1)^{\beta_1}(attribute_2)^{\beta_2}...}{nr}$$

Where

\hat{m}_{EFF} = predicted mass for mass efficient designs

r = standard error determined by the regression

n = number of standard errors below the mean for which at least three samples were observed

The amount of variation in the data which is explained by the model is quantified by the *Adjusted R squared* value. This is provided in subsequent sections for each model fit. A discussion of *Adjusted R squared* is provided in Appendix A.

- 7) A parity plot of actual subsystem mass vs. estimated mass (using the equations identified in Step 5) was used to rank mass efficiency. The distance below the parity line (45°) indicates the degree of mass efficiency.
- 8) This set of mass efficient subsystems was then used to understand the true effects of material selection on subsystem mass.

2.0 Automotive Mass Benchmarking – Detailed results

Each subsystem analysis is covered in a report section as shown in Table 2.0-1.

Table 2.0-1

Closures	Front door	Section 2.1.1
	Hood	Section 2.1.2
	Hatchback	Section 2.1.3
	Decklid	Section 2.1.4
	Liftgate	Section 2.1.5
Body systems	Front & rear bumper beam	Section 2.2.1 & 2
	Instrument panel beam	Section 2.2.3
	Front seat frame	Section 2.2.4
	Body structure	Section 2.2.5
Chassis	Lower control arm	Section 2.3.1
	Wheels	Section 2.3.2
	Front & rear suspensions	Section 2.3.3 & 4

Because each section is intended to be read independently, there is some repetition between sections.

2.1 Closures

The closure systems analyzed were front door, hood, hatchback door, decklid, and liftgate. A statistical view of a large population allows general observations not available when looking at a single design or A-B comparisons. Following are two general observations on closure mass for steel vs. aluminum designs. 1) When compared to an efficient steel design, the mass savings gap with aluminum significantly reduces. Figure 2.1-1 summarizes the structure mass ratio, also called the *Material Replacement Coefficient*, of average or nominal aluminum design to average steel design when the closure has been normalized for size (Nom). This nominal ratio varies to a low of 0.665 for the decklid to 0.939 for hatchback door. However, when the most mass efficient designs (Eff) are compared, the mass ratio increases for all closures.

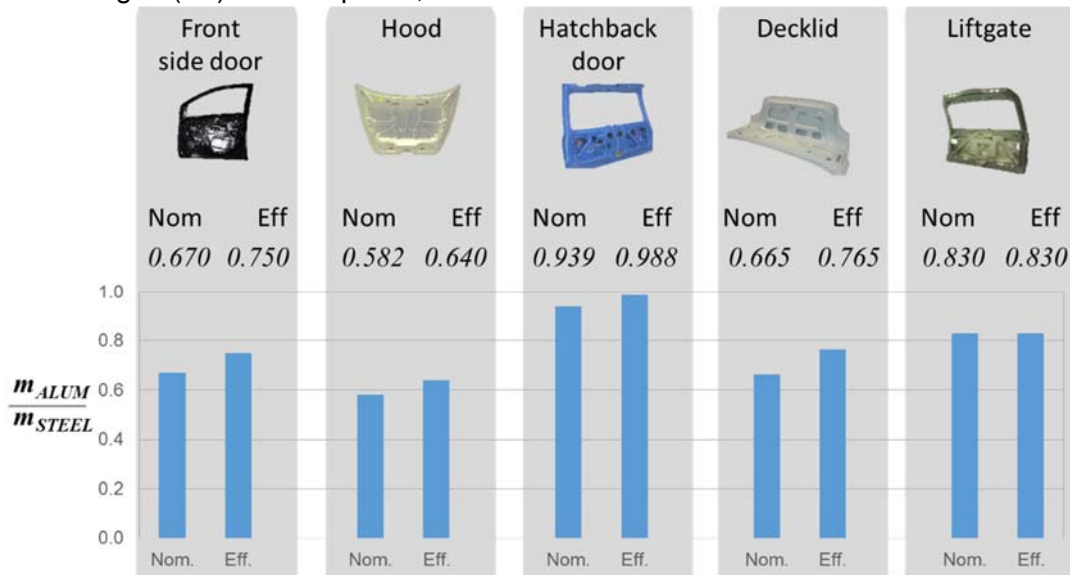


Figure 2.1-1 Closures summary

Mass ratio of aluminum to steel for closure structure for nominal and mass efficient designs

The second general observation is; 2) Mass saving achieved for the structure due to material substitution is often not realized at the system level. Figure 2.1-2 summarizes the difference in average structure mass between the aluminum closures and steel (Struct). A negative value indicates aluminum design is lighter. In the same figure, the difference between the average total system mass is also shown (System). For the front door, hatchback, and liftgate, it can be seen that the savings in the structure mass due to material selection is not fully carried over to the closure system. For the hood and decklid, the mass reduction does carry over but not completely.

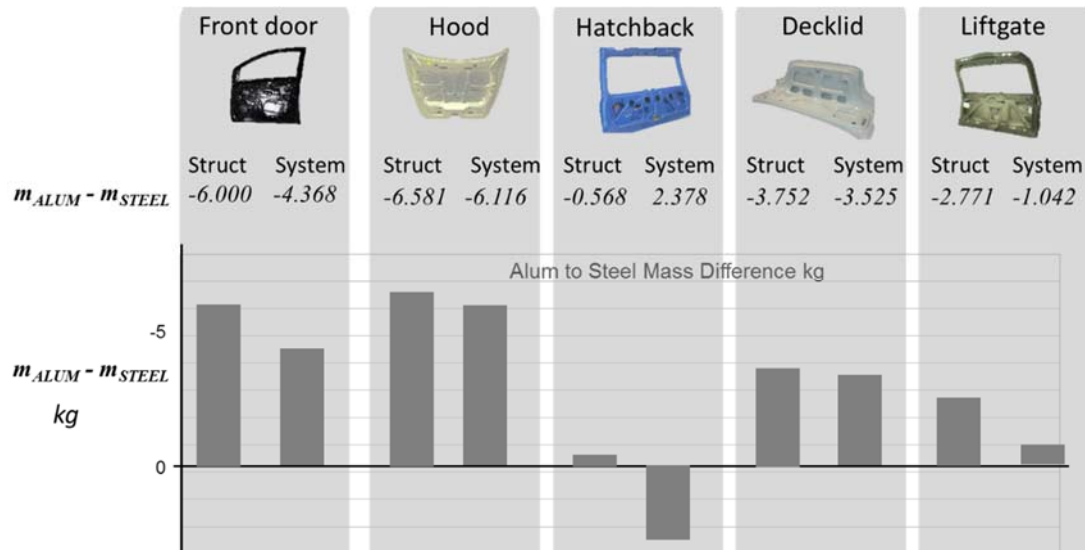


Figure 2.1-2 Closures summary
Mass difference between aluminum and mass for closure structure and for closure system

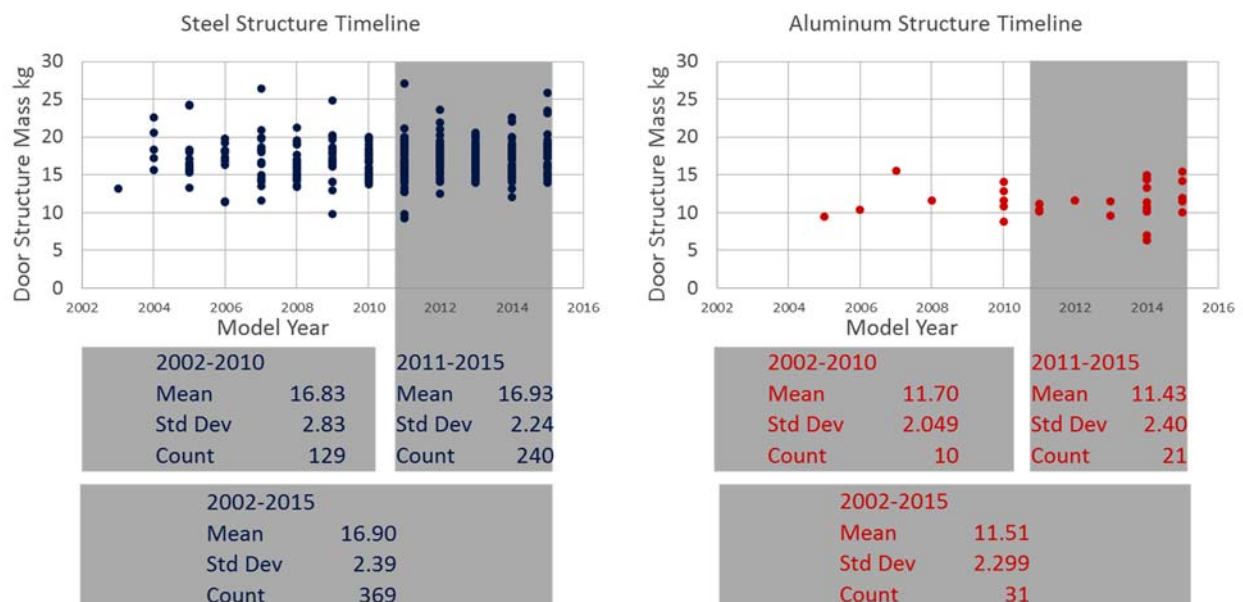
In the following sections each closure type is analyzed in detail.

2.1.1 Front side door

The front door system includes intrusion beam, glass, linkages, trim, lock & all mounting hardware. The door structure consists of the welded assembly.

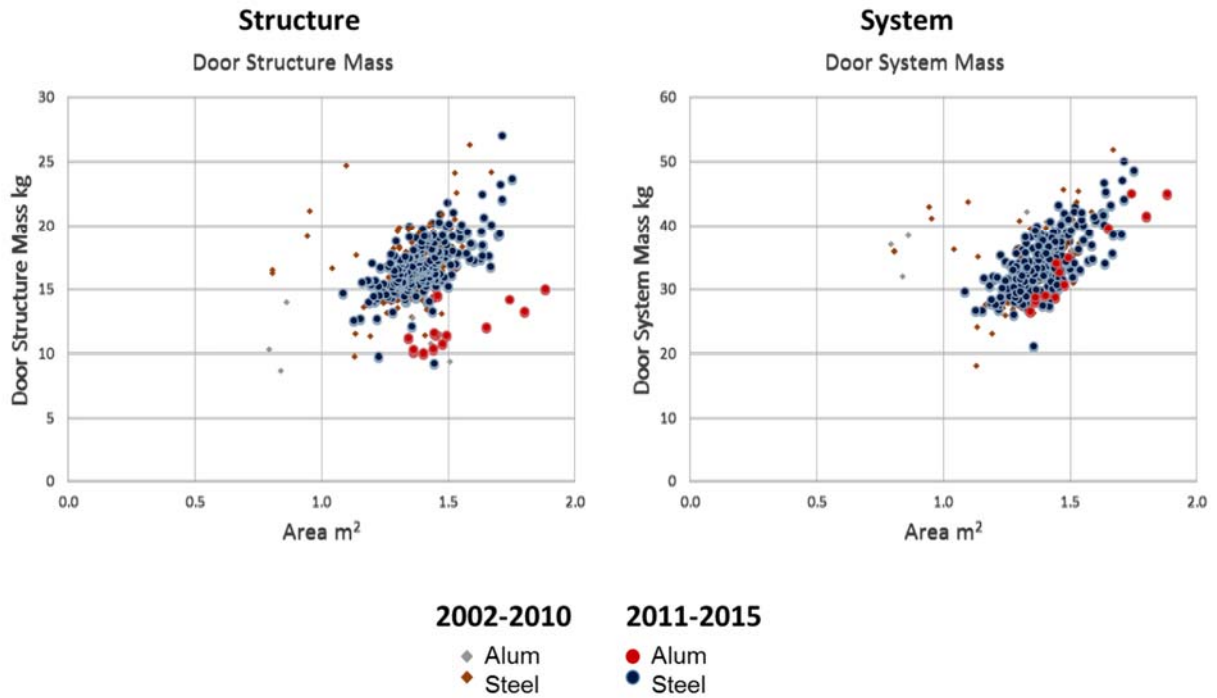


The first look at side door structure mass data is shown in Figure 2.1.1-1. The basic statistics for each material class appear to be stable.



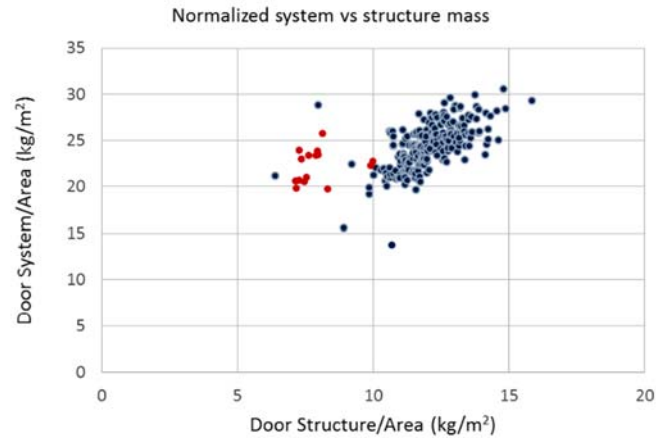
*Figure 2.1.1-1 Front door structure
Comparison of unadjusted mass statistics*

Figure 2.1.1-2 is a scatter plot of mass vs. the mass driver door side view area with data from the current study overlaid with data from the EDAG 2014 study. The data points for this study are in larger markers. The overall trend appears to be similar, however there were some heavy steel doors in the earlier study. This was confirmed by the comparison of the regression equations.



*Figure 2.1.1-2 Front door structure
Comparison of mass for two studies*

An important conclusion from the earlier study [5] was that the mass reduction in the door structure due to material substitution did not fully carry over to the door system mass. (Physical explanations of this phenomenon was examined in a follow-up study [6].) The scatter plot of Figure 2.1.1-3 shows this trend for this study; confirmed later by the regression equations.



*Figure 2.1.1-3 Front door
Comparison of normalize system mass with normalized structure*

To fit the regression models, the mass drivers from previous studies were used, Figure 2.1.1-4.

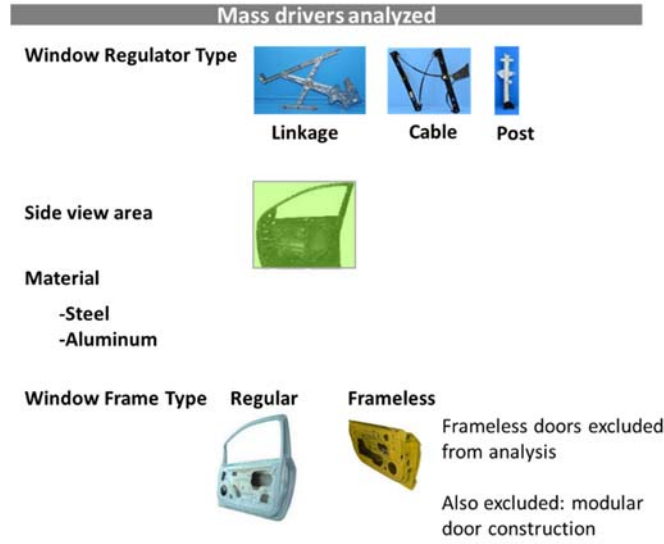


*Figure 2.1.1-4 Front door
Mass drivers considered*

Window regulator type has small effect on mass and does not affect material ratio significantly based on the equations below. Therefore it should not be considered in future models

With regulator in regression

$$m_{STRUCT} = 12.128(AREA)^{0.959} \left[\begin{matrix} 0.673 \text{ if Alum} \\ 1.000 \text{ if Steel} \end{matrix} \right] \left[\begin{matrix} 1.027 \text{ if Link} \\ 1.000 \text{ if other} \end{matrix} \right], R^2 = 0.557, r = 1.108$$

Without regulator in regression

$$m_{STRUCT} = 12.136(AREA)^{0.969} \left[\begin{matrix} 0.670 \text{ if Alum} \\ 1.000 \text{ if Steel} \end{matrix} \right], R^2 = 0.555, r = 1.109$$

Models were then fit without window regulator. These are shown below

Linear model for structure

$$m_{STRUCT} = 0.581 + 11.657 AREA - \left[\begin{matrix} 5.992 \text{ if Alum} \\ 0.000 \text{ if Steel} \end{matrix} \right], R^2 = 0.545, \sigma = 1.688$$

Power model for structure

$$m_{STRUCT} = 12.136(AREA)^{0.969} \left[\begin{matrix} 0.670 \text{ if Alum} \\ 1.000 \text{ if Steel} \end{matrix} \right], R^2 = 0.555, r = 1.109$$

Figure 2.1.1-5 shows the mass data with the power equation lines superimposed; Dotted for nominal, solid for mass efficient designs.

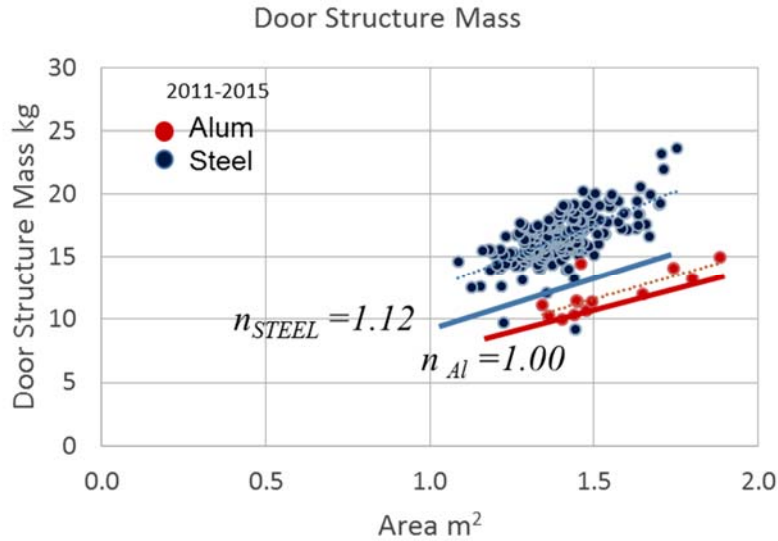


Figure 2.1.1-5 Front door
Structure mass with power model for mass efficient doors

In a similar manner, models were fit for the door system mass.
Linear model for system

$$m_{SYSTEM} = -5.498 + 28.422AREA - \begin{bmatrix} 4.368 \text{ if Alum} \\ 0.000 \text{ if Steel} \end{bmatrix}, R^2 = 0.522, s = 3.393$$

Power model for system

$$m_{SYSTEM} = 23.395(AREA)^{1.121} \begin{bmatrix} 0.876 \text{ if Alum} \\ 1.000 \text{ if Steel} \end{bmatrix}, R^2 = 0.480, r = 1.106$$

Figure 2.1.1-6 shows the mass data with the power equation line for nominal designs.

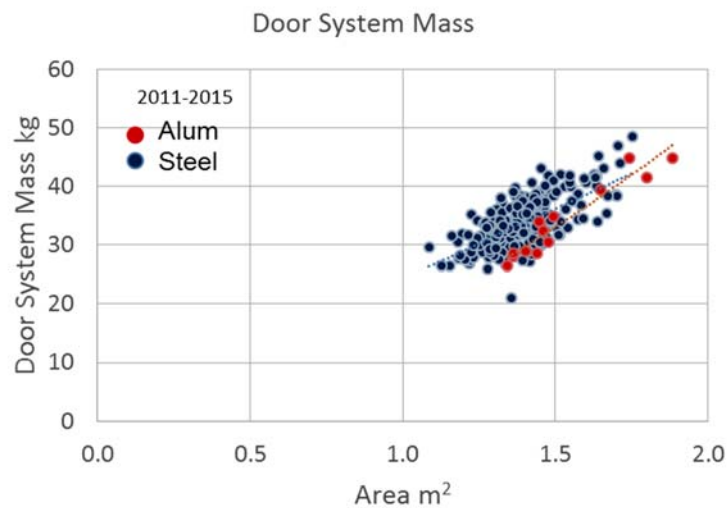


Figure 2.1.1-6 Front door
System mass with power model for nominal

Comparison of studies

A comparison of the power model equations for the three studies is presented below. The most meaningful comparison is between the current and 2014 study due to the larger number of samples. For these studies, the goodness of fit is similar. The form of the equation for the 2014 study used aluminum as the reference material while this study used steel. The prior equations were algebraically adjusted for direct comparison.

Current study

$$m_{STRUCT} = 12.136(AREA)^{0.969} \begin{bmatrix} 0.670 \text{ Alum} \\ 1.000 \text{ Steel} \end{bmatrix}, R^2 = 0.56, r=1.109$$

2014 study Equation algebraically modified for direct comparison

$$m_{STRUCT} = 11.586(AREA)^{0.884} \begin{bmatrix} 0.699 \text{ Alum} \\ 1.000 \text{ Steel} \end{bmatrix}, R^2 = 0.56, r=1.123$$

Equation as it originally appeared using a quadrilateral shape for area

$$\begin{matrix} m \text{ (kg)} \\ = 10.144(Area \text{ m}^2)^{0.884} \begin{bmatrix} 1.43 \text{ Steel} \\ 1.00 \text{ Alum} \end{bmatrix} \begin{bmatrix} 1.06 \text{ linkage} \\ 1.03 \text{ cable} \\ 1.0 \text{ post} \end{bmatrix} \end{matrix}$$

2010 study Equation algebraically modified for direct comparison

$$m_{STRUCT} = 14.347(AREA)^{0.867} \begin{bmatrix} 0.709 \text{ Alum} \\ 1.000 \text{ Steel} \end{bmatrix}, R^2 = 0.45, r=1.146$$

Equation as it originally appeared

$$\hat{m} = 11.06(Area \text{ m}^2)^{0.867} \begin{bmatrix} 1.41Fe \\ 1.00Al \end{bmatrix} \begin{bmatrix} 1 \text{ if linkage regulator} \\ 0.92 \text{ if other} \end{bmatrix}$$

Because the equations have different constant coefficients and mass driver exponents, it is difficult to compare them visually. Figure 2.1.1-7 graphs the above equations for efficient designs to allow a direct comparison. The graphs overlay very closely indicating consistent results.

Number of standard deviations below nominal for efficient designs

$$n_{STEEL}=1.25$$

$$n_{ALUM}=1.00$$

$$n_{STEEL}=1.12$$

$$n_{ALUM}=1.00$$

$$n_{STEEL}=1.12$$

$$n_{ALUM}=1.00$$

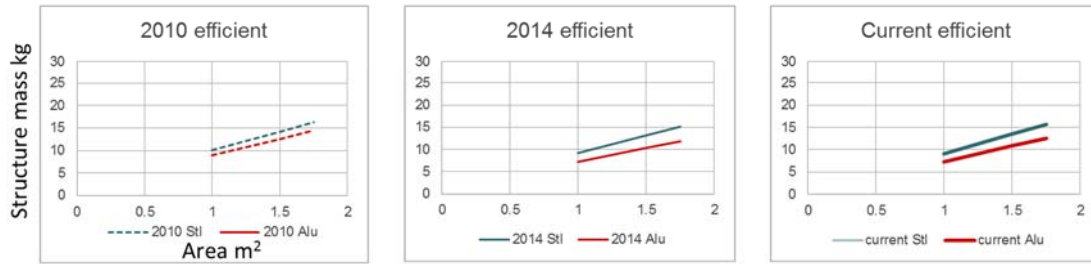


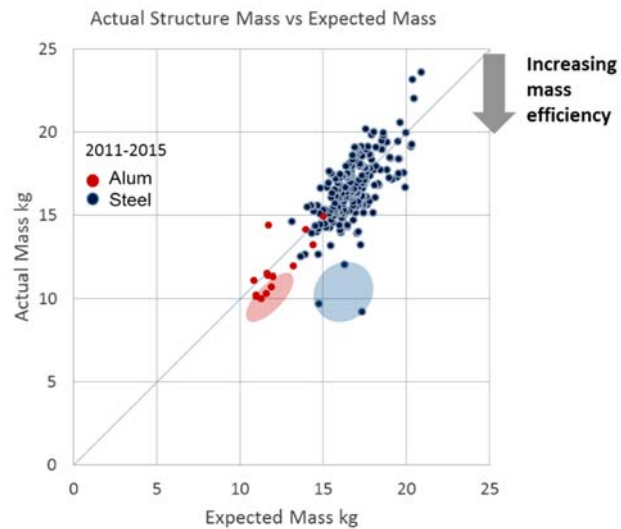
Figure 2.1.1-7 Front door
Comparison of power model for three studies

Table 2.1.1-1 compares the material mass ratio for the three studies for both nominal and efficient designs. As noted in previous studies Steel performance is better when efficient designs are compared and the ratio is slightly greater in this study of 2011-2015 doors compared with the prior study.

Table 2.1.1-1 Front door
Comparison of material mass ratio for three studies

	$\frac{m_{ALUM}}{m_{STEEL}}$	
	Nominal designs	Efficient designs
Current	0.670	0.750
2014 study	0.699	0.783
2010 study	0.709	0.886

All doors were ranked by the difference between actual mass and expected mass. This is shown graphically in the parity plot of Figure 2.1.1-8 where increasing mass efficiency is the downward distance from the 45° line where actual mass equals expected mass.



*Figure 2.1.1-8 Front door
Parity plot to evaluate mass efficiency*

2.1.2 Hood

The hood system includes hinges, mechanism, sealing and all mounting hardware. The hood structure consists of the welded assembly.



The first look at hood structure mass data is shown in Figure 2.1.2-1. There is a slight upward trend in steel mass over time, but this trend is well within the standard deviation. The reverse is true for aluminum, but it is also within the standard deviation in the data.

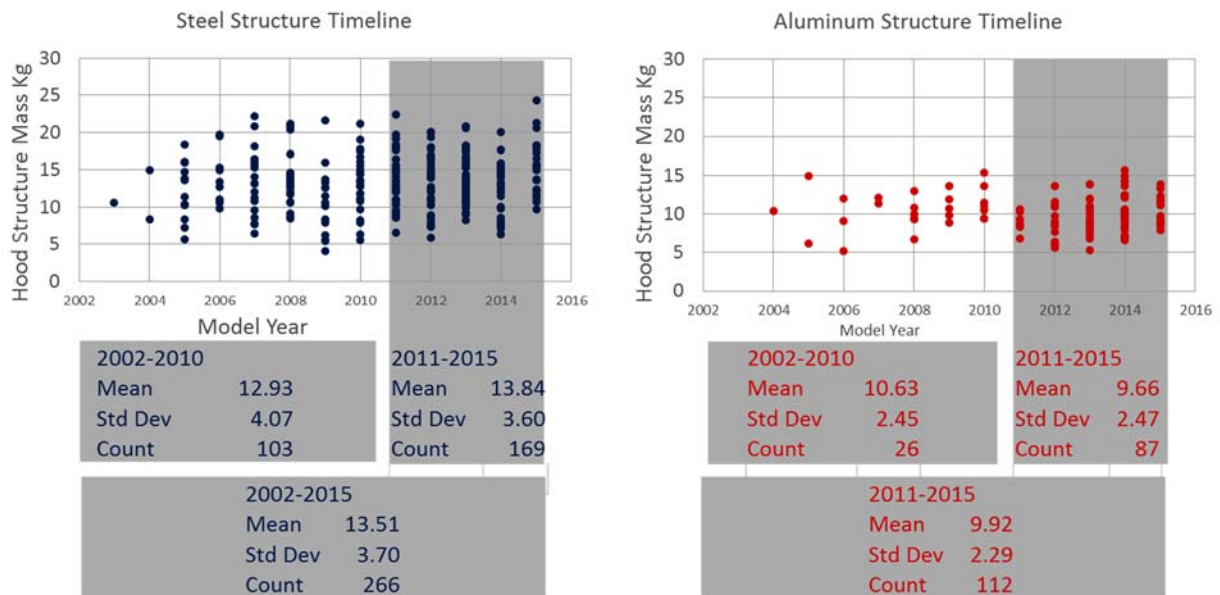
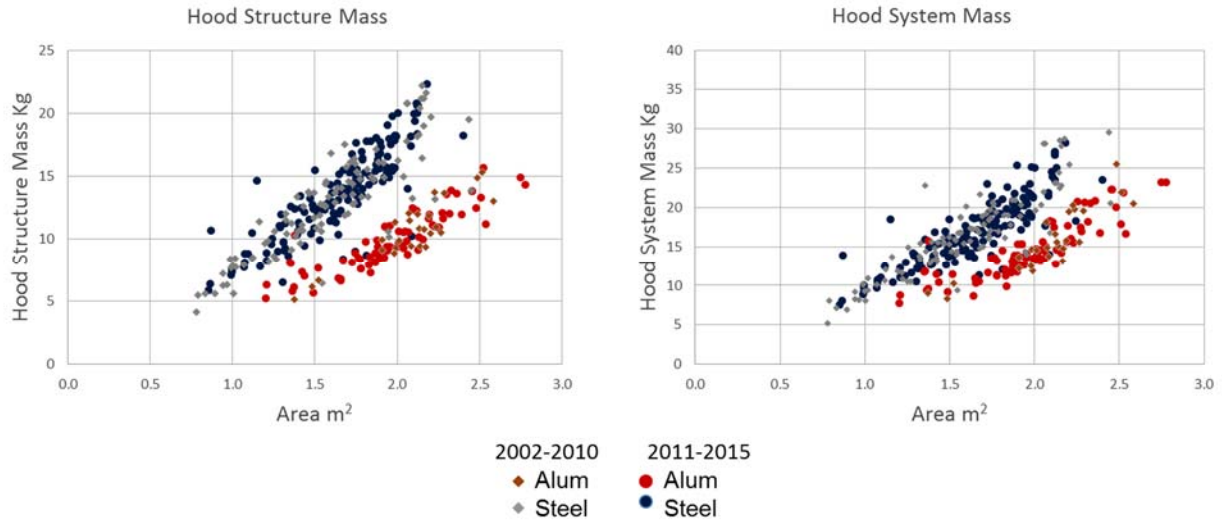


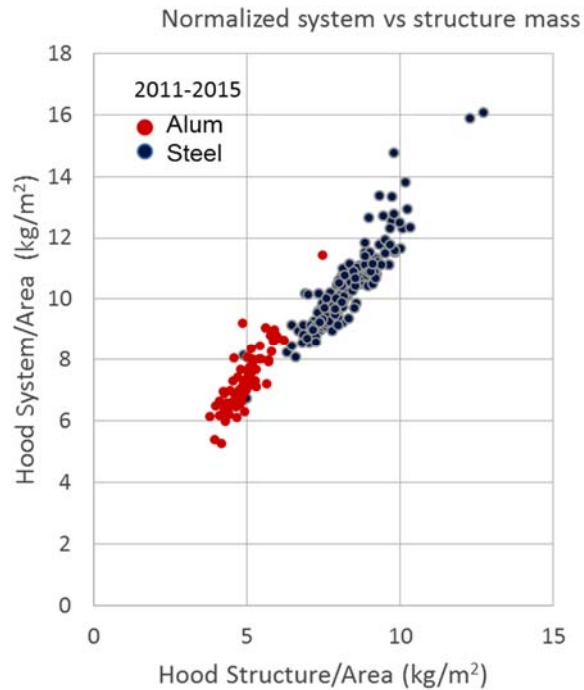
Figure 2.1.2-1 Hood
Comparison of unadjusted structure mass statistics

Figure 2.1.2-2 is a scatter plot of mass vs. the mass driver Area with data from the current study overlaid with data from the EDAG 2014 study. The data points for this study are in larger markers. The overall trend appears to be the similar.



*Figure 2.1.2-2 Hood
Comparison of mass for two studies*

As observed in an earlier study on closures [5], the mass reduction in the hood structure due to material substitution does carry over but not completely. The scatter plot of Figure 2.1.2-3 shows this trend for this study.



*Figure 2.1.2-3 Hood
Comparison of normalize system mass with normalized structure*

To fit the regression models, the mass drivers from previous studies were used, Figure 2.1.2-4.

Mass drivers analyzed

Area



Material

-Steel

-Aluminum

Figure 2.1.2-4 Hood
Mass drivers considered

Models were then fit using these mass drivers. These are shown below

Linear model for structure

$$m_{STRUCT} = 0.2579 + 8.227 AREA - \frac{6.581 Alum}{0.000 Steel}, R^2 = 0.811, \sigma = 1.582$$

Power model for structure

$$m_{STRUCT} = 7.7074 (AREA)^{1.145} \left[\frac{0.582 Alum}{1.000 Steel} \right], R^2 = 0.840, r = 1.129$$

Figure 2.1.2-5 shows the mass data with the power equation lines superimposed; Dotted for nominal, solid for mass efficient designs.

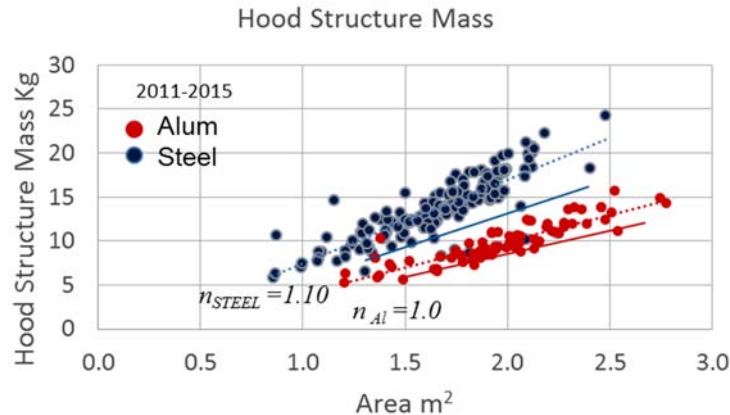


Figure 2.1.2-5 Hood
Structure mass with power model for mass efficient hoods

In a similar manner, models were fit for the system mass.

Linear model for system

$$m_{SYSTEM} = -0.446 + 10.710 AREA - \frac{6.116 Alum}{0.000 Steel}, R^2 = 0.767, \sigma = 2.017$$

Power model for system

$$m_{SYSTEM} = 9.321(AREA)^{1.176} \left[\frac{0.693 Alum}{1.000 Steel} \right], R^2 = 0.588, r = 1.224$$

Figure 2.1.2-6 shows the mass data with the power equation line for nominal designs.

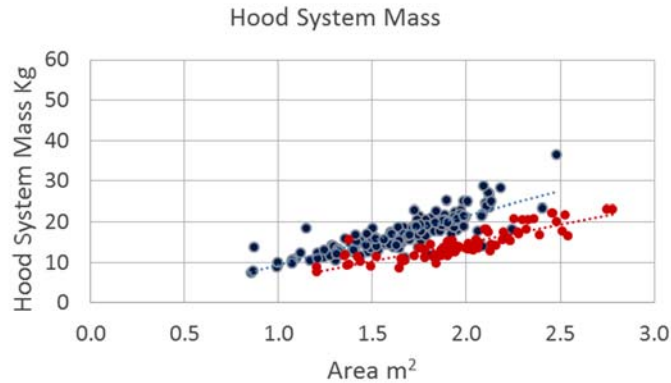


Figure 2.1.2-6 Hood
System mass with power model for nominal

Comparison of studies

A comparison of the power model equations for the three studies is presented below. The most meaningful comparison is between the current and 2014 study due to the larger number of samples. For these studies, the goodness of fit is similar. The form of the equation for the 2014 study used aluminum as the reference material while this study used steel. The prior equations were algebraically adjusted for direct comparison.

Current study

$$m_{STRUCT} = 7.7074(AREA)^{1.145} \left[\frac{0.582 Alum}{1.000 Steel} \right], R^2 = 0.84, r = 1.129$$

2014 study Equation algebraically modified for direct comparison

$$m_{STRUCT} = 7.138(AREA)^{1.23} \left[\frac{0.602 Alum}{1.000 Steel} \right], R^2 = 0.80, r = 1.177$$

Equation as it originally appeared using aluminum as reference material

$$m_{STRUCT} = 4.30(AREA)^{1.23} \left[\frac{1.66 Steel}{1.000 Alum} \right]$$

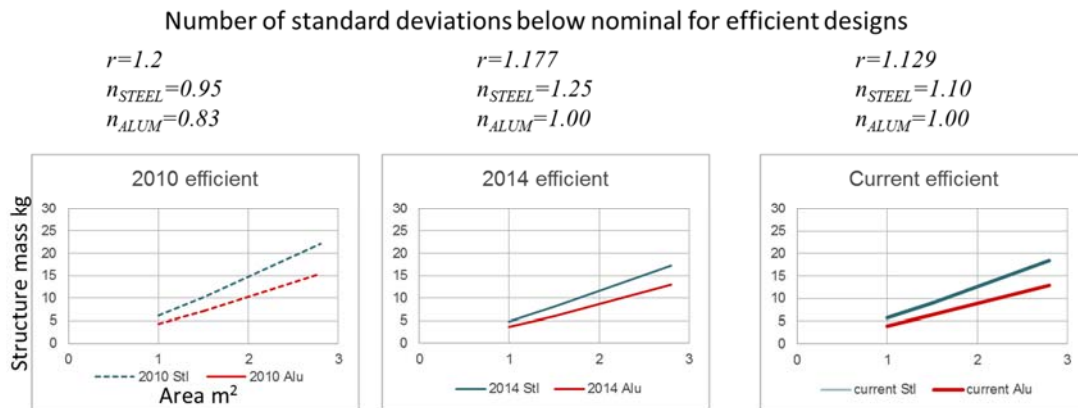
2010 study Equation algebraically modified for direct comparison

$$m_{STRUCT} = 7.062(AREA)^{1.24} \begin{bmatrix} 0.606 \text{ Alum} \\ 1.000 \text{ Steel} \end{bmatrix}, R^2=0.77, r=1.20$$

Equation as it originally appeared

$$m_{STRUCT} = 4.28(AREA)^{1.24} \begin{bmatrix} 1.650 \text{ Steel} \\ 1.000 \text{ Alum} \end{bmatrix}$$

Because the equations have different constant coefficients and mass driver exponents, it is difficult to compare them visually. Figure 2.1.2-7 graphs the above equations for efficient designs to allow a direct comparison. The graphs overlay very closely indicating consistent results.



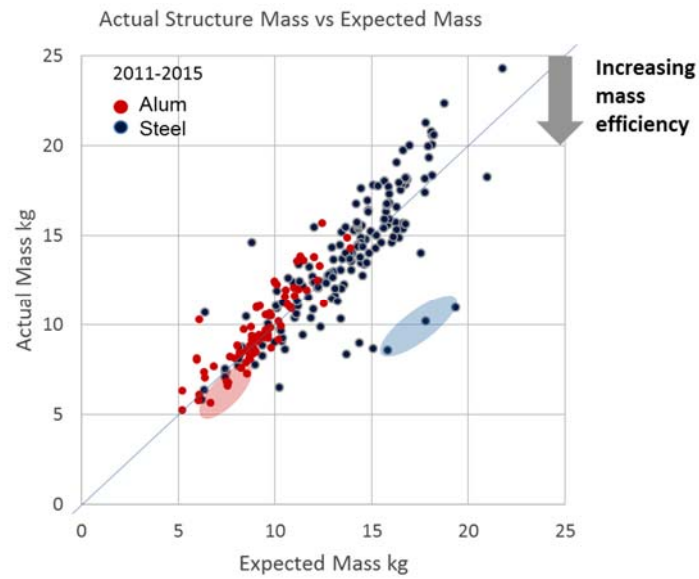
*Figure 2.1.2-7 Hood
Comparison of power model for three studies*

Table 2.1.2-1 compares the material mass ratio for the three studies for both nominal and efficient designs.

*Table 2.1.2-1 Hood
Comparison of material mass ratio for three studies*

	$\frac{m_{ALUM}}{m_{STEEL}}$	
	Nominal designs	Efficient designs
Current	0.582	0.640
2014 study	0.602	0.753
2010 study	0.606	0.694

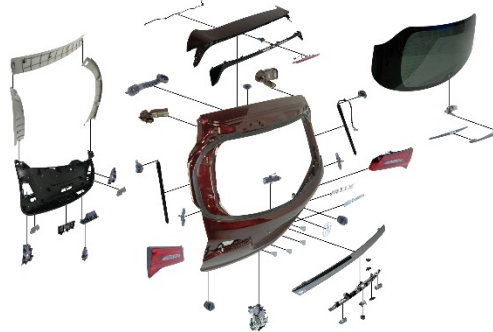
All hoods were ranked by the difference between actual mass and expected mass. This is shown graphically in the parity plot of Figure 2.1.2-8 where increasing mass efficiency is the downward distance from the 45° line where actual mass equals expected mass.



*Figure 2.1.2-8 Hood
Parity plot to evaluate mass efficiency*

2.1.3 Hatchback

Hatchback doors are defined as the cargo doors on A, B, C Class passenger cars. The hatchback system includes inner panel, glass, weather stripping, mechanisms and all mounting hardware. The hatchback structure consists of the welded assembly.



The first look at hatchback door structure mass data is shown in Figure 2.1.3-1. The basic statistics for steel appears to be stable. For aluminum, there is an increase in mean mass for the recent year, however the sample size is low.

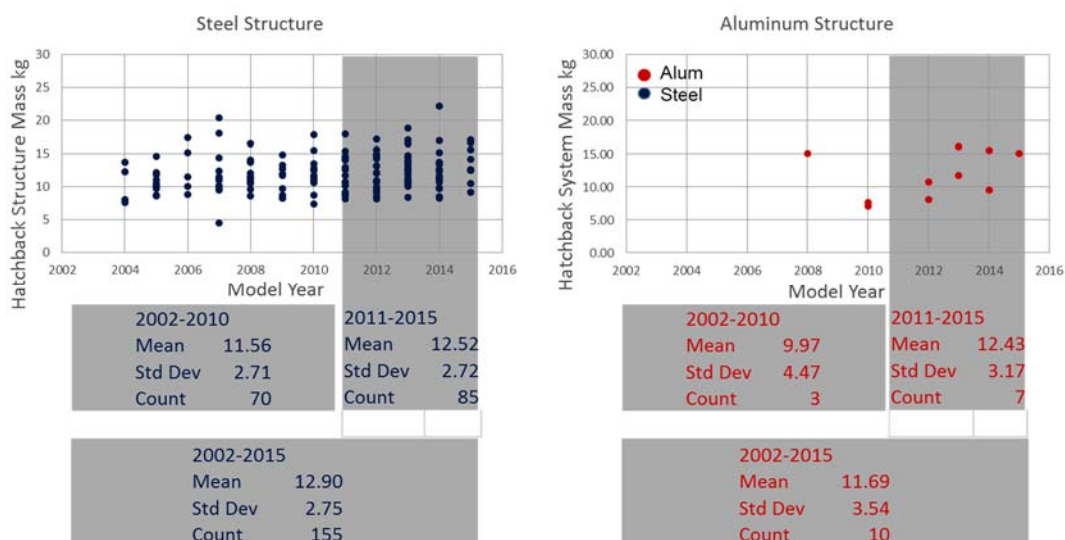
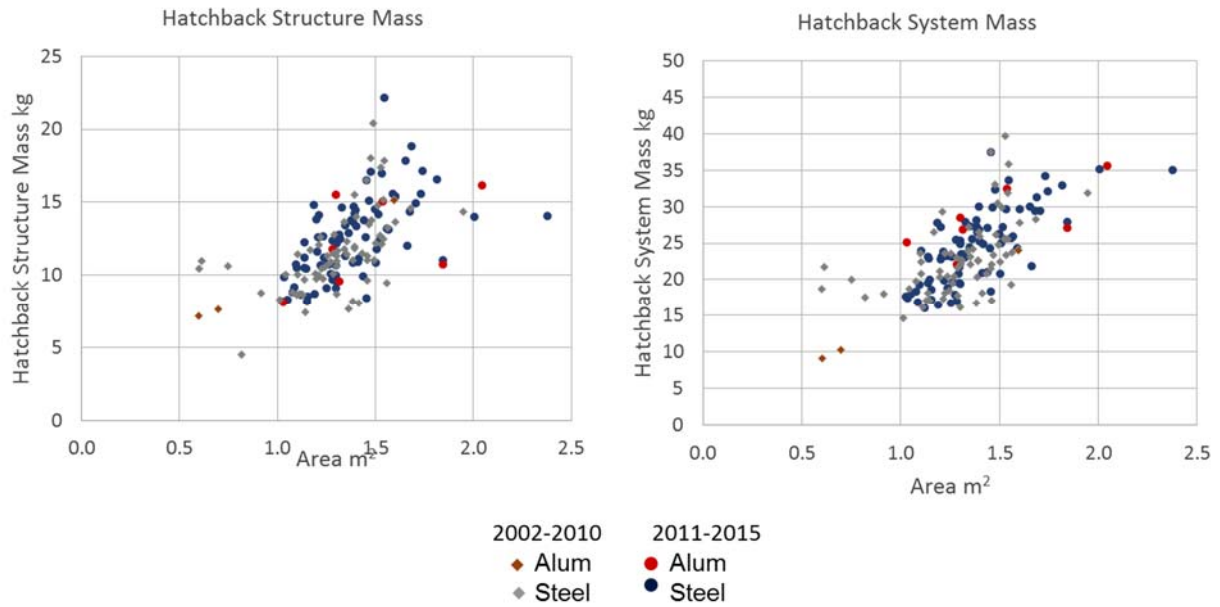


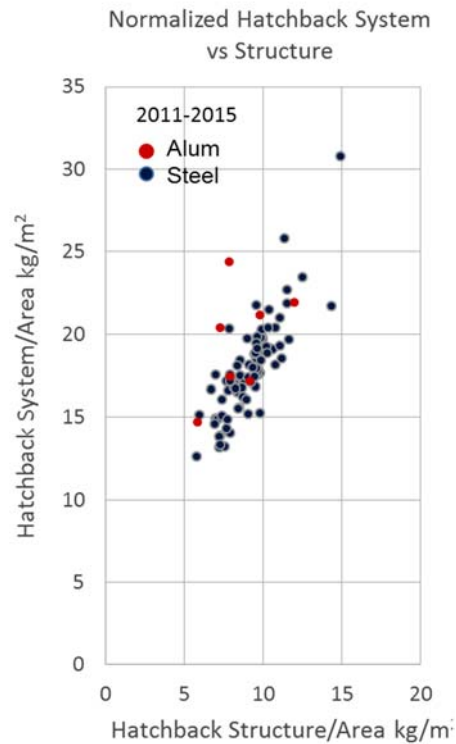
Figure 2.1.3-1 Hatchback door structure
Comparison of unadjusted mass statistics

Figure 2.1.3-2 is a scatter plot of mass vs. the mass driver area with data from the current study overlaid with data from the EDAG 2014 study. The data points for this study are in larger markers. The overall trend appears to be the similar.



*Figure 2.1.3-2 Hatchback door
Comparison of mass for two studies*

An important conclusion from the earlier study was that often the mass reduction in the structure due to material substitution did not fully carry over to the system mass. The scatter plot of Figure 2.1.3-3 shows no reduction in either structure or system mass due to aluminum.



*Figure 2.1.3-3 Hatchback door
Comparison of normalized system mass with normalized structure*

To fit the regression models, the mass drivers from previous studies were used, Figure 2.1.3-4.

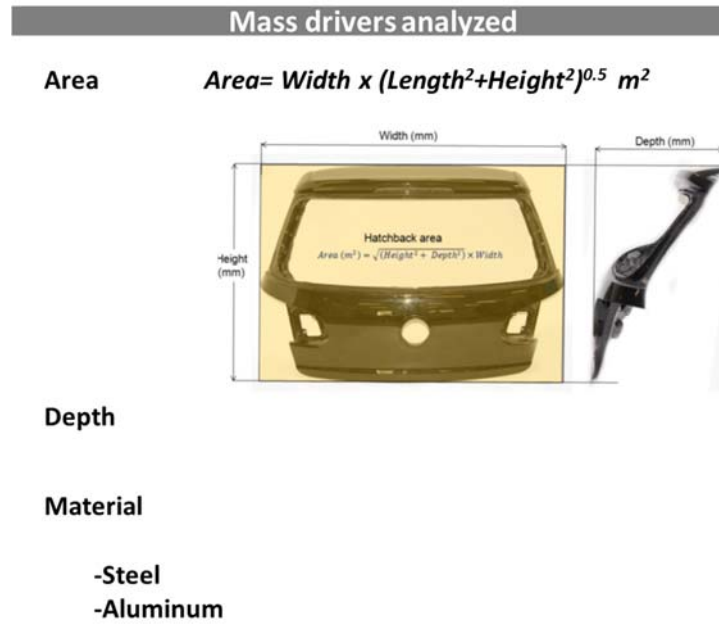


*Figure 2.1.3-4 Hatchback door
Mass drivers considered*

Models were then fit with these mass drivers. These are shown below

Linear model for structure

$$m_{STRUCT} = 4.016 + 7.407AREA - 0.003Depth - \begin{matrix} 0.568 \text{ Alum} \\ 0.000 \text{ Steel} \end{matrix}, R^2 = 0.357, \sigma = 2.12$$

Power model for structure

$$m_{STRUCT} = 16.05(AREA)^{0.890}(Depth)^{-0.088} \begin{bmatrix} 0.947 \text{ Alum} \\ 1.000 \text{ Steel} \end{bmatrix}, R^2 = 0.399, r = 1.185$$

Figure 2.1.3-5 shows the mass data with the power equation lines superimposed; Dotted for nominal, solid for mass efficient designs.

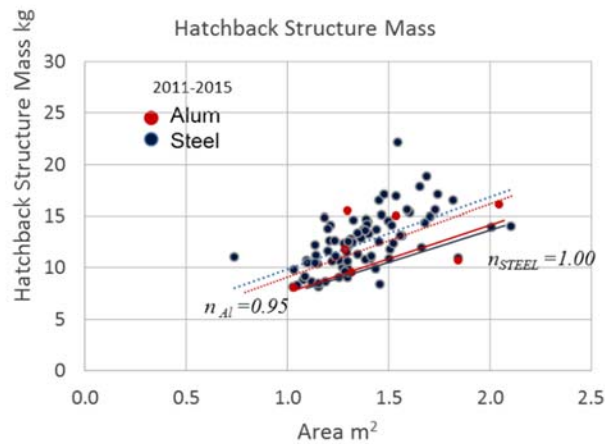


Figure 2.1.3-5 Hatchback door
Structure mass with power model for mass efficient doors

In a similar manner, models were fit for the door system mass.

Linear model for system

$$m_{SYSTEM} = 3.95 + 15.05 AREA - 0.0005 Depth + \frac{2.378 Alum}{0.000 Steel}, R^2 = 0.535, \sigma = 3.514$$

Power model for system

$$m_{SYSTEM} = 19.58 (AREA)^{0.890} (Depth)^{-0.0125} \left[\frac{1.110 Alum}{1.000 Steel} \right], R^2 = 0.530, r = 1.155$$

Figure 2.1.3-6 shows the mass data with the power equation line for nominal designs.

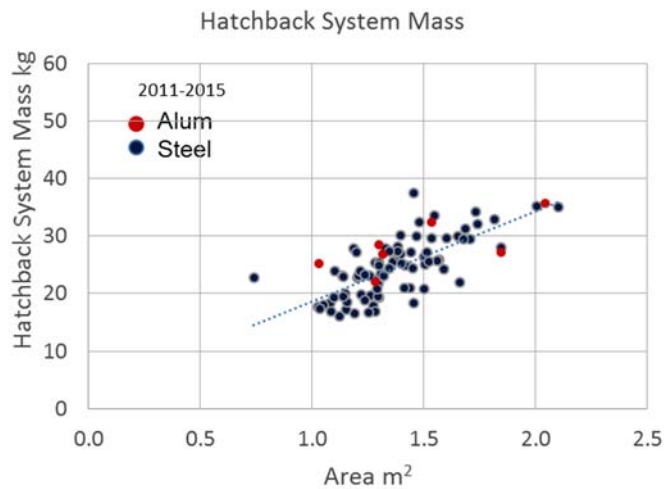


Figure 2.1.3-6 Hatchback door
System mass with power model for nominal

Comparison of studies

A comparison of the power model equations for the three studies is presented below. The most meaningful comparison is between the current and 2014 study due to the larger number of samples. The form of the equation for the 2014 study used aluminum as the reference material while this study used steel. The prior equations were algebraically adjusted for direct comparison.

Current study

$$m_{STRUCT} = 16.05(AREA)^{0.890}(Depth)^{-0.088} \left[\frac{0.947 \text{ Alum}}{1.000 \text{ Steel}} \right], R^2 = 0.399, r=1.185$$

Because of the low and negative correlation with depth, it is recommended to use the following.

$$m_{STRUCT} = 5.924(AREA)^{0.227}(Depth)^0 \left[\frac{0.939 \text{ Alum}}{1.000 \text{ Steel}} \right], R^2 = 0.34, r=1.190$$

2014 study Equation algebraically modified for direct comparison

$$m_{STRUCT} = 4.225(AREA)^{0.55} [Depth]^{0.144} \left[\frac{0.714 \text{ Alum}}{1.000 \text{ Steel}} \right], R^2 = 0.50, r=1.20$$

Equation as it originally appeared

$$m_{STRUCT} = 3.018(AREA)^{0.55} [Depth]^{0.144} \left[\frac{1.40 \text{ Steel}}{1.000 \text{ Alum}} \right]$$

2010 study Equation algebraically modified for direct comparison

$$m_{STRUCT} = 3.661(AREA)^{0.55} [Depth]^{0.177} \left[\frac{0.740 \text{ if Alum}}{1.000 \text{ if Steel}} \right], R^2 = 0.31, r=1.1$$

Equation as it originally appeared

$$m_{STRUCT} = 2.712(AREA)^{0.55} [Depth]^{0.177} \left[\frac{1.35 \text{ Steel}}{1.000 \text{ Alum}} \right]$$

Because the equations have different constant coefficients and mass driver exponents, it is difficult to compare them visually. Figure 2.1.3-7 graphs the above equations for efficient designs to allow a direct comparison.

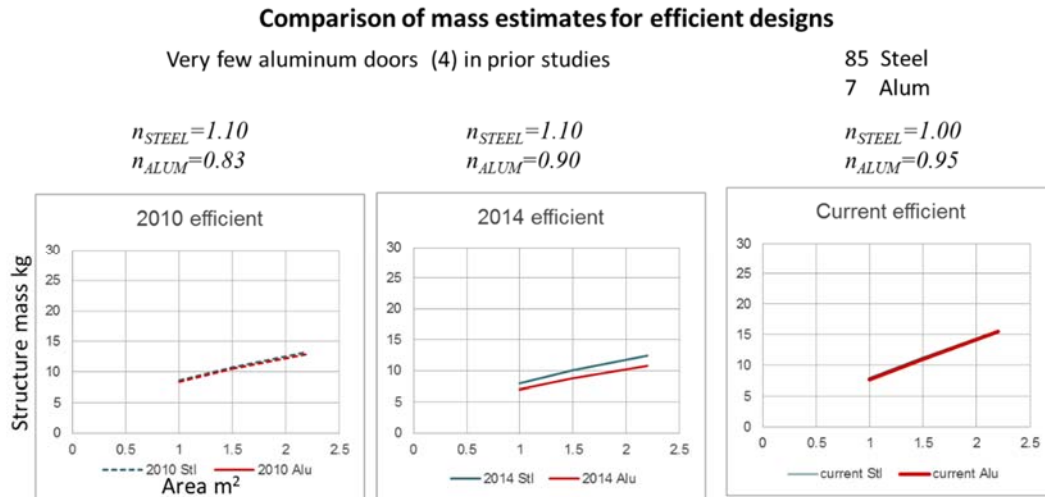


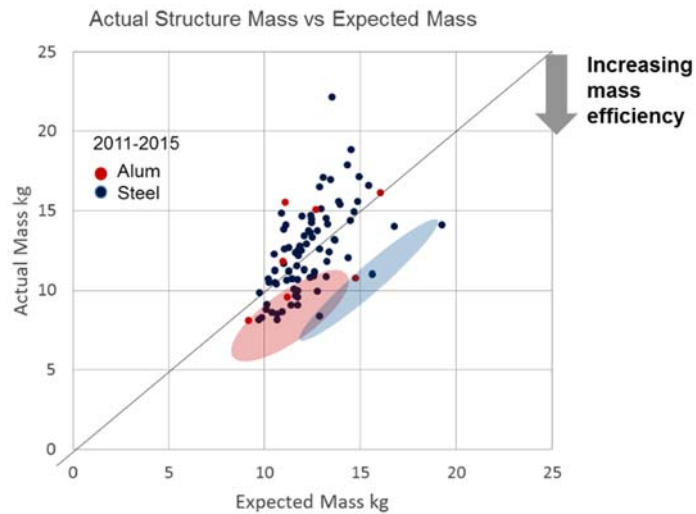
Figure 2.1.3-7 Hatchback door
Comparison of power model for three studies

Table 2.1.3-1 compares the material mass ratio for the three studies for both nominal and efficient designs. As noted in previous studies Steel performance is better when efficient designs are compared and the ratio is slightly greater in this study of 2011-2015 doors compared with the prior study.

Table 2.1.3-1 Hatchback door
Comparison of material mass ratio for three studies

	$\frac{m_{ALUM}}{m_{STEEL}}$	
	Nominal designs	Efficient designs
Current	0.939	0.988
2014 study	0.714	0.873
2010 study	0.981	0.976

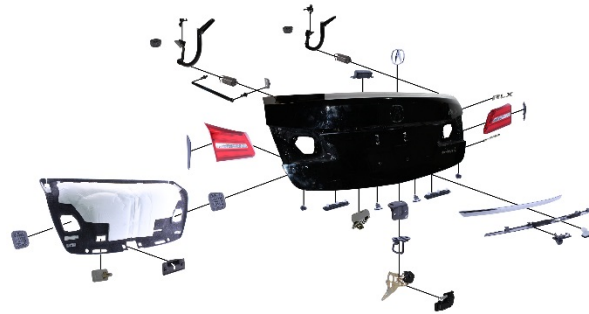
All doors were ranked by the difference between actual mass and expected mass. This is shown graphically in the parity plot of Figure 2.1.3-8 where increasing mass efficiency is the downward distance from the 45° line where actual mass equals expected mass.



*Figure 2.1.3-8 Hatchback door
Parity plot to evaluate mass efficiency*

2.1.4 Decklid

The decklid system includes inner panel, trim, weather stripping, lock and all mounting hardware. The decklid structure consists of the welded assembly.



The first look at decklid structure mass data is shown in Figure 2.1.4-1. The basic statistics for each material class appear to be stable.

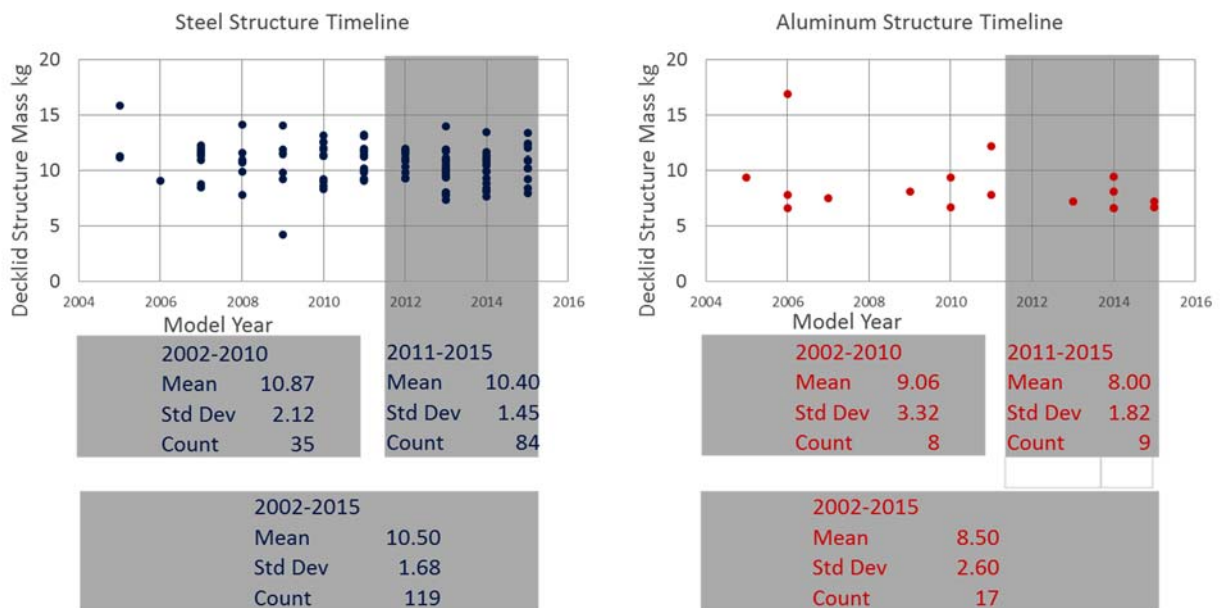
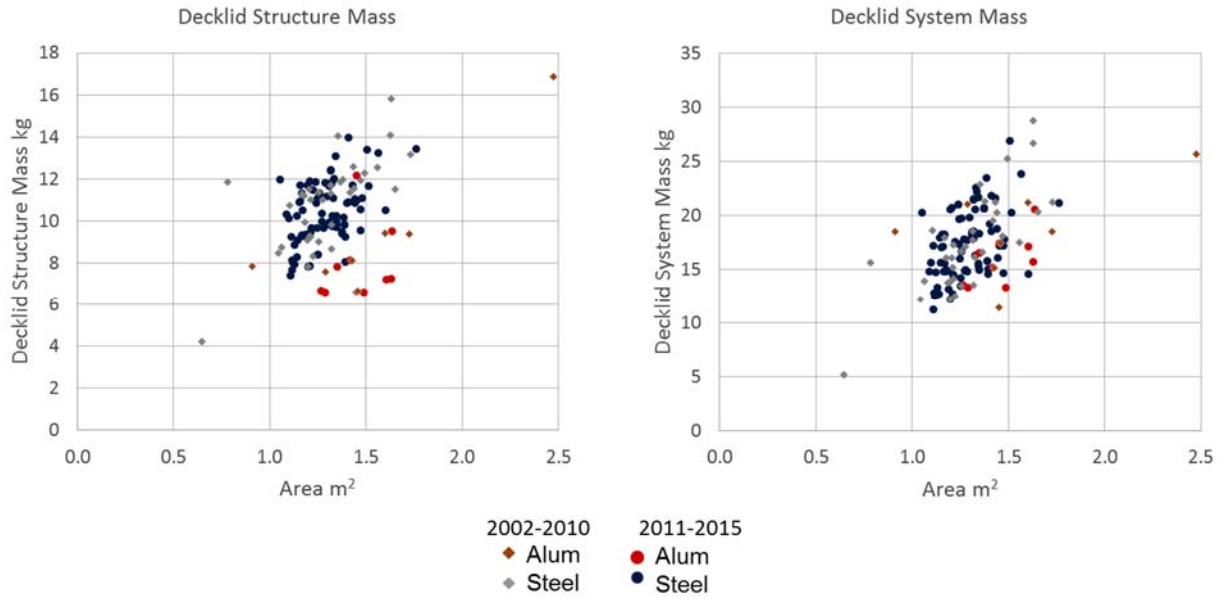


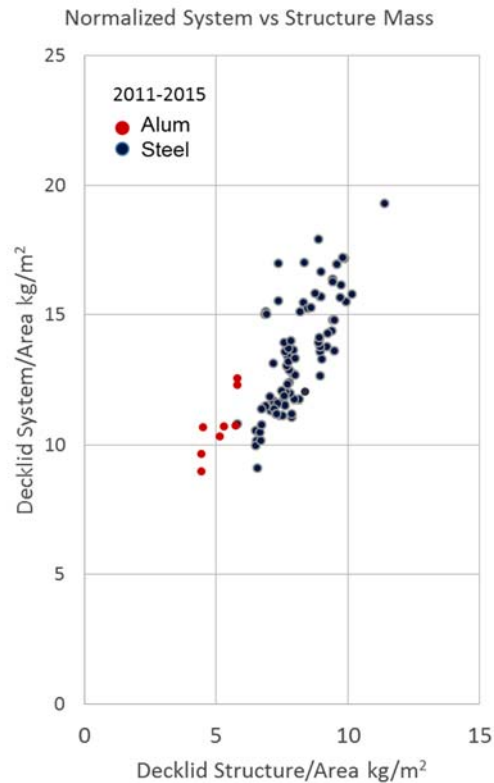
Figure 2.1.4-1 Decklid
Comparison of unadjusted mass statistics for structure

Figure 2.1.4-2 is a scatter plot of mass vs. the mass driver Area with data from the current study overlaid with data from the EDAG 2014 study. The data points for this study are in larger markers. The overall trend appears to be the similar.



*Figure 2.1.4-2 Decklid
Comparison of mass for two studies*

An important conclusion from the earlier study was that the mass reduction in the structure due to material substitution did not fully carry over to the system mass. This observation is not true for the decklid where much of the reduction does carry over. The scatter plot of Figure 2.1.4-3 shows this trend for this study; confirmed later by the regression equations.



*Figure 2.1.4-3 Decklid
Comparison of normalize system mass with normalized structure*

To fit the regression models, the mass drivers from previous studies were used, Figure 2.1.4-4.

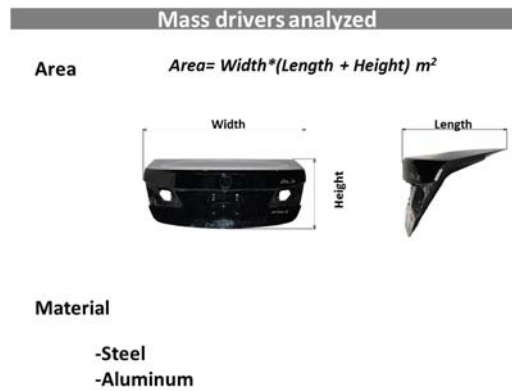


*Figure 2.1.4-4 Decklid
Mass drivers considered*

Models were then fit. These are shown below

Linear model for structure

$$m_{STRUCT} = 4.246 + 4.785 AREA - \frac{3.752 Alum}{0.000 Steel}, R^2 = 0.404, \sigma = 1.28$$

Power model for structure

$$m_{STRUCT} = 8.817 (AREA)^{0.629} \left[\frac{0.665 Alum}{1.000 Steel} \right], R^2 = 0.445, r = 1.135$$

Figure 2.1.4-5 shows the mass data with the power equation lines superimposed; Dotted for nominal, solid for mass efficient designs.

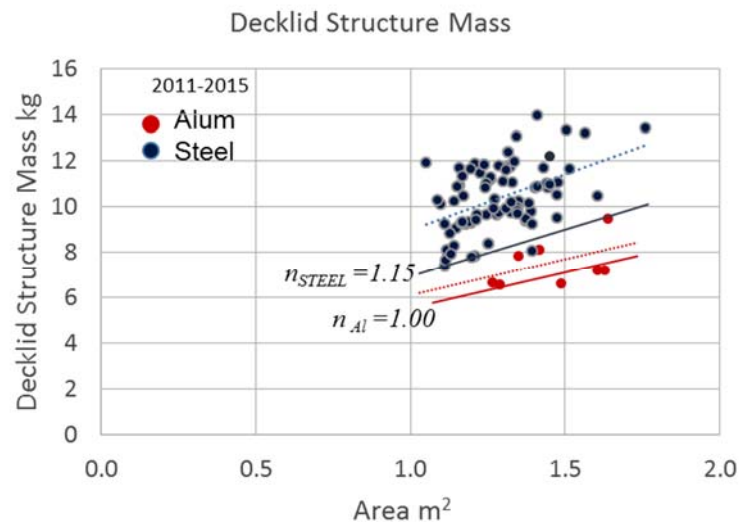


*Figure 2.1.4-5 Decklid
Structure mass with power model for mass efficient decklids*

In a similar manner, models were fit for the decklid system mass.

Linear model for system

$$m_{SYSTEM} = 3.591 + 10.693 AREA - \frac{3.525 \text{ Alum}}{0.000 \text{ Steel}}, R^2 = 0.231, \sigma = 2.772$$

Power model for system

$$m_{SYSTEM} = 13.886 (AREA)^{0.836} \left[\frac{0.818 \text{ Alum}}{1.000 \text{ Steel}} \right], R^2 = 0.221, r = 1.171$$

Figure 2.1.4-6 shows the mass data with the power equation line for nominal designs.

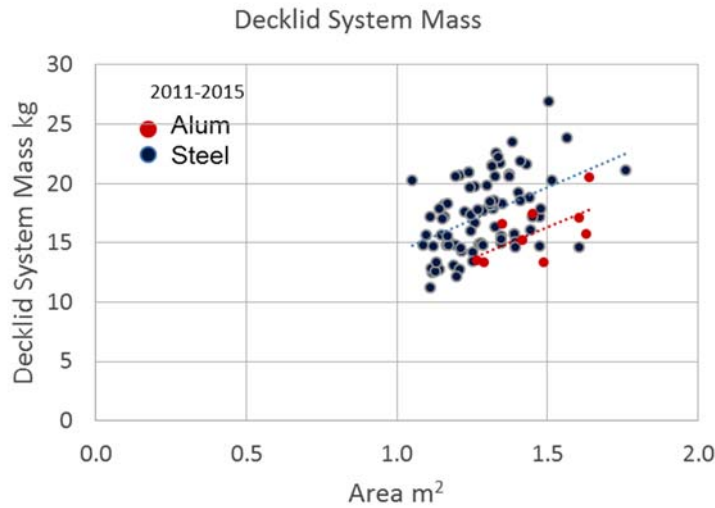


Figure 2.1.4-6 Decklid System mass with power model for nominal

Comparison of studies

A comparison of the power model equations for the three studies is presented below. The most meaningful comparison is between the current and 2014 study due to the larger number of samples. For these studies, the goodness of fit is similar. The form of the equation for the 2014 study used aluminum as the reference material while this study used steel. The prior equations were algebraically adjusted for direct comparison.

Current study

$$m_{STRUCT} = 8.817 (AREA)^{0.629} \left[\frac{0.665 \text{ Alum}}{1.000 \text{ Steel}} \right], R^2 = 0.45, r = 1.135$$

2014 study Equation algebraically modified for direct comparison

$$m_{STRUCT} = 9.055(AREA)^{0.5581} \left[\begin{array}{c} 0.757 \text{ Alum} \\ 1.000 \text{ Steel} \end{array} \right] \left[\begin{array}{c} 1.115 \text{ no LP} \\ 1.000 \text{ LP} \end{array} \right] \left[\begin{array}{c} 0.891 \text{ Tor. Spr.} \\ 1.000 \text{ Others} \end{array} \right], R^2=0.50, r=1.15$$

Equation as it originally appeared

$$m_{STRUCT} = 6.896(AREA)^{0.558} \left[\begin{array}{c} 1.32 \text{ if Steel} \\ 1.000 \text{ if Alum} \end{array} \right] \left[\begin{array}{c} 1.115 \text{ if no LP} \\ 1.000 \text{ if LP} \end{array} \right] \left[\begin{array}{c} 0.891 \text{ if Torsion Spr} \\ 1.000 \text{ if Others} \end{array} \right]$$

2010 study Equation algebraically modified for direct comparison

$$m_{STRUCT} = 8.415(AREA)^{1.176} \left[\begin{array}{c} 0.598 \text{ Alum} \\ 1.000 \text{ Steel} \end{array} \right], R^2=0.72, r=1.12$$

Equation as it originally appeared

$$m_{STRUCT} = 5.039(AREA)^{1.176} \left[\begin{array}{c} 1.67 \text{ if Steel} \\ 1.000 \text{ if Alum} \end{array} \right]$$

Because the equations have different constant coefficients and mass driver exponents, it is difficult to compare them visually. Figure 2.1.1-7 graphs the above equations for efficient designs to allow a direct comparison. The graphs overlay very closely indicating consistent results.

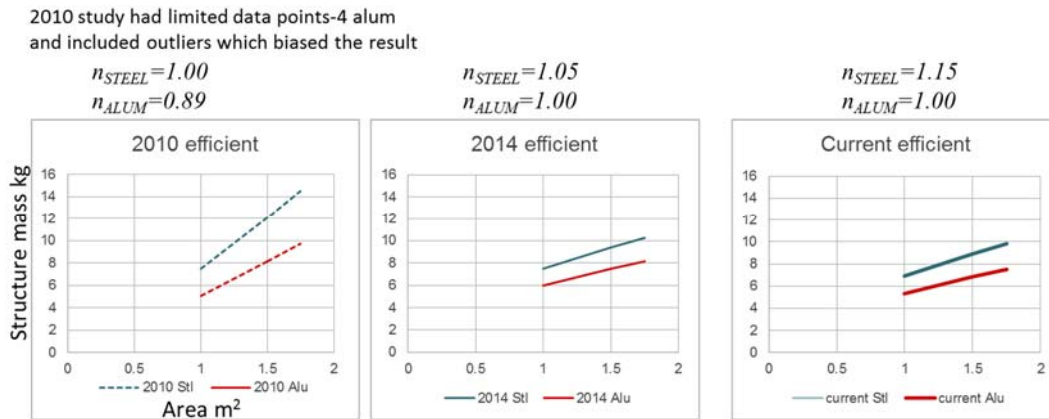


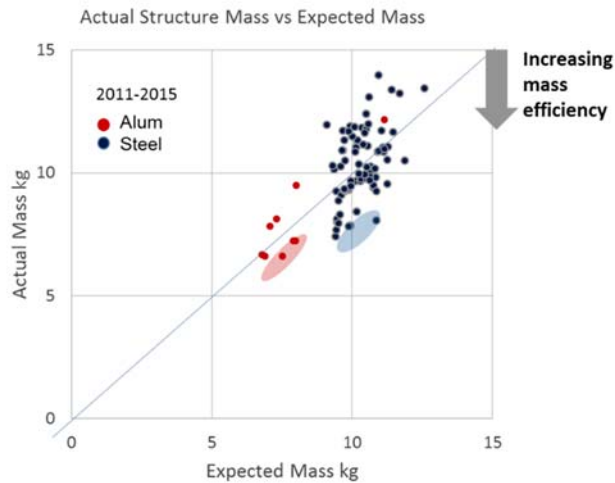
Figure 2.1.4-7 Decklid
Comparison of power model for three studies

Table 2.1.1-1 compares the material mass ratio for the three studies for both nominal and efficient designs. As noted in previous studies Steel performance is better when efficient designs are compared and the ratio is slightly greater in this study of 2011-2015 decklids compared with the prior study.

*Table 2.1.4-1 Decklid
Comparison of material mass ratio for three studies*

	$\frac{m_{ALUM}}{m_{STEEL}}$	
		Nominal designs Efficient designs
Current	<i>0.665</i>	<i>0.765</i>
2014 study	<i>0.757</i>	<i>0.795</i>
2010 study	<i>0.598</i>	<i>0.672</i>

All decklids were ranked by the difference between actual mass and expected mass. This is shown graphically in the parity plot of Figure 2.1.4-8 where increasing mass efficiency is the downward distance from the 45° line where actual mass equals expected mass.



*Figure 2.1.4-8 Decklids
Parity plot to evaluate mass efficiency*

2.1.5 Liftgate

The liftgate is the rear cargo closure on SUV vehicles. The liftgate system includes inner panel, glass, trim, weather stripping, lock and all mounting hardware.



The liftgate structure consists of the welded assembly.

The first look at liftgate structure mass data is shown in Figure 2.1.5-1. The average mass for steel has increased, for aluminum has decreased. However the changes are within the standard deviation of the data.

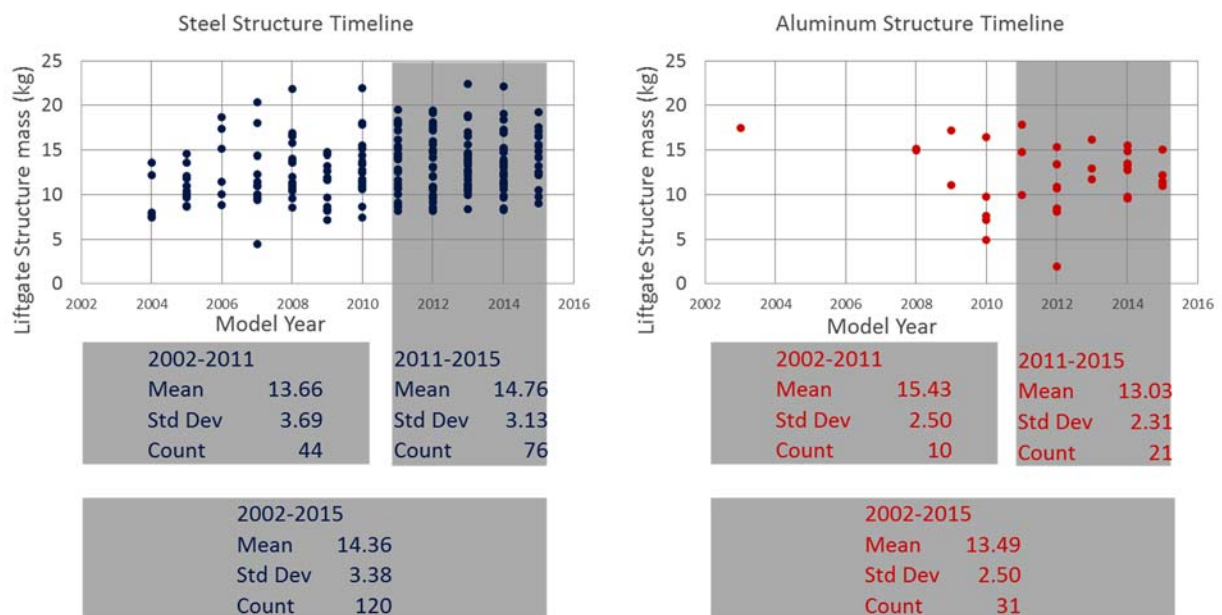


*Figure 2.1.5-1 Liftgate
Comparison of unadjusted mass statistics*

Figure 2.1.5-2 is a scatter plot of mass vs. the mass driver Area with data from the current study overlaid with data from the EDAG 2014 study. The data points for this study are in larger markers. The overall trend appears to be the similar.

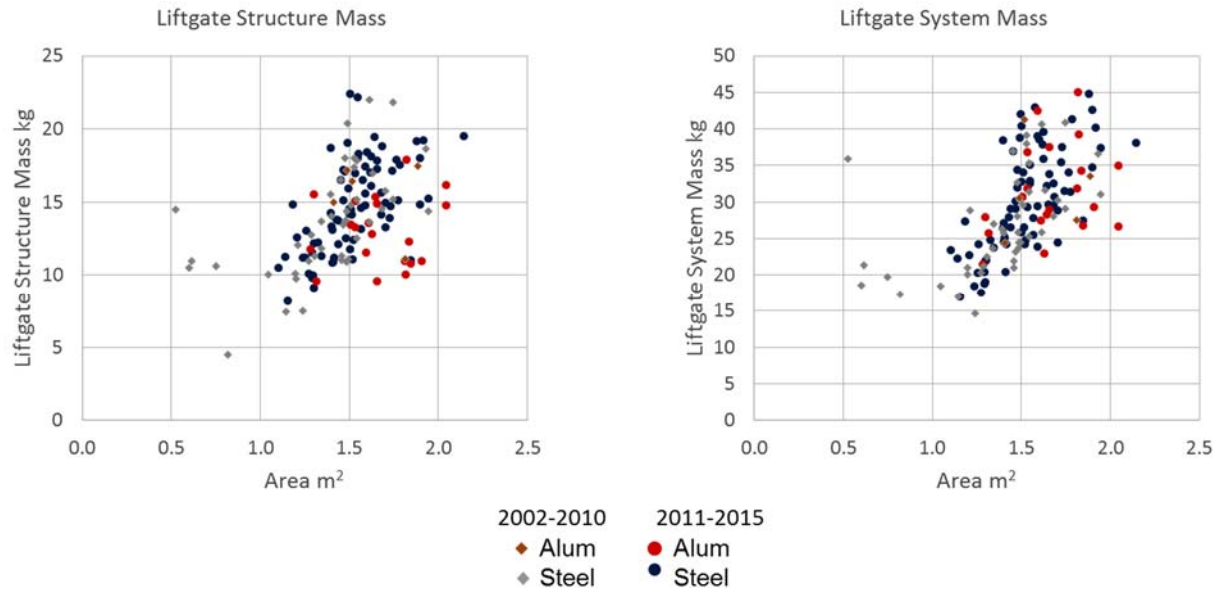


Figure 2.1.5-2 Liftgate
 Comparison of mass for two studies

An important conclusion from the earlier study was that the mass reduction in the structure due to material substitution did not fully carry over to the system mass. From the scatter plot of Figure 2.1.5-3 it is difficult to assess this effect due to the overlap of the data clouds for the two materials.

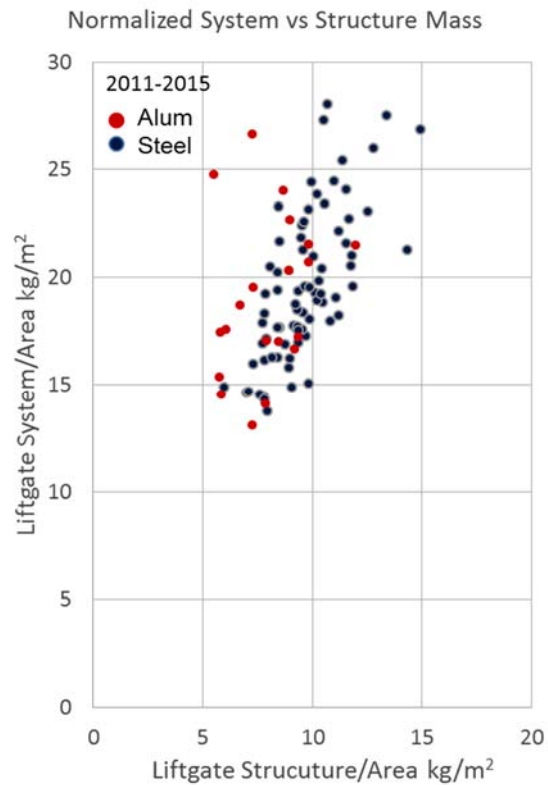
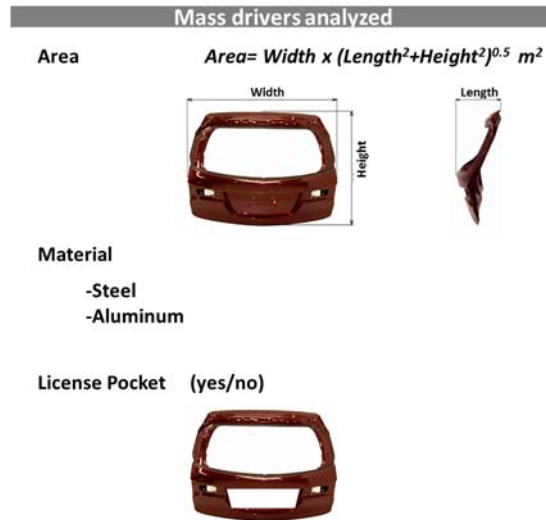


Figure 2.1.5-3 Liftgate
 Comparison of normalize system mass with normalized structure

To fit the regression models, the mass drivers from previous studies were used, Figure 2.1.5-4.



*Figure 2.1.5-4 Liftgate
Mass drivers considered*

Models were then fit. These are shown below

Linear model for structure

$$m_{STRUCT} = 4.231 + 7.371 AREA - \frac{2.771 Alum}{0.000 Steel} - \frac{0.884 LP}{0.000 no LP}, R^2 = 0.281, \sigma = 2.588$$

Power model for structure

$$m_{STRUCT} = 10.568 (AREA)^{0.848} \left[\begin{array}{c} 0.825 Alum \\ 1.000 Steel \end{array} \right] \left[\begin{array}{c} 0.952 LP \\ 1.000 no LP \end{array} \right], R^2 = 0.303, r = 1.197$$

Figure 2.1.5-5 shows the mass data with the power equation lines superimposed; Dotted for nominal, solid for mass efficient designs.

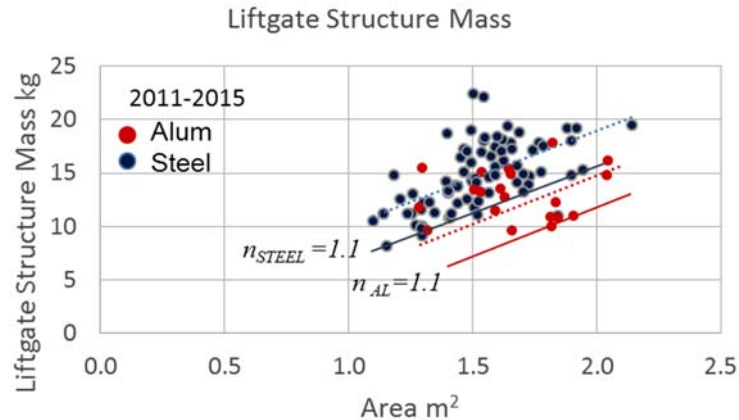


*Figure 2.1.5-5 Liftgate
Structure mass with power model for mass efficient Liftgates*

In a similar manner, models were fit for the liftgate system mass.

Linear model for system

$$m_{SYSTEM} = 0.014 + 19.201 AREA - \frac{1.042 Alum}{0.000 Steel} + \frac{0.791 LP}{0.000 no LP}, R^2 = 0.345, \sigma = 5.507$$

Power model for system

$$m_{SYSTEM} = 18.307 (AREA)^{1.074} \left[\frac{0.969 Alum}{1.000 Steel} \right] \left[\frac{1.025 LP}{1.000 no LP} \right], R^2 = 0.399, r = 1.196$$

Figure 2.1.5-6 shows the mass data with the power equation line for nominal designs.

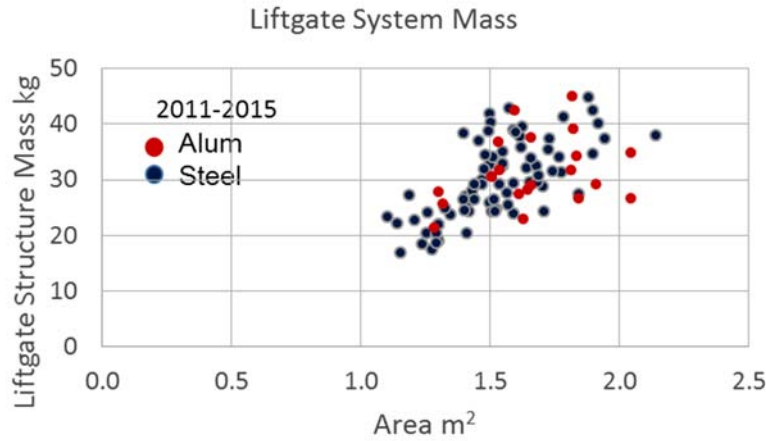


Figure 2.1.5-6 Liftgate
System mass with power model for nominal

Comparison of studies

A comparison of the power model equations for the three studies is presented below. The most meaningful comparison is between the current and 2014 study due to the larger number of samples. For these studies, the goodness of fit is similar. The form of the equation for the 2014 study used aluminum as the reference material while this study used steel. The prior equations were algebraically adjusted for direct comparison.

Current study

$$m_{STRUCT} = 10.568 (AREA)^{0.848} \left[\frac{0.825 Alum}{1.000 Steel} \right] \left[\frac{0.952 LP}{1.000 no LP} \right], R^2 = 0.303, r = 1.197$$

To be consistent with the 2014 study, the equation was modified to

$$m_{STRUCT} = 10.252 (AREA)^{0.823} \left[\frac{0.830 Alum}{1.000 Steel} \right], R^2 = 0.303, r = 1.197$$

2014 study

$$m_{STRUCT} = 10.57(AREA)^{0.491} \left[\begin{matrix} 1.000 \text{ Alum} \\ 1.000 \text{ Steel} \end{matrix} \right], R^2=0.15, r=1.194$$

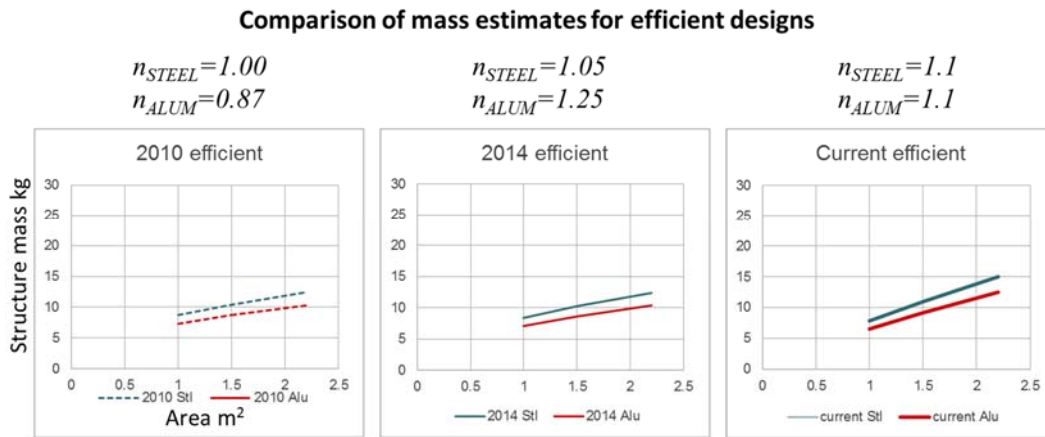
2010 study Equation algebraically modified for direct comparison

$$m_{STRUCT} = 10.050(AREA)^{0.4429} (MountedMass)^{0.1558} \left[\begin{matrix} 0.724 \text{ Alum} \\ 1.000 \text{ Steel} \end{matrix} \right] \left[\begin{matrix} 0.827 \text{ LP} \\ 1.000 \text{ no LP} \end{matrix} \right], R^2=0.72, r=1.15$$

Equation as it originally appeared

$$m_{STRUCT} = 7.283(AREA)^{0.4429} (MountedMass)^{0.1558} \left[\begin{matrix} 1.380 \text{ if Steel} \\ 1.000 \text{ if Alum} \end{matrix} \right] \left[\begin{matrix} 0.827 \text{ License Pocket} \\ 1.000 \text{ No Pocket} \end{matrix} \right]$$

Because the equations have different constant coefficients and mass driver exponents, it is difficult to compare them visually. Figure 2.1.5-7 graphs the above equations for efficient designs to allow a direct comparison. The graphs overlay very closely indicating consistent results.



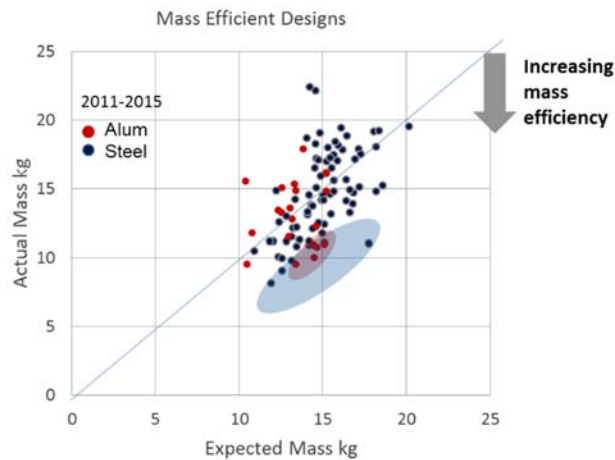
*Figure 2.1.5-7 Liftgate
Comparison of power model for three studies*

Table 2.1.5-1 compares the material mass ratio for the three studies for both nominal and efficient designs. As noted in previous studies Steel performance is better when efficient designs are compared and the ratio is slightly greater in this study of 2011-2015 liftgates compared with the prior study.

*Table 2.1.5-1 Liftgate
Comparison of material mass ratio for three studies*

	$\frac{m_{ALUM}}{m_{STEEL}}$	
	Nominal designs	Efficient designs
Current	0.830	0.830
2014 study	1.000	0.840
2010 study	0.724	0.830

All liftgates were ranked by the difference between actual mass and expected mass. This is shown graphically in the parity plot of Figure 2.1.5-8 where increasing mass efficiency is the downward distance from the 45° line where actual mass equals expected mass.



*Figure 2.1.5-8 Liftgate
Parity plot to evaluate mass efficiency*

2.2 Body Subsystems

The body systems analyzed were front bumper beam, rear bumper beam, instrument panel beam, seat structure, and body structure.

2.2.1 Front bumper

The front bumper structure includes the beam and all mounting hardware.



The first look at front bumper structure mass data is shown in Figure 2.2.1-1. The basic statistics for each material class appear to be stable.

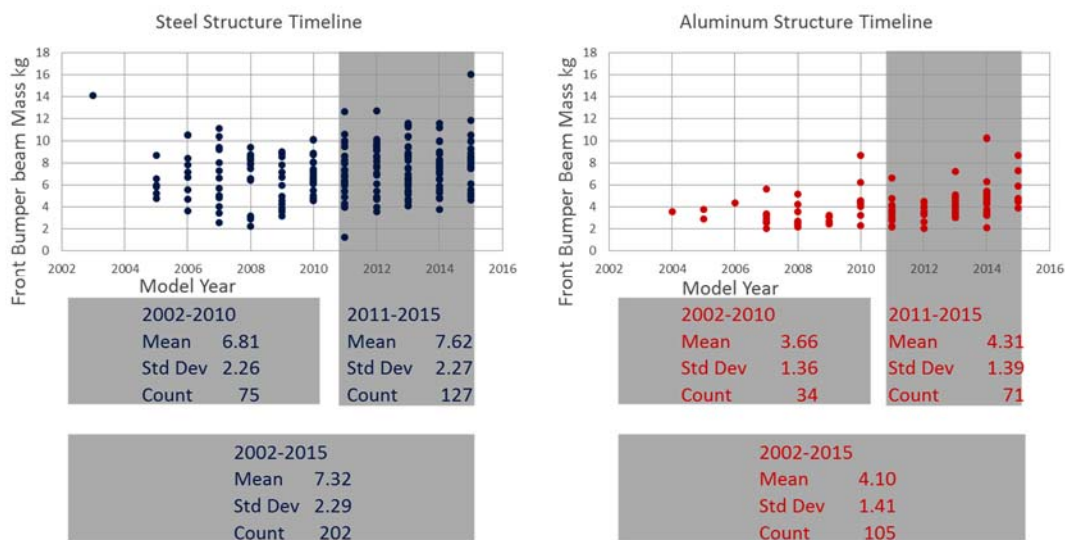


Figure 2.2.1-1 Front bumper
Comparison of unadjusted mass statistics

Figure 2.2.1-2 shows scatter plots of mass vs. the mass drivers **Beam length** and **Curb mass** with data from the current study overlaid with data from the EDAG 2014 study. The data points for this study are in larger markers. The overall trends appear to be similar.

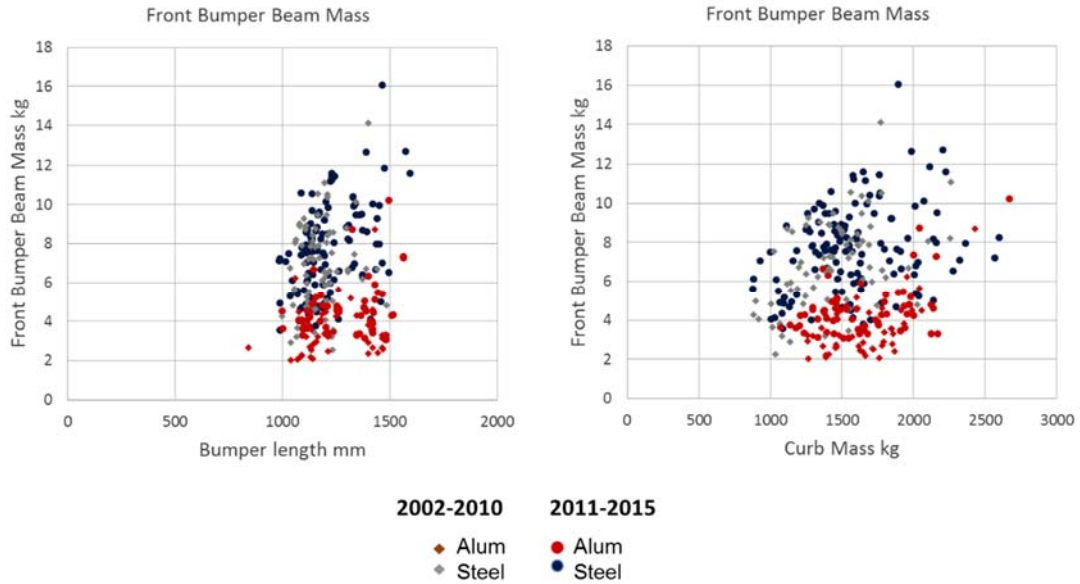


Figure 2.2.1-2 Front bumper
Comparison of mass for two studies

To fit the regression models, the mass drivers from previous studies were used, Figure 2.2.1-3.

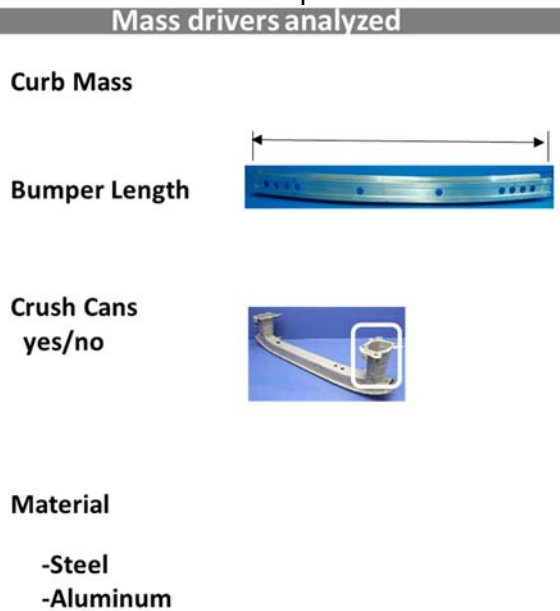


Figure 2.2.1-3 Front bumper
Mass drivers considered

Models were then fit. These are shown below

Linear model for structure

$$m_{STRUC} = -4.094 + 0.002CurbMass + 0.005BLength - \frac{2.477 Alum}{0.000 Steel} + \frac{2.660 Crush Can}{0.000 No Crush Can}$$

$$R^2 = 0.655, \sigma = 1.44$$

Power model for structure

$$m_{STRUC} = 3.6 \times 10^{-4} (CurbMass)^{0.501} (BLength)^{0.838} \begin{bmatrix} 0.658 \text{ Alum} \\ 1.000 \text{ Steel} \end{bmatrix} \begin{bmatrix} 1.471 \text{ Crush Can} \\ 1.000 \text{ No Crush Can} \end{bmatrix}$$

$$R^2 = 0.687, r = 1.23$$

Figure 2.2.1-4 shows the mass data with the power equation lines superimposed; Dotted for nominal, solid for mass efficient designs.

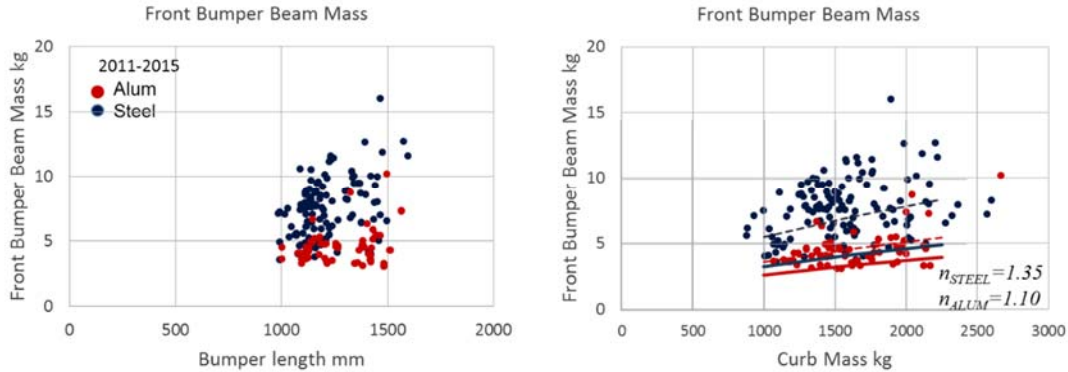


Figure 2.2.1-4 Front bumper
Structure mass with power model for mass efficient Front bumpers

Comparison of studies

A comparison of the power model equations for the three studies is presented below. The most meaningful comparison is between the current and 2014 study due to the larger number of samples. For these studies, the goodness of fit is similar. The form of the equation for the 2014 study used aluminum as the reference material while this study used steel. The prior equations were algebraically adjusted for direct comparison.

Current study

$$m_{STRUC} = 3.6 \times 10^{-4} (CurbMass)^{0.501} (BLength)^{0.838} \begin{bmatrix} 0.658 \text{ Alum} \\ 1.000 \text{ Steel} \end{bmatrix} \begin{bmatrix} 1.471 \text{ Crush Can} \\ 1.000 \text{ No Crush Can} \end{bmatrix}$$

$$R^2 = 0.687, r = 1.25$$

2014 study Equation algebraically modified for direct comparison

$$m_{STRUC} = 2.14 \times 10^{-4} (CurbMass)^{0.845} (BLength)^{0.587} \begin{bmatrix} 0.668 \text{ Alum} \\ 1.000 \text{ Steel} \end{bmatrix} \begin{bmatrix} 1.266 \text{ Crush Can} \\ 1.000 \text{ no Crush Can} \end{bmatrix} \begin{bmatrix} 0.870 \text{ Pick Up - SUV} \\ 1.000 \text{ Passenger Cars} \end{bmatrix}$$

$$R^2 = 0.48, r = 1.346$$

As equation appeared in original report

$$m_{STRUC} = 0.000157 (CurbMass)^{0.845} (RailWidth)^{0.587} \begin{bmatrix} 1.497 \text{ if Steel} \\ 1.000 \text{ if Alum} \end{bmatrix} \begin{bmatrix} 1.266 \text{ Crush Can} \\ 1.000 \text{ no Crush Can} \end{bmatrix} \begin{bmatrix} 0.87 \text{ Pick Up - SUV} \\ 1.000 \text{ Passenger Cars} \end{bmatrix}$$

where Rail width ~ 0.85 (Bumper length)

2010 study Equation algebraically modified for direct comparison

$$m_{STRUC} =$$

$$1.00 \times 10^{-6} (CurbMass)^{0.55} (BumperLength)^{1.64} \left[\begin{array}{c} 0.671 \text{ Alum} \\ 1.000 \text{ Steel} \end{array} \right] \left[\begin{array}{c} 1.3 \text{ Crush Can} \\ 1.0 \text{ no Crush Can} \end{array} \right], R^2=0.49, r=1.37$$

As equation appeared in original report

$$m_{STRUC} = 7.375 \times 10^{-7} (CurbMass)^{0.55} (BumperLength)^{1.053} (RailWidth)^{0.587} \left[\begin{array}{c} 1.49 \text{ if Steel} \\ 1.000 \text{ if Alum} \end{array} \right] \left[\begin{array}{c} 1.3 \text{ Crush Can} \\ 1.000 \text{ no Crush Can} \end{array} \right]$$

where Rail width ~ 0.85 (Bumper length)

Because the equations have different constant coefficients and mass driver exponents, it is difficult to compare them visually. Figure 2.2.1-5 graphs the above equations for efficient designs to allow a direct comparison. The graphs overlay very closely indicating consistent results.

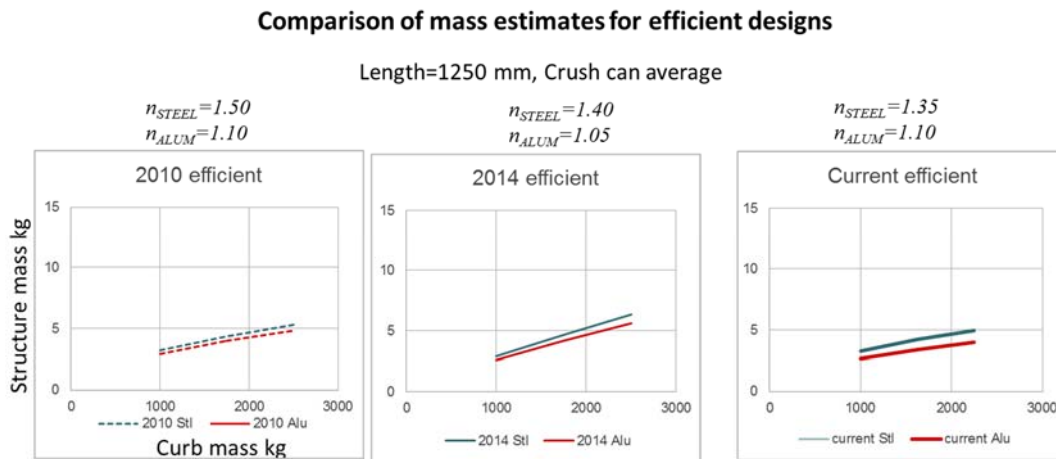


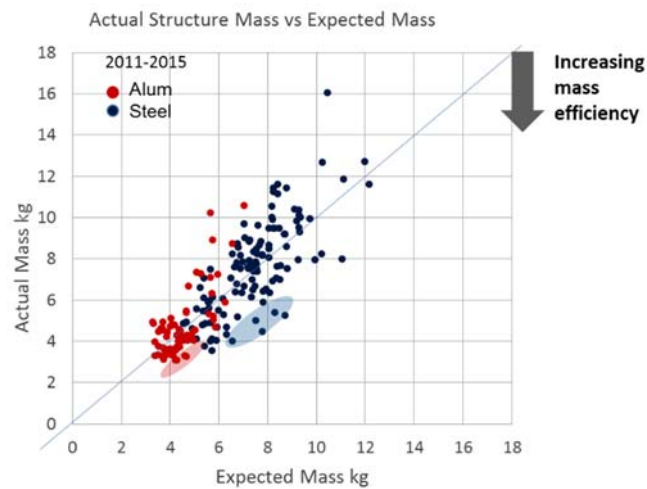
Figure 2.2.1-5 Front bumper
Comparison of power model for three studies

Table 2.2.1-1 compares the material mass ratio for the three studies for both nominal and efficient designs. As noted in previous studies steel performance is better when efficient designs are compared.

Table 2.2.1-1 Front bumper
Comparison of material mass ratio for three studies

	$\frac{m_{ALUM}}{m_{STEEL}}$	
	Nominal designs	Efficient designs
Current	0.658	0.808
2014 study	0.668	0.891
2010 study	0.671	0.915

All front bumpers were ranked by the difference between actual mass and expected mass. This is shown graphically in the parity plot of Figure 2.2.1-6 where increasing mass efficiency is the downward distance from the 45° line where actual mass equals expected mass.



*Figure 2.2.1-6 Front bumper
Parity plot to evaluate mass efficiency*

2.2.2 Rear bumper

The rear bumper structure includes the beam and all mounting hardware.



The first look at rear bumper structure mass data is shown in Figure 2.2.2-1. The basic statistics for each material class appear to be stable.

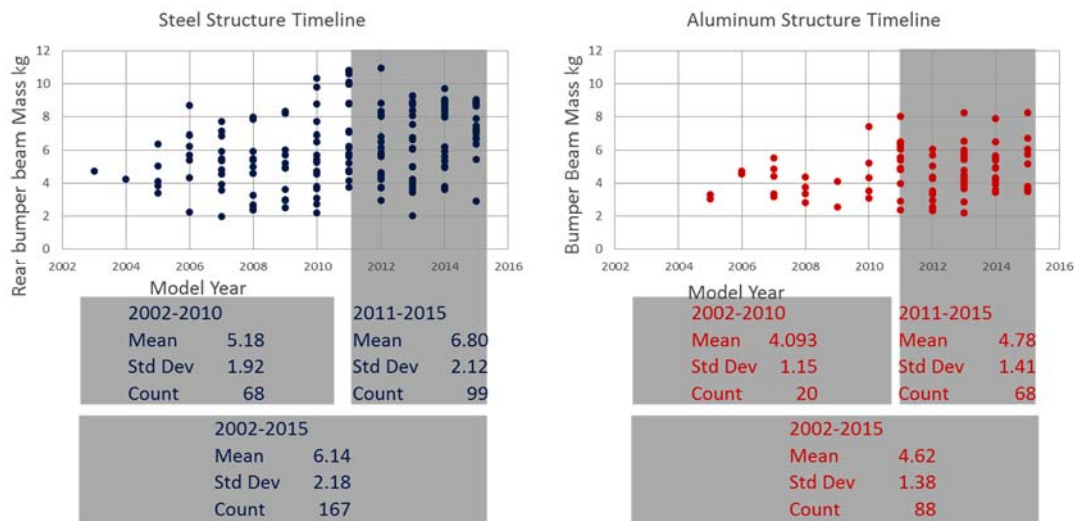


*Figure 2.2.2-1 Rear bumper
Comparison of unadjusted mass statistics*

Figure 2.2.2-2 is a scatter plot of mass vs. the mass driver **Curb mass** with data from the current study overlaid with data from the EDAG 2014 study. The data points for this study are in larger markers. The overall trend appears to be the similar.

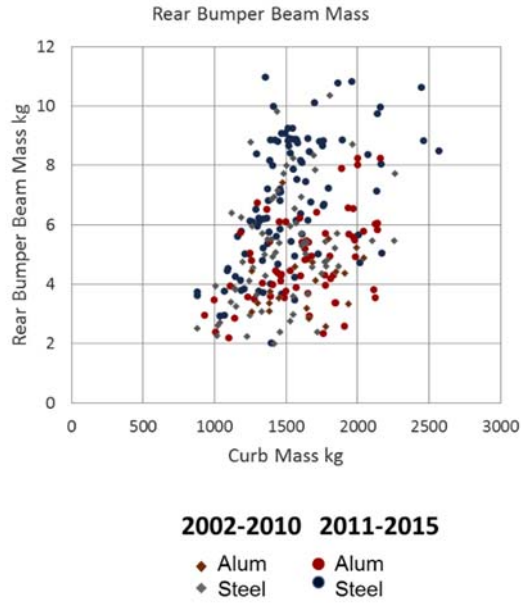


Figure 2.2.2-2 Rear bumper
Comparison of mass for two studies

To fit the regression models, the mass drivers from previous studies were used, Figure 2.2.2-3. Note that, unlike the front bumper, the rear bumper mass dependence on bumper length and crush can presence was not found to be statistically significant in these earlier studies.

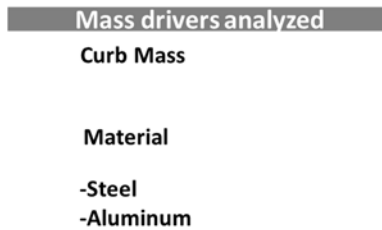


Figure 2.2.2-3 Rear bumper
Mass drivers considered

Models were then fit. These are shown below

Linear model for structure

$$m_{STRUC} = 2.396 + 0.002881CurbMass - \begin{matrix} 2.285 \text{ if Alum} \\ 0.000 \text{ if Steel} \end{matrix}$$

$$R^2 = 0.404, \sigma = 1.62$$

Power model for structure

$$m_{STRUC} = 0.0145(CurbMass)^{0.833} \begin{bmatrix} 0.676 \text{ if Alum} \\ 1.000 \text{ if Steel} \end{bmatrix}$$

$$R^2 = 0.41, r = 1.328$$

Figure 2.2.2-4 shows the mass data with the power equation lines superimposed; Dotted for nominal, solid for mass efficient designs.

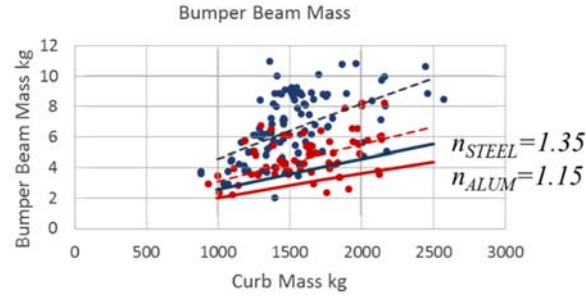


Figure 2.2.2-4 Rear bumper
Structure mass with power model for mass efficient Rear bumpers

Comparison of studies

A comparison of the power model equations for the three studies is presented below. The most meaningful comparison is between the current and 2014 study due to the larger number of samples. For these studies, the goodness of fit is similar. The form of the equation for the 2014 study used aluminum as the reference material while this study used steel. The prior equations were algebraically adjusted for direct comparison.

Current study

$$m_{STRUC} = 0.0145(CurbMass)^{0.833} \begin{bmatrix} 0.676 \text{ if Alum} \\ 1.000 \text{ if Steel} \end{bmatrix}, R^2 = 0.41, r = 1.32$$

2014 study Equation algebraically modified for direct comparison

$$m_{STRUC} = 0.0082(CurbMass)^{0.882} \begin{bmatrix} 0.685 \text{ if Alum} \\ 1.000 \text{ if Steel} \end{bmatrix} \begin{bmatrix} 1.388 \text{ North America} \\ 1.000 \text{ Europe} \end{bmatrix}, R^2 = 0.41, r = 1.44$$

Equation as it originally appeared

$$m_{STRUC} = 0.0056(CurbMass)^{0.882} \begin{bmatrix} 1.459 \text{ if Steel} \\ 1.000 \text{ if Alum} \end{bmatrix} \begin{bmatrix} 1.388 \text{ North America} \\ 1.000 \text{ Europe} \end{bmatrix}$$

2010 study Equation algebraically modified for direct comparison

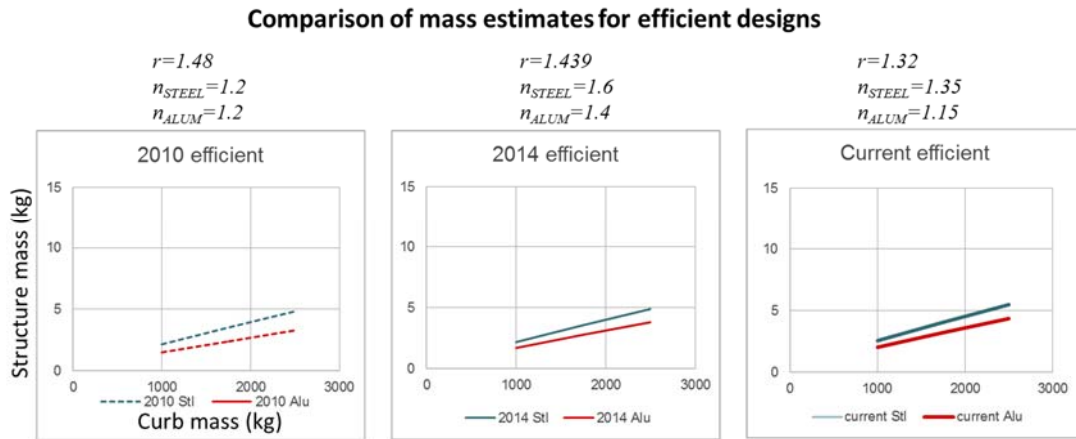
$$m_{STRUC} = 0.0092(CurbMass)^{0.874} \begin{bmatrix} 0.686 \text{ if Alum} \\ 1.000 \text{ if Steel} \end{bmatrix}, R^2 = 0.31, r = 1.48$$

Equation as it originally appeared

$$m_{STRUC} = 0.0063(CurbMass)^{0.874} \begin{bmatrix} 1.457 \text{ if Steel} \\ 1.000 \text{ if Alum} \end{bmatrix}$$

Because the equations have different constant coefficients and mass driver exponents, it is difficult to compare them visually. Figure 2.2.2-5 graphs the above equations for efficient

designs to allow a direct comparison. The graphs overlay very closely indicating consistent results.



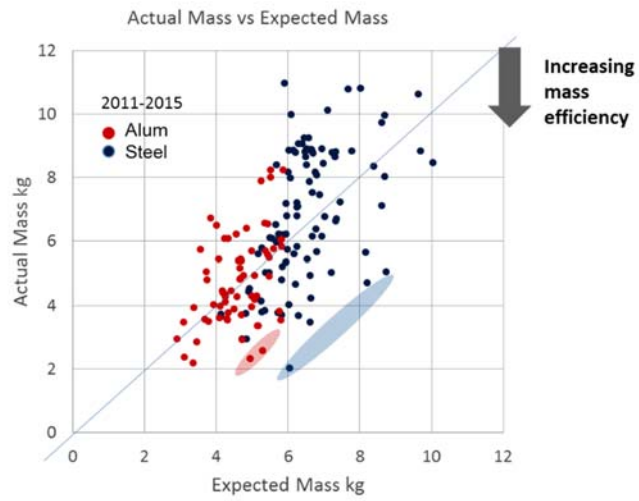
*Figure 2.2.2-5 Rear bumper
Comparison of power model for three studies*

Table 2.2.2-1 compares the material mass ratio for the three studies for both nominal and efficient designs.

*Table 2.2.2-1 Rear bumper
Comparison of material mass ratio for three studies*

	$\frac{m_{ALUM}}{m_{STEEL}}$	
	Nominal designs	Efficient designs
Current	0.676	0.794
2014 study	0.685	0.783
2010 study	0.686	0.686

All rear bumpers were ranked by the difference between actual mass and expected mass. This is shown graphically in the parity plot of Figure 2.2.2-6 where increasing mass efficiency is the downward distance from the 45° line where actual mass equals expected mass.



*Figure 2.2.2-6 Rear bumper
Parity plot to evaluate mass efficiency*

2.2.3 Instrument panel beam

The IP Beam includes the beam, bracketry, and mounting hardware.



The first look at IP beam structure mass data is shown in Figure 2.2.3-1. The basic statistics for each material class appear to be stable.

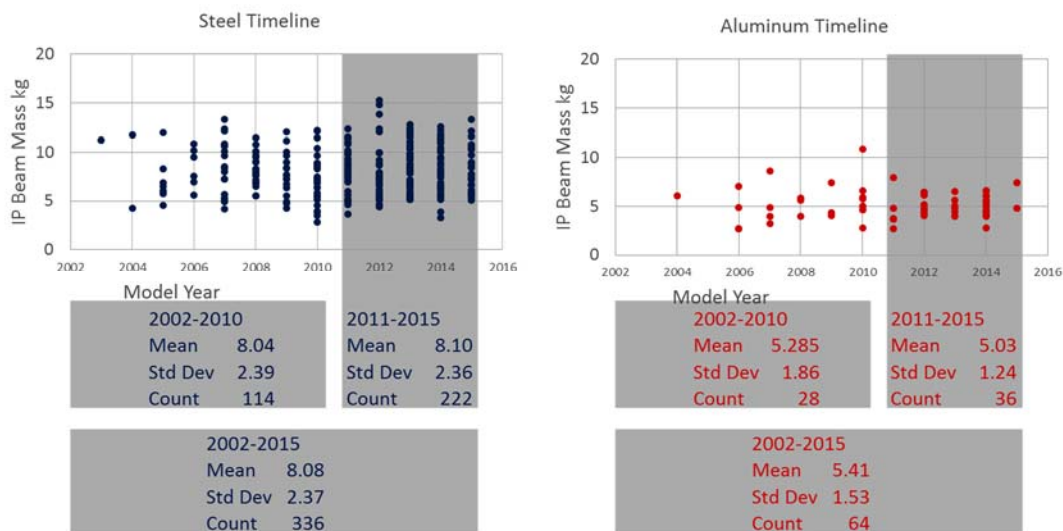


*Figure 2.2.3-1 IP beam
Comparison of unadjusted mass statistics*

Figure 2.2.3-2 is a scatter plot of mass vs. vehicle width with data from the current study overlaid with data from the EDAG 2014 study. The data points for this study are in larger markers. The overall data appears to be the similar.

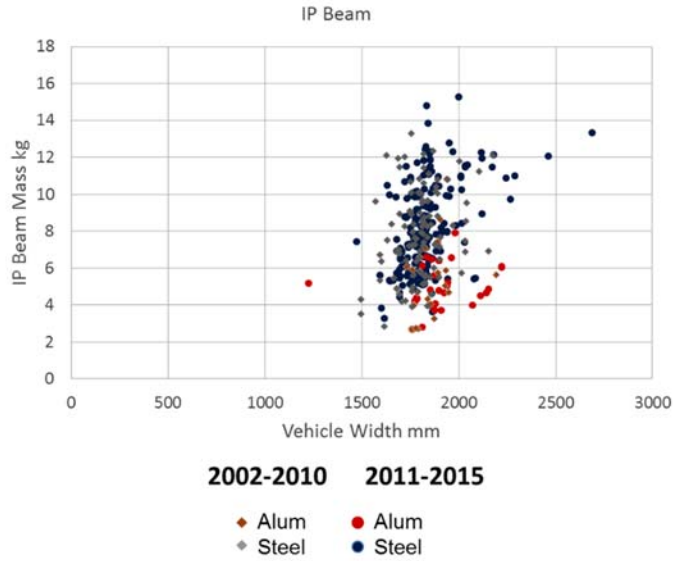


Figure 2.2.3-2 IP beam
Comparison of mass for two studies

To fit the regression models, the mass drivers from previous studies were used, Figure 2.2.3-3.

Mass drivers analyzed

Vehicle Width

Material Type

Figure 2.2.3-3 IP beam
Mass drivers considered

Models were then fit. These are shown below

Linear model for structure

$$m_{STRUC} = -4.77 + 8.75 \times 10^{-4} (\text{Vehicle Width}) - \begin{bmatrix} 3.640 \text{ Alum} \\ 0.000 \text{ Steel} \end{bmatrix}, R^2 = 0.341, \sigma = 2.011$$

Power model for structure

$$m_{STRUC} = 17.8 \times 10^{-6} (\text{Vehicle Width})^{1.729} \begin{bmatrix} 0.581 \text{ Alum} \\ 1.000 \text{ Steel} \end{bmatrix}, R^2 = 0.374, r = 1.30$$

Figure 2.2.3-4 shows the mass data with the power equation lines superimposed; Dotted for nominal, solid for mass efficient designs.

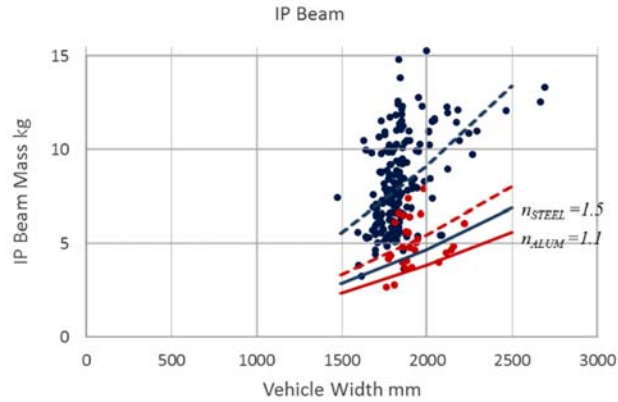


Figure 2.2.3-4 IP beam
Structure mass with power model for mass efficient IP beams

Comparison of studies

A comparison of the power model equations for the three studies is presented below. The most meaningful comparison is between the current and 2014 study due to the larger number of samples. For these studies, the goodness of fit is similar. The form of the equation for the 2014 study used aluminum as the reference material while this study used steel. The prior equations were algebraically adjusted for direct comparison.

Current study

$$m_{STRUC} = 17.8 \times 10^{-6} (\text{Vehicle Width})^{1.729} \left[\begin{array}{c} 0.581 \text{ Alum} \\ 1.000 \text{ Steel} \end{array} \right], R^2 = 0.374, r = 1.30$$

2014 study Equation algebraically modified for direct comparison

$$m_{STRUC} = 3.478 \times 10^{-6} (\text{Vehicle Width})^{1.954} \left[\begin{array}{c} 0.603 \text{ Alum} \\ 1.000 \text{ Steel} \end{array} \right], R^2 = 0.36, r = 1.31$$

Equation as it originally appeared

$$m_{STRUC} = 2.1 \times 10^{-6} (\text{Vehicle Width})^{1.954} \left[\begin{array}{c} 1.656 \text{ Steel} \\ 1.000 \text{ Al} \end{array} \right]$$

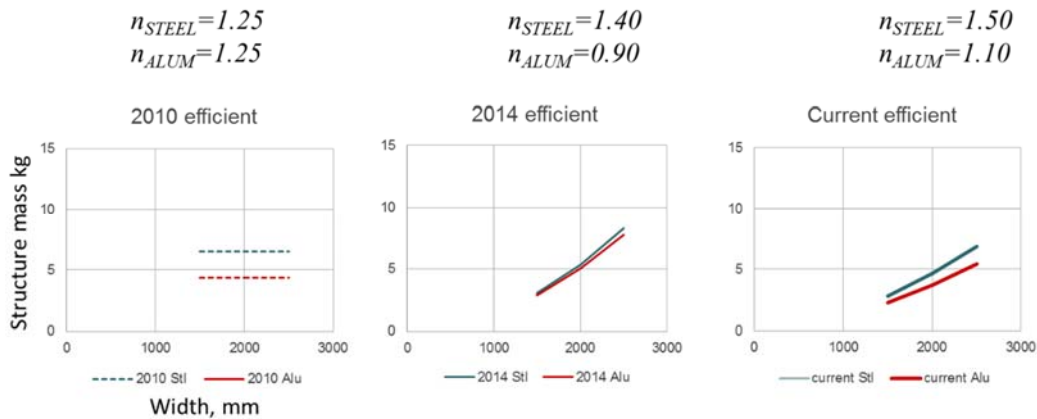
2010 study Equation algebraically modified for direct comparison

$$m_{STRUC} = 10.20 \left[\begin{array}{c} 1.000 \text{ Steel} \\ 0.670 \text{ Alloy} \\ 1.166 \text{ Plastic} \end{array} \right], R^2 = 0.24, r = 1.26$$

Equation as it originally appeared

$$m_{STRUC} = 8.75 \left[\begin{array}{c} 0.858 \text{ Steel} \\ 0.575 \text{ Alloy} \\ 1.000 \text{ Plastic} \end{array} \right]$$

Because the equations have different constant coefficients and mass driver exponents, it is difficult to compare them visually. Figure 2.2.3-5 graphs the above equations for efficient designs to allow a direct comparison. The graphs for 2014 and the current study overlay closely indicating consistent results.



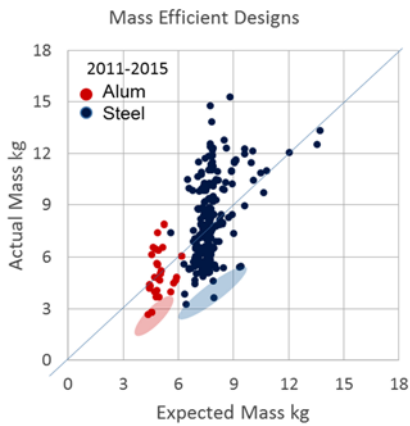
*Figure 2.2.3-5 IP beam
Comparison of power model for three studies*

Table 2.2.3-1 compares the material mass ratio for the three studies for both nominal and efficient designs.

*Table 2.2.3-1 IP beam
Comparison of material mass ratio for three studies*

	$\frac{m_{ALUM}}{m_{STEEL}}$	
	Nominal designs	Efficient designs
Current	0.581	0.792
2014 study	0.603	0.938
2010 study	0.670	0.670

All IP beams were ranked by the difference between actual mass and expected mass. This is shown graphically in the parity plot of Figure 2.2.3-6 where increasing mass efficiency is the downward distance from the 45° line where actual mass equals expected mass.



*Figure 2.2.3-6 IP beam
Parity plot to evaluate mass efficiency*

2.2.4 Front seat frame

The seat system includes headrest, cushion, power adjusters, support system and all mounting hardware. The seat structure consists of the welded assemblies of seat back and base.



The first look at seat frame structure is shown in Figure 2.2.4-1. The basic statistics appear to be stable. Note that all seat frames in the 2011-2015 timeframe are steel with the exception of two variants of a CFRP/Steel design found on related models.

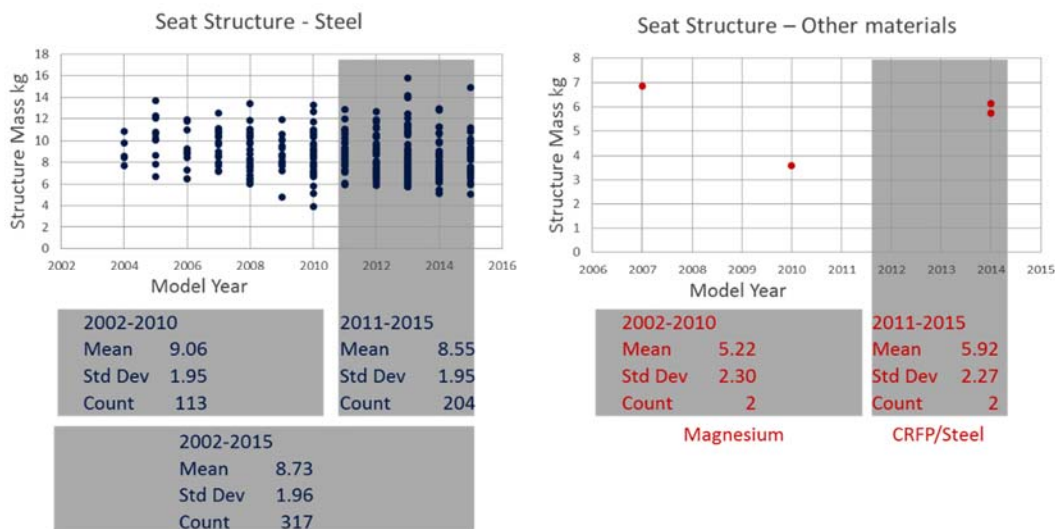
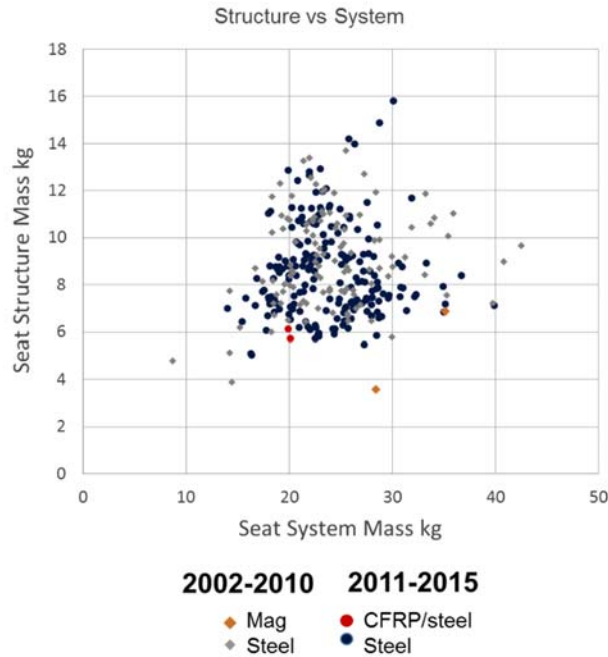


Figure 2.2.4-1 Seat structure (left) and seat system (right)
Comparison of unadjusted mass statistics

Figure 2.2.4-2 is a scatter plot of seat structure mass vs. seat system mass for the current study overlaid with data from the EDAG 2014 study. The data points for this study are in larger markers. The overall data cloud appears to be the similar.



*Figure 2.2.4-2 Seat structure mass vs. seat system mass
Comparison of mass for two studies*

An important conclusion from the earlier closure studies was that often the mass reduction in the structure due to material substitution did not fully carry over to the system mass (e.g. Front door). For the case of seats, there were insufficient data samples for materials other than steel to determine this effect.

To fit the regression models, the mass drivers from previous studies were used, Figure 2.2.4-3. For seats, the only mass driver is material.

Mass drivers analyzed
Material
-Steel
-CFRP/steel

*Figure 2.2.4-3 Seat frame
Mass drivers considered*

Models were fit and are shown below. In general there is high residual variability as indicated by the very low R^2 values.

Linear model for structure

$$m_{STRUCT} = 8.552 - \begin{bmatrix} 2.623 \text{ CFRP/Steel} \\ 0.000 \text{ Steel} \end{bmatrix}, R^2 = 0.12, \sigma = 1.95$$

Power model for structure

$$m_{STRUCT} = 8.345 \begin{bmatrix} 0.710 \text{ CFRP/Steel} \\ 1.000 \text{ Steel} \end{bmatrix}, R^2 = 0.18, r = 1.25$$

In a similar manner, models were fit for the seat frame system mass.
Linear model for system

$$m_{SYSTEM} = 24.00 - \frac{3.975 CFRP/Steel}{0.000 Steel}, R^2 = 0.003, \sigma = 4.29$$

Power model for system

$$m_{SYSTEM} = 23.63 \left[\frac{0.848 CFRP/Steel}{1.000 Steel} \right], R^2 = 0.003, r = 1.19$$

Figure 2.2.4-4 shows the mass data for seat structure and seat system mass for the 2011-2015 timeframe.

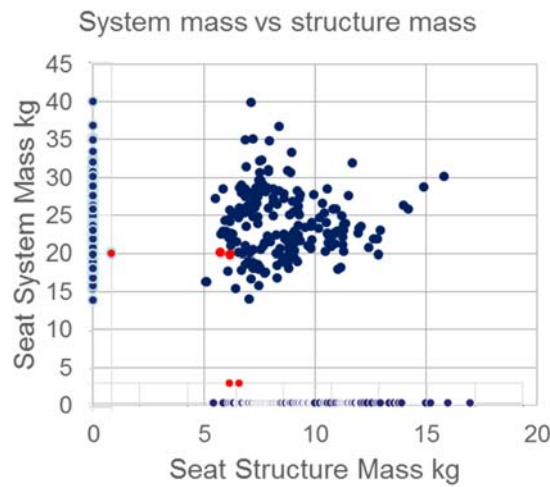


Figure 2.2.4-4 Seat structure and seat system mass

Comparison of studies

The equations for the three studies are presented below. Because of the very low goodness of fit, no graphical comparisons were attempted.

Current study

$$m_{STRUCT} = 8.345 \left[\frac{0.710 CRFP/Steel}{1.000 Steel} \right], R^2 = 0.18, r = 1.25$$

2014 study Only linear model was fit.

$$m_{STRUCT} = 5.368 + 0.175(SeatTotalMass) - \left[\begin{array}{l} 1.639 \text{ if Motorised} \\ 0.000 \text{ if Manual Adjust} \end{array} \right], R^2 = 0.135, r = 1.84$$

2010 study Used only the average

$$m_{STRUCT} = 9.155 kg$$

All seat frames were ranked by the difference between actual mass and expected mass. This is shown graphically in the parity plot of Figure 2.2.4-5 where increasing mass efficiency is the downward distance from the 45° line where actual mass equals expected mass.

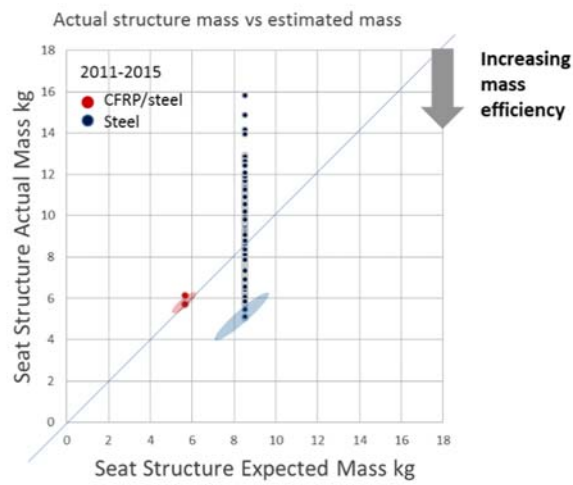


*Figure 2.2.4-5 Seat frame
Parity plot to evaluate mass efficiency*

2.2.5 Body structure with front sub-frame

The body structure consists of the body-in-white with front sub-frame less doors and including paint, sealer and mastic sound treatments. Vehicles with full frames have been excluded. (An analysis without the sub-frame was also performed. This is found in Appendix B.)



The first look at body structure mass data is shown in Figure 2.2.5-1. The basic statistics for each material class appear to be stable.

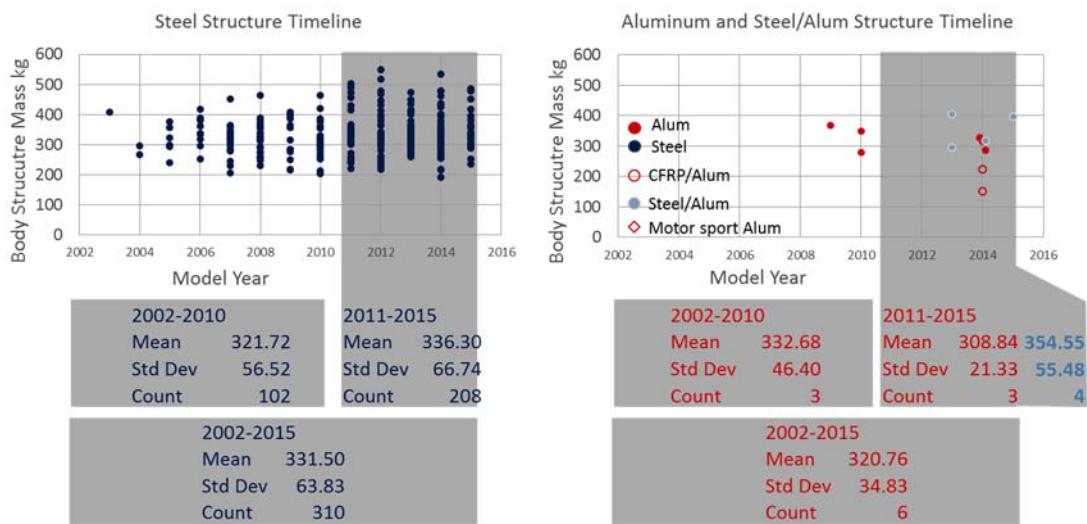


Figure 2.2.5-1 Body structure
Comparison of unadjusted mass statistics

Figure 2.2.5-2 shows scatter plots of mass vs. the mass drivers plan view **Area** and gross vehicle mass, **GVM**, with data from the current study overlaid with data from the EDAG 2014 study. The data points for this study are in larger markers. The overall trend appears to be the similar.

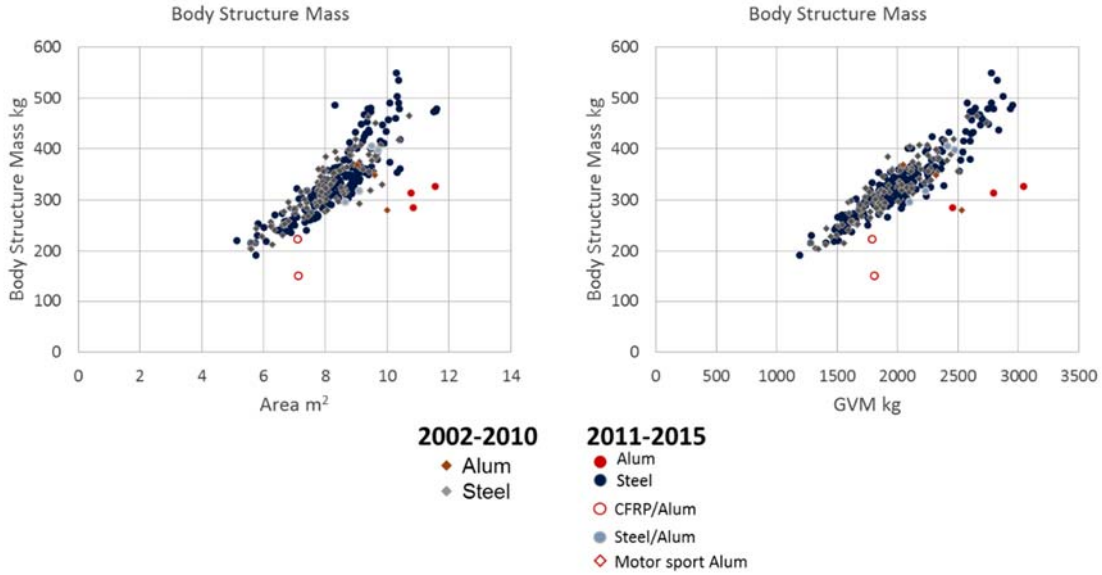


Figure 2.2.5-2 Body structure
Comparison of mass for two studies

To fit the regression models, the mass drivers from previous studies were used, Figure 2.2.5-3.

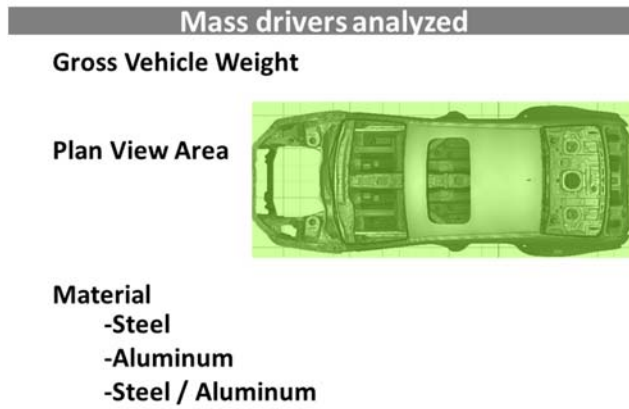


Figure 2.2.5-3 Body structure
Mass drivers considered

Models were then fit. These are shown below.
Linear model for structure

$$m_{STRUCT} = -64.78 + 0.131GVW + 16.036AREA + \begin{bmatrix} -166.70 \text{ Alum} \\ -31.21 \text{ St.Al} \\ 0 \text{ Steel} \end{bmatrix}, R^2 = 0.88, \sigma = 21.80$$

Power model for structure

$$m_{STRUCT} = 0.448(GVW)^{0.753} (AREA)^{0.416} \begin{bmatrix} 0.652 \text{ Alum} \\ 0.917 \text{ St.Al} \\ 1.000 \text{ Steel} \end{bmatrix}, R^2 = 0.89, r = 1.0637$$

Figure 2.2.5-4 shows the mass data with the power equation lines superimposed; Dotted for nominal, solid for mass efficient designs.

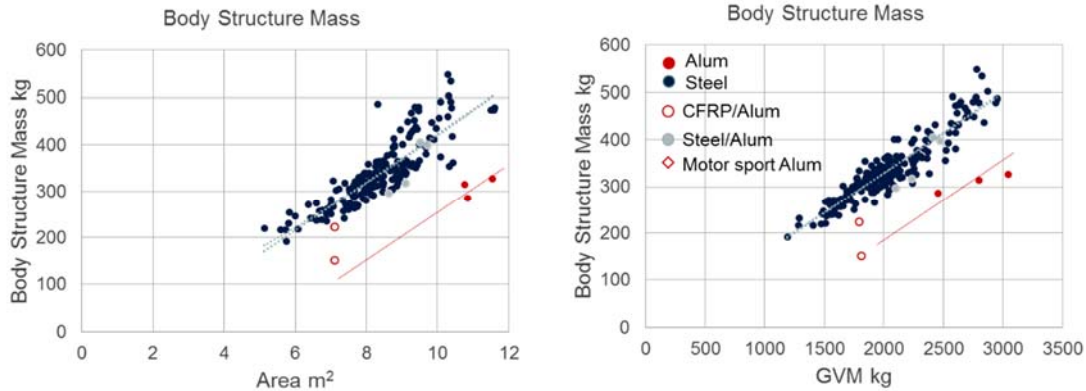


Figure 2.2.5-4 Body structure
Structure mass with power model for mass efficient body structures

Comparison of studies

A comparison of the power model equations for the three studies is presented below. The most meaningful comparison is between the current and 2014 study due to the larger number of samples. For these studies, the goodness of fit is similar. The form of the equation for the 2014 study used aluminum as the reference material while this study used steel. The prior equations were algebraically adjusted for direct comparison.

Current study

$$m_{STRUCT} = 0.448(GVW)^{0.753}(AREA)^{0.416} \begin{bmatrix} 0.652 \text{ Alum} \\ 0.917 \text{ St.Al} \\ 1.000 \text{ Steel} \end{bmatrix}, R^2 = 0.89, r=1.063$$

2014 study Equation algebraically modified for direct comparison

$$m_{STRUCT} = 1.59(GVW)^{0.546}(AREA)^{0.579} \begin{bmatrix} 0.656 \text{ Alum} \\ 0.947 \text{ St.Al} \\ 1.000 \text{ Steel} \end{bmatrix}, R^2=0.87, r=1.085$$

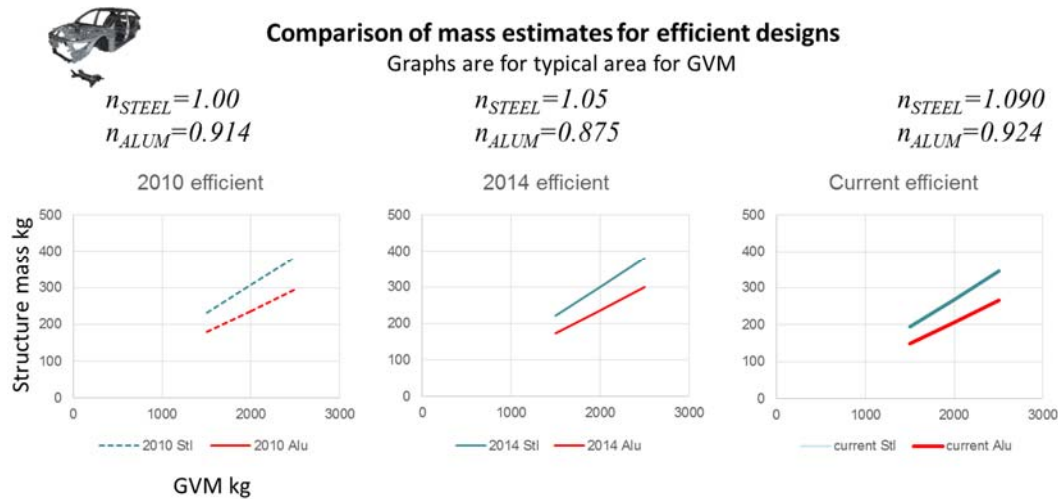
Equation as it originally appeared

$$m_{STRUCT} = 1.0437(GVW)^{0.546}(AREA)^{0.579} \begin{bmatrix} 1.000 \text{ Alum} \\ 1.443 \text{ St.Al} \\ 1.524 \text{ Steel} \end{bmatrix}$$

2010 study Equation algebraically modified for direct comparison

$$m_{STRUCT} = 3.418(GVM)^{0.438}(AREA)^{0.599} \begin{bmatrix} 0.704 \text{ if Alum} \\ 1.000 \text{ if Steel} \end{bmatrix} \begin{bmatrix} 1.02 \text{ if FWD} \\ 1.00 \text{ if RWD} \\ 1.08 \text{ if AWD} \end{bmatrix}, R^2=0.83, r=1.094$$

Because the equations have different constant coefficients and mass driver exponents, it is difficult to compare them visually. Figure 2.2.5-5 graphs the above equations for efficient designs to allow a direct comparison. The graphs overlay very closely indicating consistent results.



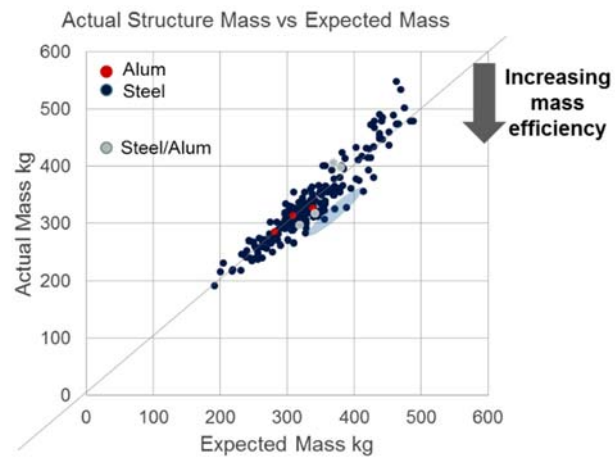
*Figure 2.2.5-5 Body structure
 Comparison of power model for three studies*

Table 2.2.5-1 compares the material mass ratio for the three studies for both nominal and efficient designs. As noted in previous studies Steel performance is better when efficient designs are compared and the ratio is slightly greater in this study of 2011-2015 body structures compared with the prior study.

*Table 2.2.5-1 Body structure
 Comparison of material mass ratio for three studies*

	$\frac{m_{ALUM}}{m_{STEEL}}$	
	Nominal designs	Efficient designs
Current	0.652	0.769
2014 study	0.656	0.783
2010 study	0.704	0.770

All body structures were ranked by the difference between actual mass and expected mass. This is shown graphically in the parity plot of Figure 2.2.5-6 where increasing mass efficiency is the downward distance from the 45° line where actual mass equals expected mass.



*Figure 2.2.5-6 Body structure
Parity plot to evaluate mass efficiency*

2.3 Chassis

The chassis systems analyzed were lower control arms for both McPherson and SLA type suspensions, wheels, front suspension, and rear suspension.

2.3.1 Lower Control Arm

The lower control arm is found on both McPherson strut and Short and Long Arm—SLA—suspensions. The lower control arm includes arm assembly with bushings and ball joints. In some designs, there are multiple parts forming the arm



single part



multiple parts

The first look at lower control arm mass data is shown in Figure 2.3.1-1. The basic statistics for each material class appear to be stable.

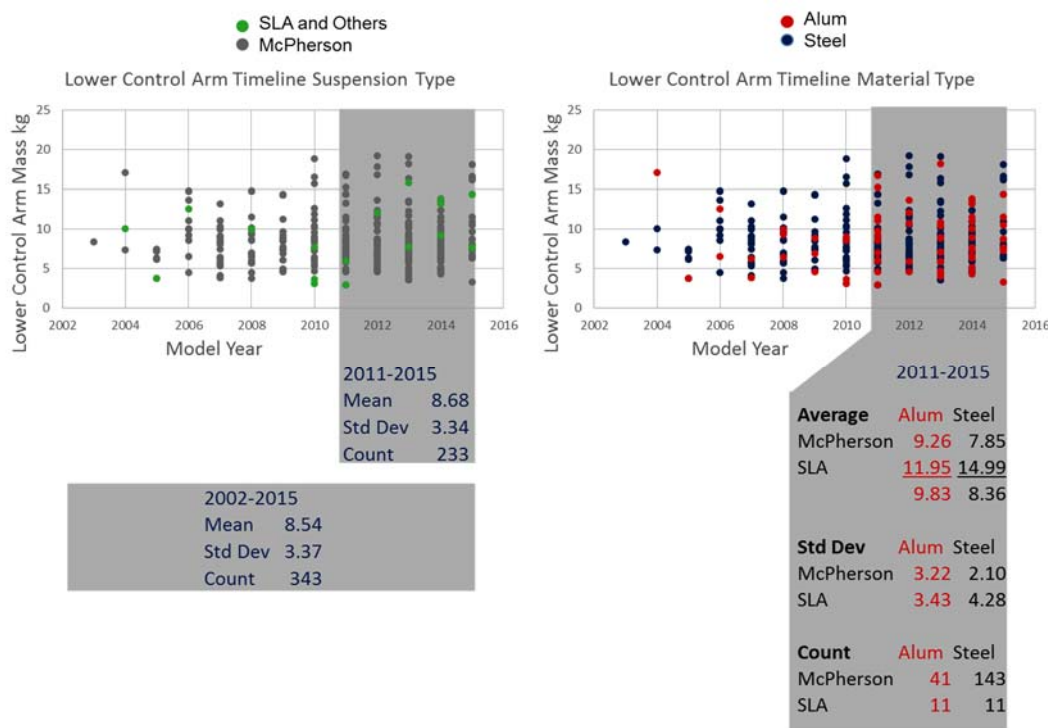


Figure 2.3.1-1 Lower control arm
Comparison of unadjusted mass statistics

Figure 2.3.1-2 is a scatter plot of mass vs. the mass driver **FGAM**, front gross axle mass, with data from the current study overlaid with data from the EDAG 2014 study. The data points for this study are in larger markers. The data clouds are similar.

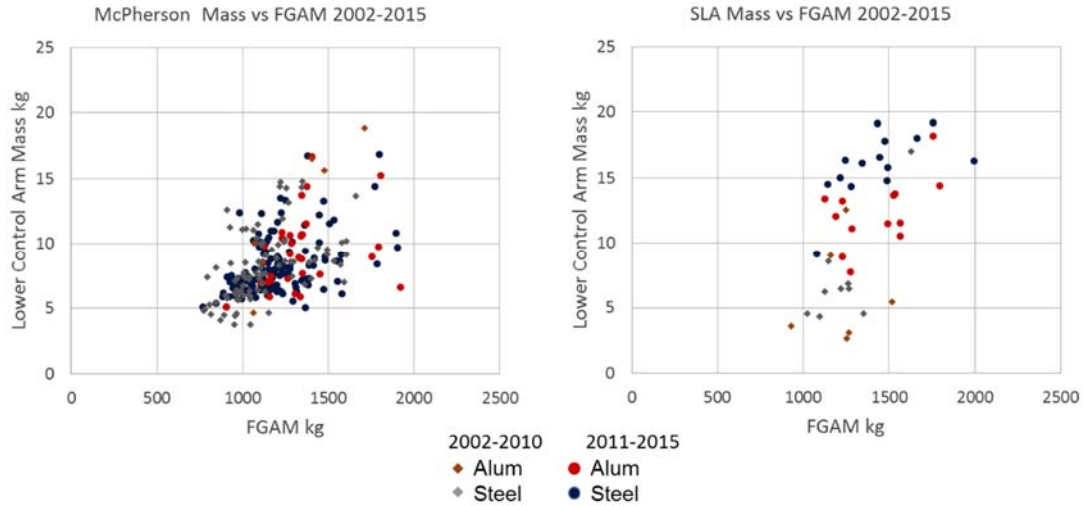


Figure 2.3.1-2 Lower control arm
Comparison of mass for two studies

To fit the regression models, the mass drivers from previous studies were used, Figure 2.3.1-3.

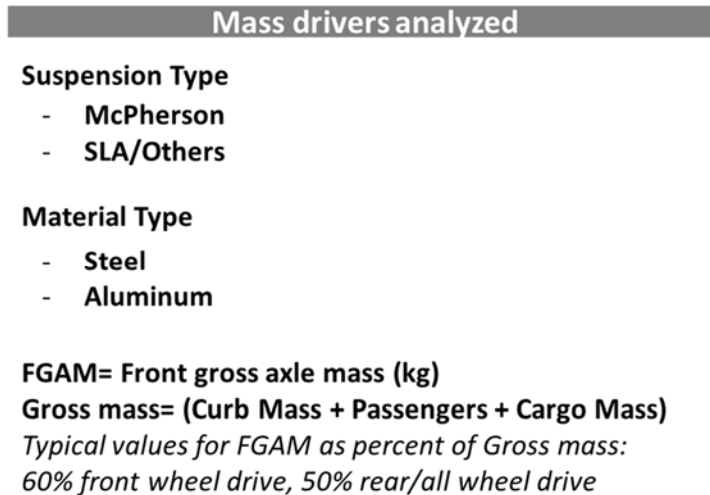


Figure 2.3.1-3 Lower control arm
Mass drivers considered

Models were then fit. These are shown below

Linear model for lower control arm using data for both suspension types

$$m_{SYSTEM} = 1.613 + 0.0055(FGAM) - \begin{bmatrix} 0.0620 \text{ Alum} \\ 0.000 \text{ Steel} \end{bmatrix} + \begin{bmatrix} 0.00 \text{ McPherson} \\ 4.32 \text{ SLA/Others} \end{bmatrix}, R^2 = 0.487, \sigma = 2.22$$

Power model for lower control arm using data for both suspension types

$$m_{SYSTEM} = 0.0398(FGAM)^{0.747} \begin{bmatrix} 1.014 \text{ Alum} \\ 1.000 \text{ Steel} \end{bmatrix} \begin{bmatrix} 1.000 \text{ McPherson} \\ 1.464 \text{ SLA/Others} \end{bmatrix}, R^2 = 0.47, r = 1.25$$

To see if the goodness of fit could be improved by separating the data by suspension type, two additional power models were fit: one using only data for the McPherson strut type, and one for only the SLA type.

McPherson strut type suspension

$$m_{SYSTEM} = 0.0522(FGAM)^{0.7078} \begin{bmatrix} 1.070 \text{ Alum} \\ 1.000 \text{ Steel} \end{bmatrix}, R^2 = 0.246, r=1.24$$

SLA type suspension

$$m_{SYSTEM} = 0.1044(FGAM)^{0.691} \begin{bmatrix} 0.766 \text{ Alum} \\ 1.000 \text{ Steel} \end{bmatrix}, R^2 = 0.475, r=1.19$$

Because the R^2 value did not improve, the combined model was used in the flowing analysis.

Figure 2.3.1-4 and 2.3.1-5 shows the mass data with the power equation lines superimposed; Dotted for nominal, solid for mass efficient designs.

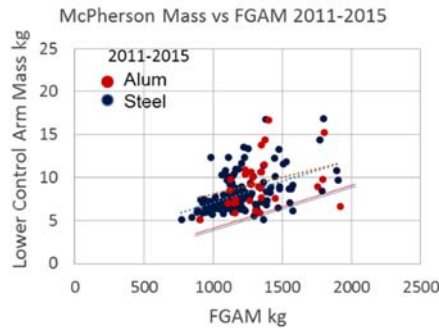


*Figure 2.3.1-4 Lower control arm
Mass with power model for mass efficient McPherson strut lower control arms*

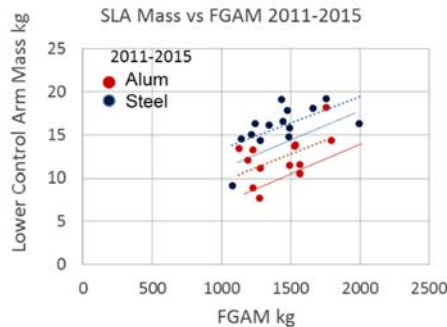


*Figure 2.3.1-5 Lower control arm
Mass with power model for mass efficient SLA lower control arms*

Comparison of studies

A comparison of the power model equations for the three studies is presented below. The most meaningful comparison is between the current and 2014 study due to the larger number of samples. For these studies, the goodness of fit is similar. The form of the equation for the 2014

study used aluminum as the reference material while this study used steel. The prior equations were algebraically adjusted for direct comparison.

Current study

$$m_{SYSTEM} = 0.0398(FGAM)^{0.747} \left[\frac{1.014 \text{ Alum}}{1.000 \text{ Steel}} \right] \left[\frac{1.000 \text{ McPherson}}{1.464 \text{ SLA/Others}} \right], R^2 = 0.47, r=1.25$$

2014 study Equation algebraically modified for direct comparison

$$m_{SYSTEM} = 0.0142(FGAM)^{0.919} \left[\frac{0.709 \text{ Alum}}{1.000 \text{ Steel}} \right] \left[\frac{1.175 \text{ Cast/Forged}}{1.000 \text{ Stamped}} \right] \left[\frac{1.00 \text{ McPhe}}{1.30 \text{ Others}} \right], R^2=0.494, r=1.325$$

Equation as it originally appeared

$$m_{SYSTEM} = 0.01313(FGAM)^{0.919} \left[\frac{1.000 \text{ Alum}}{1.411 \text{ Steel}} \right] \left[\frac{1.175 \text{ Cast/Forged}}{1.000 \text{ Stamped}} \right] \left[\frac{0.769 \text{ McPhe}}{1.000 \text{ Others}} \right]$$

2010 study

The 2010 study fit an equation for McPherson strut and for SLA independently.

Equations algebraically modified for direct comparison

McPherson

$$m_{SYSTEM} = 0.0102(FGAM)^{0.899} \left[\frac{1.427 \text{ Steel}}{1.000 \text{ Alum}} \right] \left[\frac{1.390 \text{ Cast/Forged}}{1.202 \text{ StampedClosed}} \right] \left[\frac{1.000 \text{ Stamped Open}}{1.000 \text{ Stamped Open}} \right], R^2=0.36, r=1.26$$

SLA

$$m_{SYSTEM} = 0.00283(FGAM)^{1.039} (LinkageRatio)^{2.766} \left[\frac{1.49 \text{ Alum}}{1.000 \text{ Steel}} \right], R^2=0.80, r=1.12$$

Because the equations have different constant coefficients and mass driver exponents, it is difficult to compare them visually. Figure 2.3.1-6 and 2.3.1-7 graph the above equations for efficient designs to allow a direct comparison. The graphs overlay very closely indicating consistent results.

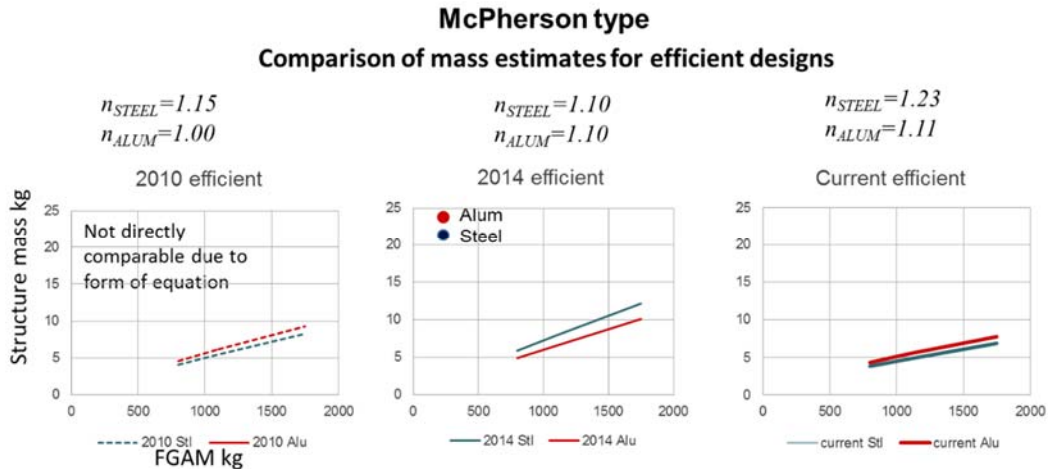


Figure 2.3.1-6 Lower control arm
Comparison of power model for three studies, McPherson strut lower control arms

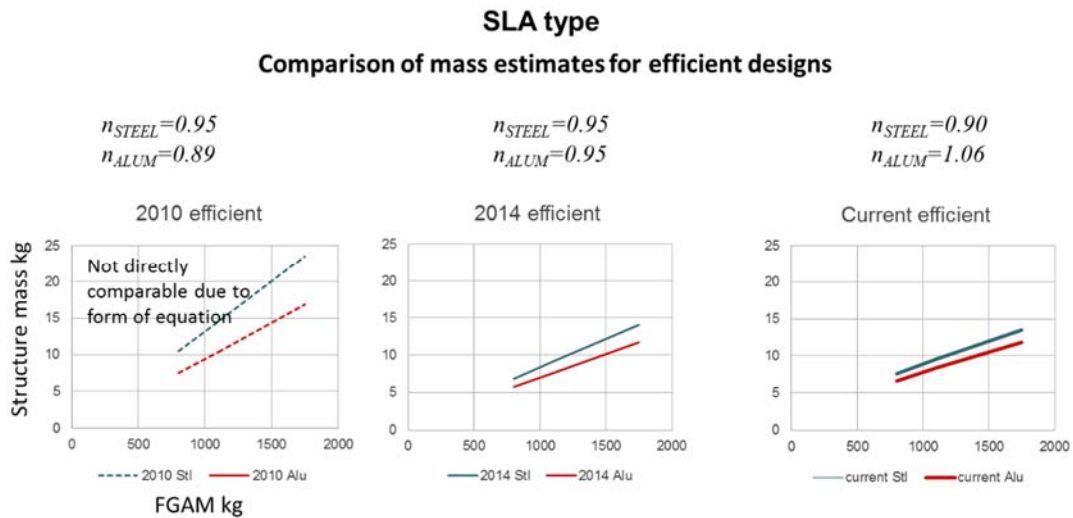


Figure 2.3.1-7 Lower control arm
Comparison of power model for three studies, SLA lower control arms

Table 2.3.1-1 compares the material mass ratio for the three studies for both nominal and efficient designs. As noted in previous studies Steel performance is better when efficient designs are compared and the ratio is slightly greater in this study of 2011-2015 lower control arms compared with the prior study.

Table 2.3.1-1 Lower control arm
Comparison of material mass ratio for three studies

	McPherson type		SLA type	
	$\frac{m_{ALUM}}{m_{STEEL}}$		$\frac{m_{ALUM}}{m_{STEEL}}$	
	Nominal designs	Efficient designs	Nominal designs	Efficient designs
Current	1.014	1.124	1.014	0.861
2014 study	0.833	0.833	0.833	0.833
2010 study	0.974	1.120	0.670	0.715

All Lower control arms were ranked by the difference between actual mass and expected mass. This is shown graphically in the parity plot of Figure 2.3.1-8 where increasing mass efficiency is the downward distance from the 45° line where actual mass equals expected mass.

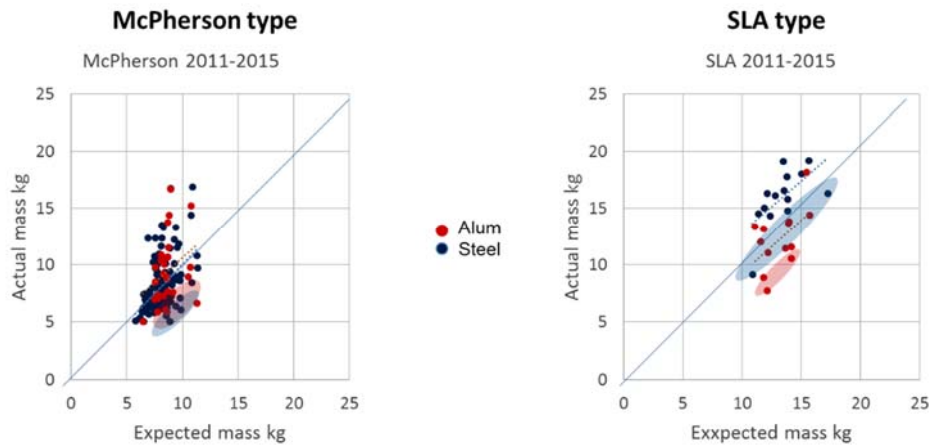


Figure 2.3.1-8 Lower control arm
Parity plot to evaluate mass efficiency

2.3.2 Wheels

The wheel system includes the rim, wheel cover, and hub cap.



The first look at wheel mass data is shown in Figure 2.3.2-1. The basic statistics for each material class appear to be stable.

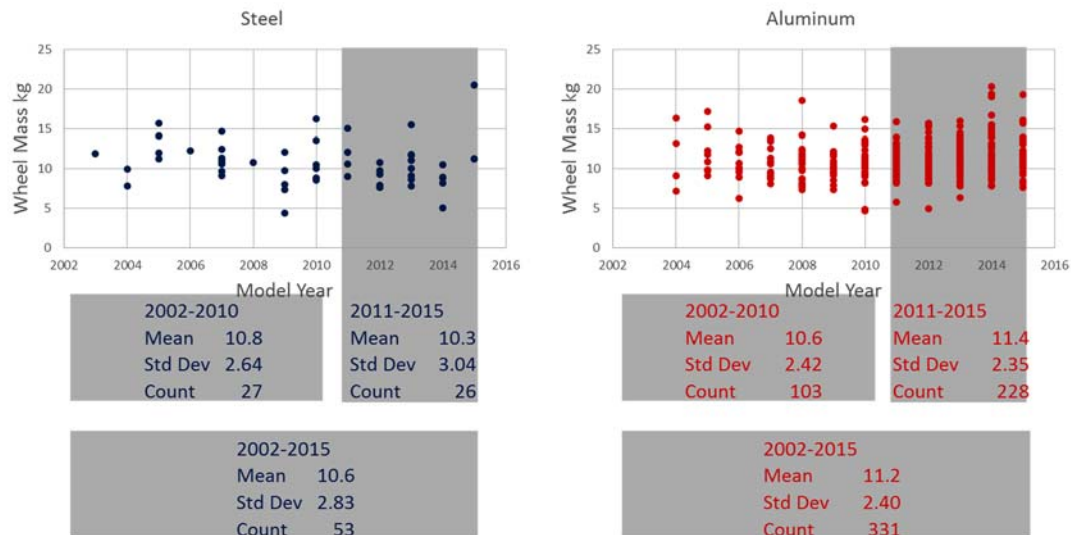
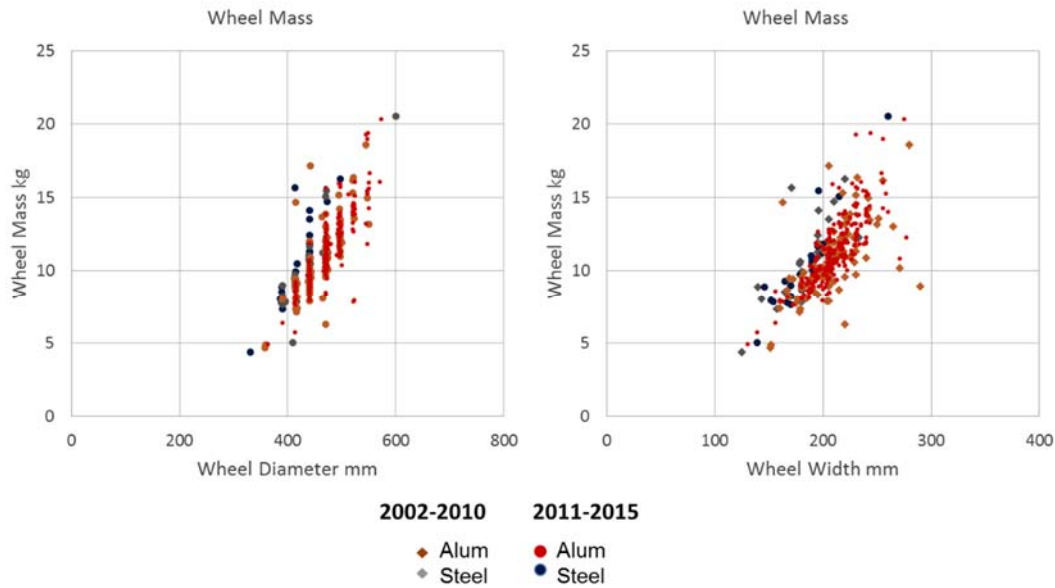


Figure 2.3.2-1 Wheel
Comparison of unadjusted mass statistics

Figure 2.3.2-2 is a scatter plot of mass vs. the mass drivers *wheel Diameter* and *Width* with data from the current study overlaid with data from the EDAG 2014 study. The data points for this study are in larger markers. The overall trend appears to be the similar.



*Figure 2.3.2-2 Wheel
Comparison of mass for two studies*

To fit the regression models, the mass drivers from previous studies were used, Figure 2.3.2-3. Note that this study does not address the level of aesthetic performance for the wheels, and only compares mass based on objective attributes.

Mass drivers analyzed

Wheel Diameter

Wheel Width

Material

-Steel

-Aluminum

*Figure 2.3.2-3 Wheel
Mass drivers considered*

Models were then fit. These are shown below

Linear model for system

$$m_{SYSTEM} = -13.178 + 0.037Diameter + 0.039Width - \begin{matrix} 1.493 \text{ Alum} \\ 0.000 \text{ Steel} \end{matrix}, R^2 = 0.771, \sigma = 1.137$$

Power model for system

$$m_{SYSTEM} = 0.0000264(Diameter)^{1.359}(Width)^{0.883} \begin{bmatrix} 0.872 \text{ Alum} \\ 1.000 \text{ Steel} \end{bmatrix}, R^2 = 0.800, r = 1.098$$

Figure 2.3.2-4 shows the mass data for the 2011-2015 timeframe.

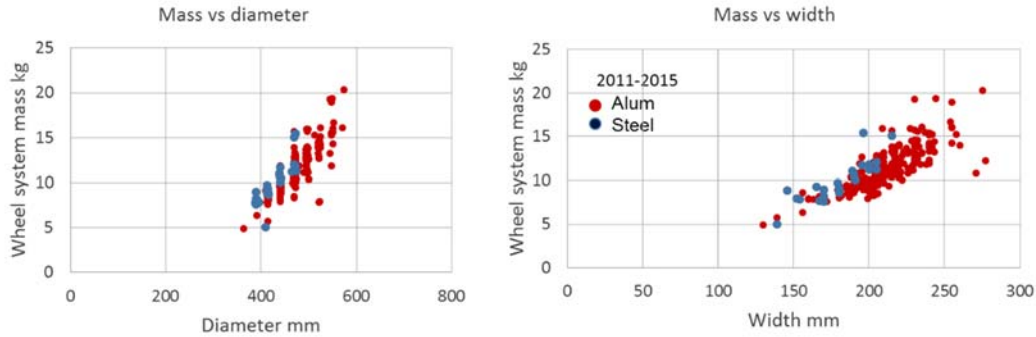


Figure 2.3.2-4 Wheel System mass for wheels

Comparison of studies

A comparison of the power model equations for the three studies is presented below. The most meaningful comparison is between the current and 2014 study due to the larger number of samples. For these studies, the goodness of fit is similar. The form of the equation for the 2014 study used aluminum as the reference material while this study used steel. The prior equations were algebraically adjusted for direct comparison.

Current study

$$m_{SYSTEM} = 2.64 \times 10^{-5} (DIAMETER)^{1.359} (WIDTH)^{0.883} \begin{bmatrix} 0.872 \text{ if Alum} \\ 1.000 \text{ if Steel} \end{bmatrix}, R^2 = 0.800, r = 1.098$$

2014 study

Equation algebraically modified for direct comparison

$$m_{SYSTEM} = 5.13 \times 10^{-5} (DIAMETER)^{1.466} (WIDTH)^{0.628} \begin{bmatrix} 0.896 \text{ if Alum} \\ 1.000 \text{ if Steel} \end{bmatrix}, R^2 = 0.56, r = 1.158$$

Equation as it originally appeared

$$m_{struct} = 0.000046 (DIAMETER)^{1.466} (WIDTH)^{0.628} \begin{bmatrix} 1.115 \text{ if Steel} \\ 1.000 \text{ if Alum} \end{bmatrix}$$

2010 study

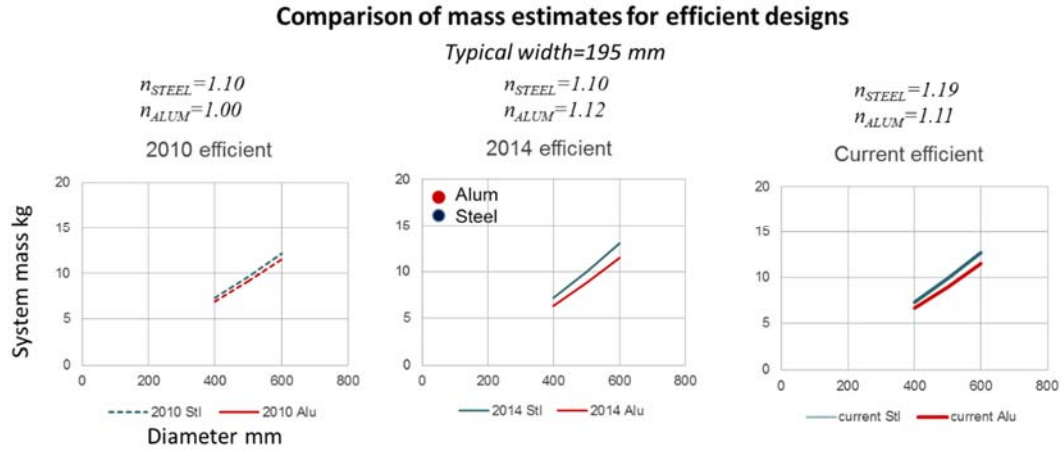
Equation algebraically modified for direct comparison

$$m_{SYSTEM} = 17.17 \times 10^{-5} (DIAMETER)^{1.266} (WIDTH)^{0.633} \begin{bmatrix} 0.862 \text{ if Alum} \\ 1.000 \text{ if Steel} \end{bmatrix}, R^2 = 0.38, r = 1.19$$

Equation as it originally appeared

$$m_{struct} = 0.000148 (DIAMETER)^{1.266} (WIDTH)^{0.633} \begin{bmatrix} 1.160 \text{ if Steel} \\ 1.000 \text{ if Alum} \end{bmatrix}$$

Because the equations have different constant coefficients and mass driver exponents, it is difficult to compare them visually. Figure 2.3.2-5 graphs the above equations for efficient designs to allow a direct comparison. The graphs overlay very closely indicating consistent results.



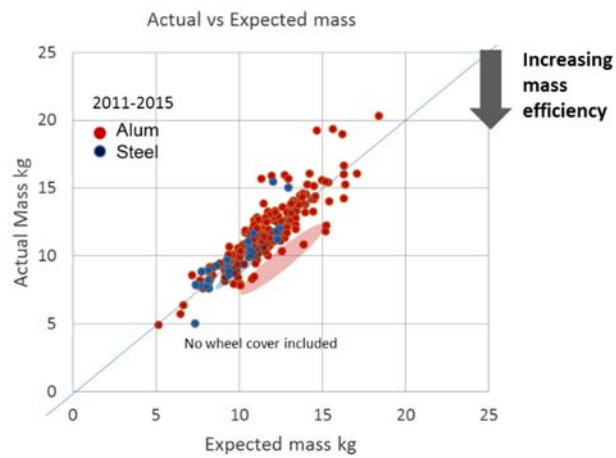
*Figure 2.3.2-5 Wheel
Comparison of power model for three studies*

Table 2.3.2-1 compares the material mass ratio for the three studies for both nominal and efficient designs. As noted in previous studies Steel performance is better when efficient designs are compared and the ratio is slightly greater in this study of 2011-2015 wheels compared with the prior study.

*Table 2.3.2-1 Wheel
Comparison of material mass ratio for three studies*

	$\frac{m_{ALUM}}{m_{STEEL}}$	
	Nominal designs	Efficient designs
Current	0.872	0.935
2014 study	0.896	0.880
2010 study	0.862	0.948

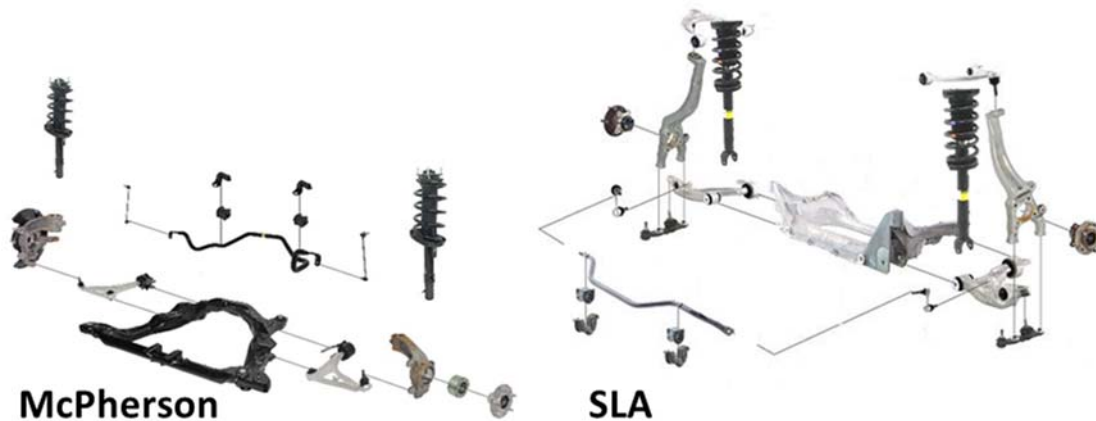
All wheels were ranked by the difference between actual mass and expected mass. This is shown graphically in the parity plot of Figure 2.3.2-6 where increasing mass efficiency is the downward distance from the 45° line where actual mass equals expected mass.



*Figure 2.3.2-6 Wheel
Parity plot to evaluate mass efficiency*

2.3.3 Front Suspension

The front suspension includes engine cradle, stabilizer bar, all control arms, spring / damper strut, steering knuckle and all mounting hardware.



The raw front suspension system mass data is shown in Figure 2.3.3-1.

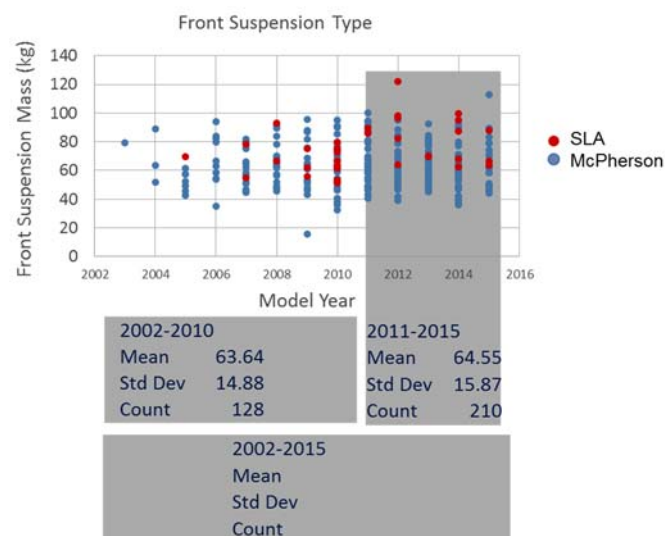
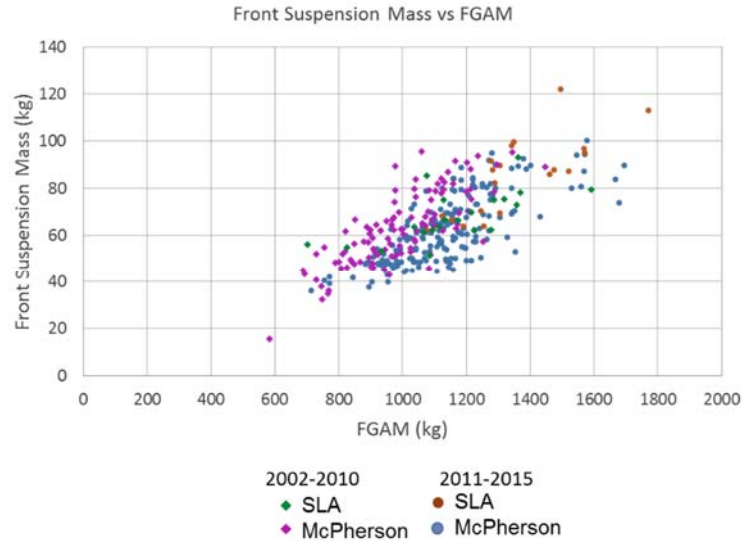


Figure 2.3.3-1 Front suspension
Comparison of unadjusted mass statistics

Figure 2.3.3-2 is a scatter plot of mass vs. the mass driver *Front gross axle mass, FGAM*, with data from the current study overlaid with data from the EDAG 2014 study. The data points for this study are in larger markers. The overall trend appears to be the similar.



*Figure 2.3.3-2 Front suspension
Comparison of mass for two studies*

To fit the regression models, the mass drivers from previous studies were used, Figure 2.3.3-3. As the suspension is an assembly parts of different materials, material is not a mass driver.

Mass drivers analyzed
Suspension Type <ul style="list-style-type: none"> - McPherson - SLA/Others
Drivetrain Type <ul style="list-style-type: none"> - Front Wheel Drive - Others
FGAM= % total mass on front axle Total mass=(Curb Mass + Passengers + Cargo) <i>Typical values: 60% front wheel drive, 50% rear/all wheel drive</i>

*Figure 2.3.3-3 Front suspension
Mass drivers considered*

Models were then fit. These are shown below

Linear model for system

$$m_{SYSTEM} = -12.963 + 0.0652(FGAM) + \begin{bmatrix} 0.000 \text{ McPherson} \\ 3.698 \text{ SLA} \end{bmatrix} + \begin{bmatrix} 0.000 \text{ FWD} \\ 7.151 \text{ Others} \end{bmatrix}, R^2 = 0.663, \sigma = 9.27$$

Power model for system

$$m_{SYSTEM} = 0.0164(FGAM)^{1.187} \begin{bmatrix} 0.964 \text{ McPherson} \\ 1.000 \text{ SLA} \end{bmatrix} \begin{bmatrix} 0.902 \text{ FWD} \\ 1.000 \text{ Other} \end{bmatrix}, R^2 = 0.661, r = 1.149$$

Figure 2.3.3-4 shows the 2011-2015 mass data.

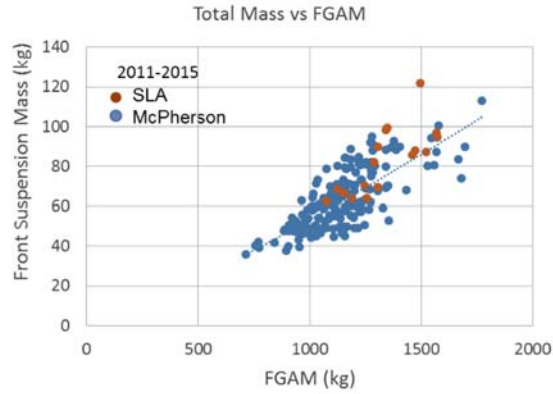


Figure 2.3.3-4 Front suspension
System mass

Comparison of studies

A comparison of the power model equations for the three studies is presented below. The most meaningful comparison is between the current and 2014 study due to the larger number of samples. For these studies, the goodness of fit is similar.

Current study

$$m_{SYSTEM} = 0.0164(FGAM)^{1.187} \left[\begin{array}{c} 0.964 \text{ McPherson} \\ 1.000 \text{ SLA} \end{array} \right] \left[\begin{array}{c} 0.902 \text{ FWD} \\ 1.000 \text{ Other} \end{array} \right], R^2 = 0.661, r=1.149$$

2014 study

$$m_{SYSTEM} = 0.0018(FGAM)^{1.475} \left[\begin{array}{c} 0.924 \text{ McPherson} \\ 1.000 \text{ SLA} \end{array} \right] \left[\begin{array}{c} 1.120 \text{ FWD} \\ 1.000 \text{ Other} \end{array} \right], R^2 = 0.74, r=1.183$$

2010 study Note: Definition of system is not comparable for this study

$$m_{SYSTEM} = 1.45(FGAM)^{0.5392} \left[\begin{array}{c} 0.733 \text{ McPhe} \\ 1.000 \text{ SLA} \end{array} \right] \left[\begin{array}{c} 0.881 \text{ FWD} \\ 1.000 \text{ Other} \end{array} \right], R^2 = 0.66$$

Because the equations have different constant coefficients and mass driver exponents, it is difficult to compare them visually. Figure 2.3.3-5 graphs the above equations for efficient designs to allow a direct comparison. The graphs for the current and 2014 studies overlay very closely indicating consistent results.

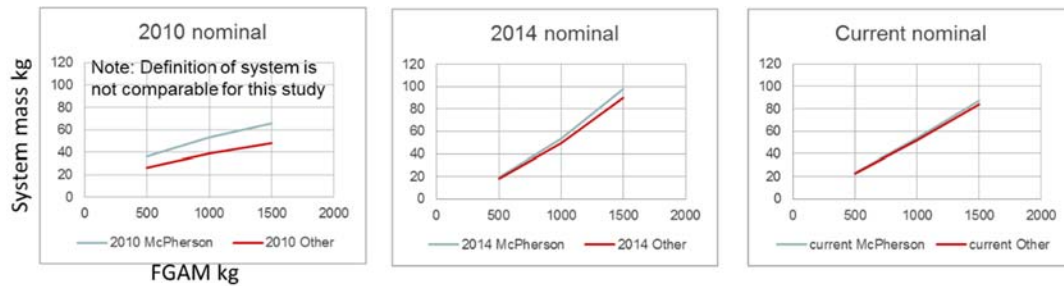


*Figure 2.3.3-5 Front suspension
Comparison of power model for three studies*

All front suspensions were ranked by the difference between actual mass and expected mass. This is shown graphically in the parity plot of Figure 2.3.3-6 where increasing mass efficiency is the downward distance from the 45° line where actual mass equals expected mass.

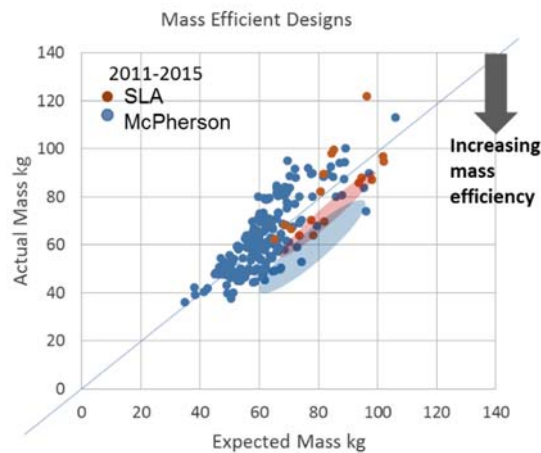
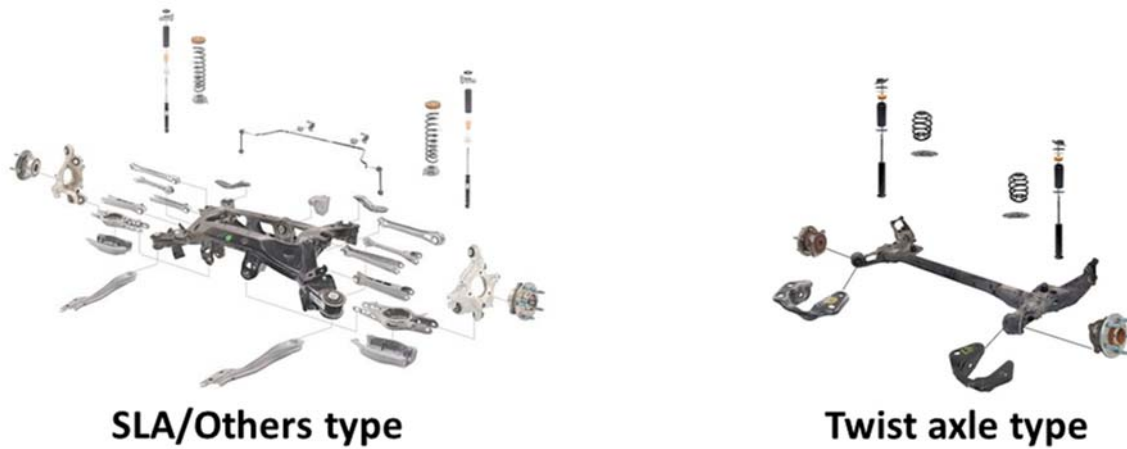


*Figure 2.3.3-6 Front suspension
Parity plot to evaluate mass efficiency*

For SLA front suspensions the mass varied considerably between body-frame integral construction in which there is generally a front sub-frame included in the front suspension mass, and for full frame vehicles where the frame mass is not included as part of the suspension.

2.3.4 Rear Suspension

The rear suspension includes the sub frame, twist axle beam if present, roll bar, all control arms, springs, shock absorber, knuckle and all mounting hardware.



The raw rear suspension system mass data is shown in Figure 2.3.4-1. .

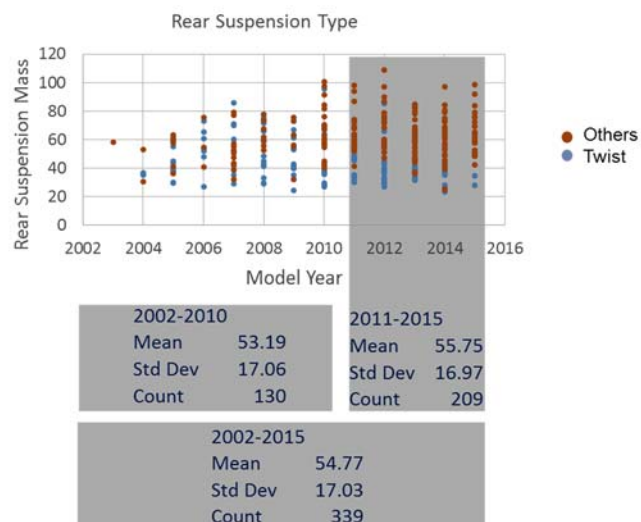


*Figure 2.3.4-1 Rear suspension
Comparison of unadjusted mass statistics*

Figure 2.3.4-2 is a scatter plot of mass vs. the mass driver *Rear gross axle mass, **RGAM***, with data from the current study overlaid with data from the EDAG 2014 study. The data points for this study are in larger markers. The overall trend appears to be the similar.

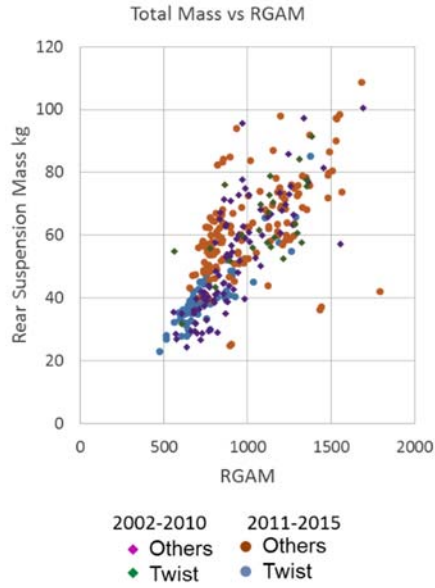


Figure 2.3.4-2 Rear suspension
Comparison of mass for two studies

To fit the regression models, the mass drivers from previous studies were used, Figure 2.3.4-3. As the suspension is an assembly parts of different materials, material is not a mass driver.

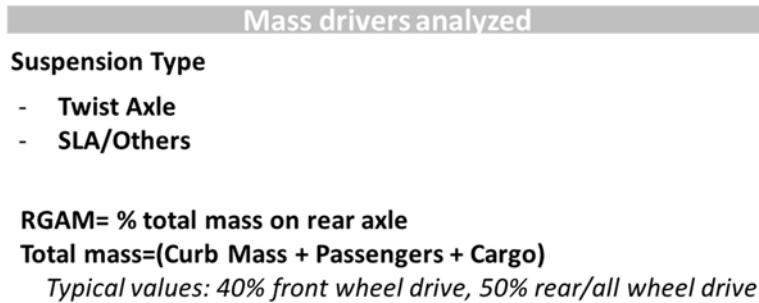


Figure 2.3.4-3 Rear suspension
Mass drivers considered

Models were then fit. These are shown below

Linear model for system

$$m_{SYSTEM} = 15.195 + 0.0332RGAM + \begin{bmatrix} 14.043 \text{ Other} \\ 0.000 \text{ Twist Axle} \end{bmatrix}, R^2 = 0.607, \sigma = 10.65$$

Power model for system

$$m_{SYSTEM} = 1.058(RGAM)^{0.589} \begin{bmatrix} 0.759 \text{ Twist Axle} \\ 1.000 \text{ Other} \end{bmatrix}, R^2 = 0.642, r = 1.208$$

Figure 2.3.4-4 shows the 2011-2015 mass data.

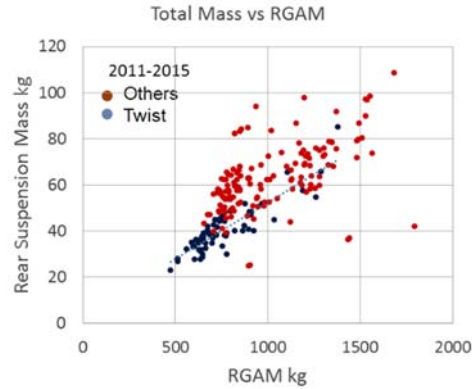


Figure 2.3.4-4 Rear suspension
System mass

Comparison of studies

A comparison of the power model equations for the three studies is presented below. The most meaningful comparison is between the current and 2014 study due to the larger number of samples. For these studies, the goodness of fit is similar.

Current study

$$m_{SYSTEM} = 1.058(RGAM)^{0.589} \left[\begin{matrix} 0.759 \text{ Twist Axle} \\ 1.000 \text{ Other} \end{matrix} \right], R^2 = 0.642, r=1.208$$

2014 study

$$m_{SYSTEM} = 0.02644(RGAM)^{1.128} \left[\begin{matrix} 0.797 \text{ Twist} \\ 1.000 \text{ Others} \end{matrix} \right], R^2=0.79, r=1.175$$

2010 study

$$m_{SYSTEM} = 0.0714(RGAM)^{0.900} \left[\begin{matrix} 1.160 \text{ FWD} \\ 1.000 \text{ Other} \end{matrix} \right], R^2=0.43$$

Because the equations have different constant coefficients and mass driver exponents, it is difficult to compare them visually. Figure 2.3.4-5 graphs the above equations for efficient designs to allow a direct comparison.

Comparison of mass estimates for nominal designs

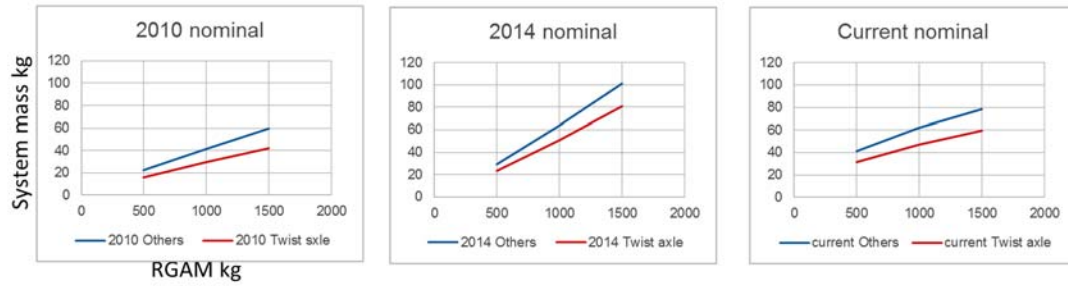


*Figure 2.3.4-5 Rear suspension
Comparison of power model for three studies*

All rear suspensions were ranked by the difference between actual mass and expected mass. This is shown graphically in the parity plot of Figure 2.3.4-6 where increasing mass efficiency is the downward distance from the 45° line where actual mass equals expected mass.

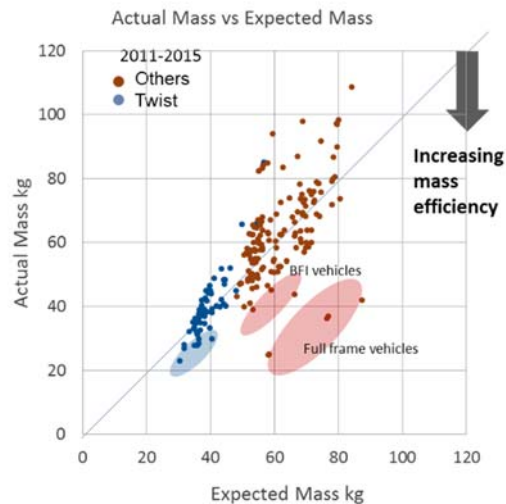


*Figure 2.3.4-6 Rear suspension
Parity plot to evaluate mass efficiency*

For rear suspensions other than twist axle, the mass varied considerably between body-frame integral construction in which there is generally a rear sub-frame included in the rear suspension mass, and for full frame vehicles where the frame mass is not included as part of the suspension.

3.0 Observations

A statistical view of a large population allows general observations not available when looking at a single design or at A-B comparisons. Following are three general observations enabled by this methodology.

1) When comparing steel components of the same size and mass drivers, there is a considerable range of mass. For example, consider steel doors with Area= 1.5 m^2 , Figure 3.0-1. There is a range of approximately 5 kg between the lightest and heaviest.

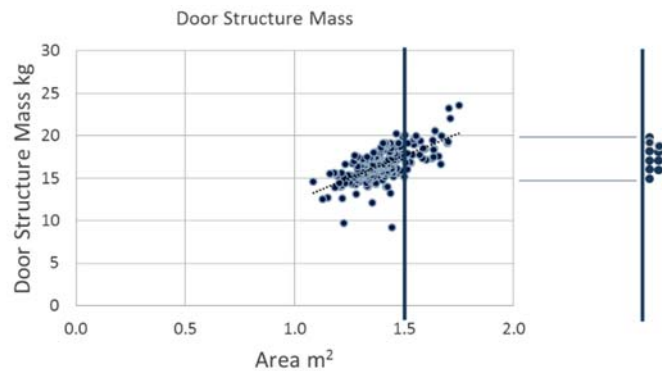


*Figure 3.0-1 Variability in mass for steel door structures of the same size
Example for steel front door structures*

There are several possible causes for this variability:

- Functional performance differences.
- Program differences in mass allocation targets during the design stage.
- Differences in applying efficient steel design practices – Opportunity.

This last cause indicates that an opportunity exists to more effectively use steel grades available today for lightweighting. Further, the statistical approach used in this paper has identified these mass efficient designs so that design details may be examined and learnings applied to future designs.

2) When compared to an efficient steel design, the mass savings gap with aluminum significantly reduces and in some cases reverses. Figure 3.0-2a shows the *average* mass for steel and aluminum as the blue and red regression lines respectively. The mass difference between average steel and average aluminum designs is shown by the bold arrow. Figure 3.0-2b shows the corresponding relationship for *mass efficient* designs—those at the lower boundary for each material type. The mass difference between efficient steel and efficient aluminum is typically less than for nominal designs.

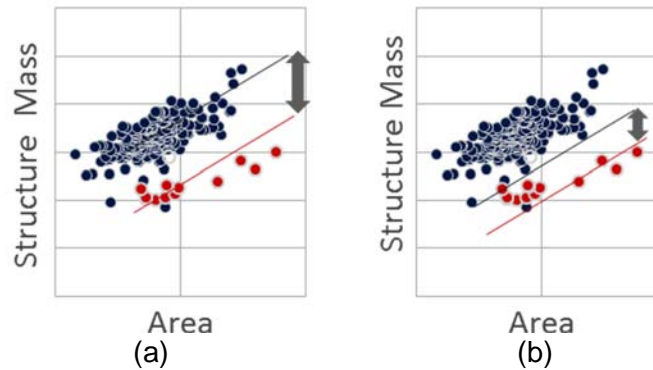


Figure 3.0-2 Mass comparison for (a) nominal designs, and for (b) mass-efficient designs
Example for steel and aluminum front door structures

Table 3.0-1 is a summary of the ratio of aluminum mass to steel mass for each subsystem analyzed for both nominal designs and efficient designs. It can be seen that the mass reduction performance of aluminum is reduced—larger ratio—when efficient designs are compared.

Table 3.0-1 Structure mass ratio, aluminum to steel

Subsystem	Nominal designs	Efficient designs
Front Door	0.670	0.750
Hood	0.582	0.640
Hatchback	0.939	0.988
Decklid	0.665	0.765
Liftgate	0.830	0.830
Front Bumper	0.658	0.808
Rear Bumper	0.676	0.794
Instrument panel beam	0.581	0.792
Front seat frame	insufficient data	
Body Structure <i>with</i> sub frame	0.652	0.769
Body Structure <i>without</i> sub frame	0.637	0.761
Lower Control Arm	1.014 McP 1.014 SLA	1.124 McP 0.861 SLA
Wheels	0.872	0.935
Front suspension	-	-
Rear suspension	-	-

3) For many closures, the full mass saving achieved at the structure level due to material substitution is often not realized at the system level. Figure 3.0-3 illustrates this concept for the side door where the horizontal arrow indicates the average structure mass reduction from steel—blue points to aluminum—red points. The vertical line indicates the mass reduction for the complete door system.

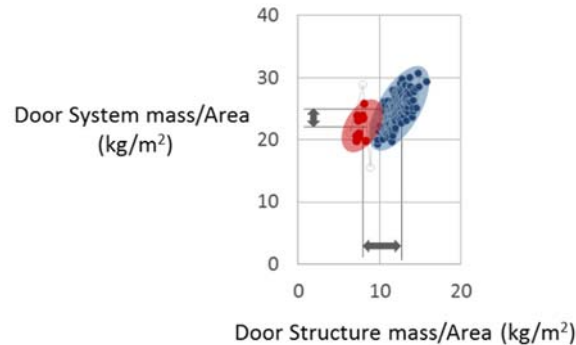


Figure 3.0-3 Normalized system mass vs. normalized structure mass
Example for steel and aluminum front door systems and structures

The figure below, *Figure 2.1-2 REPEATED*, quantifies this phenomenon based on the data of this study. For each closure type, the left bar is the difference between average *structure mass* between aluminum and steel (Struct). A negative value indicates aluminum structure is lighter. The right bar is the difference between the average total *system mass* (System).

For the front door and liftgate, while there is a mass reduction for aluminum *structure* the reduction does not fully carry over to reducing *system mass*. For hatchback doors, aluminum results in a heavier system, while for hood and decklid the mass reduction does carry over but not completely.

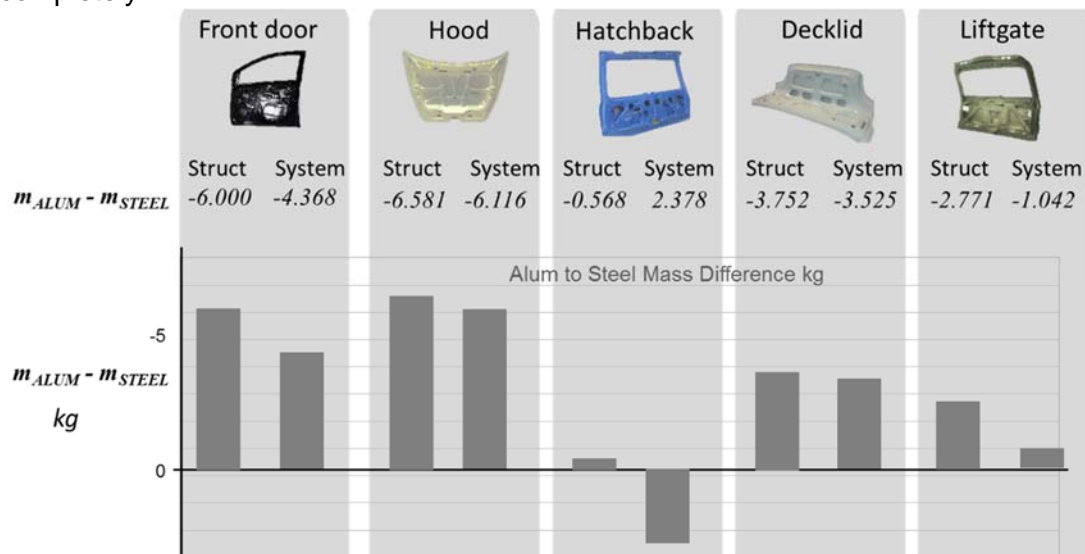


Figure 2.1-2 REPEATED
Closures summary

Mass difference between aluminum and mass for closure structure and for closure system

References

1. Malen, D., Automotive Mass Benchmarking, USAMP and Auto/Steel Partnership, May 15, 2010.
2. Singh, H., Automotive Mass Benchmarking, WorldAutoSteel, January 15, 2014.
3. --, A New Paradigm for Automotive Mass Benchmarking, WorldAutoSteel, October 2014.
4. A2Mac1.com, Automotive Benchmarking, 8393 Rawsonville Rd., Belleville, MI 48111.
5. Malen, D. and Hughes, J., "Mass Benchmarking Using Statistical Methods Applied to Automotive Closures," *SAE Int. J. Mater. Manf.* 8(3):2015, doi:10.4271/2015-01-0574.
6. Malen, D., & Nagaraj, B., Side Door: Structure Mass / System Mass, WorldAutoSteel, April 12, 2016.

Appendix A – Model Equations

Table A-1 is a summary of the power model equations for nominal designs.

To obtain the equations for efficient designs, divide the nominal design equations by the product,

$$(r \cdot n_{\text{MATERIAL}})$$

where

r =the 1 standard deviation value determined by regression
(same for both steel and aluminum)

n_{MATERIAL} =the number of standard deviations for which there were at least three observations in the data
(n will differ for each material)

Values for r , n_{ALUM} , and n_{STEEL} are found in Table A-2.

For example, from Table A-1 the mass of a nominal door structure is

$$m_{\text{STRUCT}} = 12.136(\text{AREA})^{0.969} \begin{bmatrix} 0.670 \text{ if Alum} \\ 1.000 \text{ if Steel} \end{bmatrix}$$

The mass of an efficient door structure design is

$$m_{\text{STRUCT}} = \frac{12.136(\text{AREA})^{0.969}}{r \cdot n_{\text{MATERIAL}}} \begin{bmatrix} 0.670 \text{ Alum} \\ 1.000 \text{ Steel} \end{bmatrix}$$

From Table A-2 values for r , n_{ALUM} , and n_{STEEL} may be found yielding

$$m_{\text{STRUCT STEEL}} = \frac{12.136(\text{AREA})^{0.969}}{1.109 \cdot 1.12} \begin{bmatrix} 0.670 \text{ Alum} \\ 1.000 \text{ Steel} \end{bmatrix}, \text{ and } m_{\text{STRUCT ALUM}} = \frac{12.136(\text{AREA})^{0.969}}{1.109 \cdot 1.00} \begin{bmatrix} 0.670 \text{ Alum} \\ 1.000 \text{ Steel} \end{bmatrix}$$

If the ratio of efficient steel mass to efficient aluminum mass is desired, take the ratio of these equations,

$$\frac{m_{\text{STRUCT ALUM}}}{m_{\text{STRUCT STEEL}}} = \frac{1.109 \cdot 1.12}{1.109 \cdot 1.00} \begin{bmatrix} 0.670 \\ 1.000 \end{bmatrix} = 0.75$$

The accuracy of the mass predicted by these equations is indicated by the R^2 value calculated by the regression analysis. For example, an R^2 value of 0.60 indicates that 60% variation in the mass data is accounted for by the chosen mass drivers in the equation. A comparison of the R^2 values for all subsystems and for prior studies is shown in Table A-3, and on the same page is a discussion of R^2 value.

When interpreting the results one should also understand that the A2Mac1 data base could have measurement and recording errors as the vehicle teardown process involve manual part disassembly, weighing and recording of mass and material data. Some of the data for material class was corrected in this study.

Table A-1: Equations for nominal designs

Subsystem	Mass drivers	Power model equation
Front Door	Area	$m_{STRUCT} = 12.136(AREA)^{0.969} \begin{bmatrix} 0.670 \text{ if Alum} \\ 1.000 \text{ if Steel} \end{bmatrix}$
Hood	Area	$m_{STRUCT} = 7.7074(AREA)^{1.145} \begin{bmatrix} 0.582 \text{ Alum} \\ 1.000 \text{ Steel} \end{bmatrix}$
Hatchback	Area	$m_{STRUCT} = 5.924(AREA)^{0.227} \begin{bmatrix} 0.939 \text{ Alum} \\ 1.000 \text{ Steel} \end{bmatrix}$
Decklid	Area	$m_{STRUCT} = 8.817(AREA)^{0.629} \begin{bmatrix} 0.665 \text{ Alum} \\ 1.000 \text{ Steel} \end{bmatrix}$
Liftgate	Area	$m_{STRUCT} = 10.252(AREA)^{0.823} \begin{bmatrix} 0.830 \text{ Alum} \\ 1.000 \text{ Steel} \end{bmatrix}$
Front Bumper	Curb mass Bumper length Crush can	$m_{STRUCT} = 3.6 \times 10^{-4} (CurbMass)^{0.501} (Length)^{0.838} \begin{bmatrix} 0.658 \text{ Alum} \\ 1.000 \text{ Steel} \end{bmatrix} \begin{bmatrix} 1.471 \text{ Can} \\ 1.000 \text{ No Can} \end{bmatrix}$
Rear Bumper	Curb mass Vehicle Width	$m_{STRUCT} = 0.0145 (CurbMass)^{0.833} \begin{bmatrix} 0.676 \text{ if Alum} \\ 1.000 \text{ if Steel} \end{bmatrix}$
Instrument panel beam	Vehicle Width	$m_{STRUCT} = 17.8 \times 10^{-6} (VehicleWidth)^{1.729} \begin{bmatrix} 0.581 \text{ Alum} \\ 1.000 \text{ Steel} \end{bmatrix}$
Front seat frame	None	$m_{STRUCT} = 8.345 \begin{bmatrix} 0.710 \text{ CRFP/Steel} \\ 1.000 \text{ Steel} \end{bmatrix}$
Body Structure with sub frame	GVM Plan view area	$m_{STRUCT} = 0.448 (GVW)^{0.753} (AREA)^{0.416} \begin{bmatrix} 0.652 \text{ Alum} \\ 0.917 \text{ St.Al} \\ 1.000 \text{ Steel} \end{bmatrix}$
Body Structure without sub frame	GVM Plan view area	$m_{STRUCT} = 0.429 (GVW)^{0.750} (AREA)^{0.421} \begin{bmatrix} 0.637 \text{ Alum} \\ 0.924 \text{ St.Al} \\ 1.000 \text{ Steel} \end{bmatrix}$
Lower Control Arm	Gross axle mass	$m_{SYSTEM} = 0.0398 (FGAM)^{0.747} \begin{bmatrix} 1.014 \text{ Alum} \\ 1.000 \text{ Steel} \end{bmatrix} \begin{bmatrix} 1.000 \text{ McPherson} \\ 1.464 \text{ SLA/Others} \end{bmatrix}$
Wheels	Diameter Width	$m_{SYSTEM} = 2.64 \times 10^{-5} (DIAMETER)^{1.359} (WIDTH)^{0.883} \begin{bmatrix} 0.872 \text{ if Alum} \\ 1.000 \text{ if Steel} \end{bmatrix}$
Front suspension	Gross axle mass Type	$m_{SYSTEM} = 0.0018 (FGAM)^{1.475} \begin{bmatrix} 0.924 \text{ McPherson} \\ 1.000 \text{ SLA} \end{bmatrix} \begin{bmatrix} 1.120 \text{ FWD} \\ 1.000 \text{ Other} \end{bmatrix}$
Rear suspension	Gross axle mass Type	$m_{SYSTEM} = 1.058 (RGAM)^{0.589} \begin{bmatrix} 0.759 \text{ Twist Axle} \\ 1.000 \text{ Other} \end{bmatrix}$

Table A-2: Values for r , n_{ALUM} , and n_{STEEL}

Subsystem	r	n_{ALUM}	n_{STEEL}
Front Door	1.109	1.00	1.12
Hood	1.129	1.00	1.10
Hatchback	1.185	0.95	1.00
Decklid	1.135	1.00	1.15
Liftgate	1.197	1.10	1.10
Front Bumper	1.250	1.10	1.35
Rear Bumper	1.320	1.15	1.35
Instrument panel beam	1.300	1.10	1.50
Front seat frame	1.250	-	-
Body Structure with sub frame	1.063	0.924	1.09
Body Structure without sub frame	1.061	0.912	1.09
Lower Control Arm	1.250	1.11 McP 1.06 SLA	1.23 McP 0.90 SLA
Wheels	1.098	1.11	1.19
Front suspension	1.149	-	-
Rear suspension	1.208	-	-

R Square and Adjusted R Square

R^2 is the *Coefficient of multiple determination*. *Adjusted R Squared* modifies R^2 based on the number of coefficients fit. Both these statistics show how much of the variability in the data is explained by the model.

$$R^2 = 1 - SSE/SST = (SST - SSE)/SST$$

Where

Sum of Squares Total, SST , is the variability of the raw data about the mean.

$$SST = \sum_n (y_i - \bar{y})^2, \bar{y} \text{ is the mean}$$

Sum of Squares for Error, SSE , is the variability of the raw data about the fit equation.

$$SSE = \sum_n (y_i - \hat{y}_i)^2, y_i \text{ is observed data, } \hat{y}_i \text{ is estimated by model}$$

$(SST - SSE)$ is the variability remaining after fitting the function.

By merely adding more coefficients, we can make R^2 larger. Therefore, the *Adjusted R Squared* value is the more important statistic in that it adjusts for the number of coefficients included.

$$\text{Adjusted } R^2 = 1 - \left(1 - R^2\right) \frac{n-1}{n-p}, \text{ where } n = \text{number of data points, } p = \text{number of coefficients fit.}$$

For mass benchmarking, *Adjusted R Square* $> \sim 0.50$ is desired and indicates a meaningful model. When the factors have direct physical significance, a model with an *Adjusted R Squared* > 0.30 can be directionally valid.

Adjusted R Squared is the value shown in this paper.

Table A-3: Comparison of R^2 Values

Subsystem	U Mich 2010	EDAG 2014	A2Mac1 2016
Front Door	0.45	0.56	0.56
Hood	0.77	0.80	0.84
Hatchback	0.31	0.50	0.34
Decklid	0.72	0.50	0.45
Liftgate	0.72	0.15	0.30
Front Bumper	0.49	0.48	0.69
Rear Bumper	0.31	0.44	0.41
Instrument panel beam	0.24	0.36	0.37
Front seat frame	-	0.13	0.44
Body Structure with sub frame	0.83	0.87	0.89
Body Structure without sub frame	-	-	0.89
Lower Control Arm	0.36 McP 0.80 SLA	0.49	0.47
Wheels	0.38	0.56	0.80
Front suspension	0.66	0.74	0.66
Rear suspension	0.43	0.79	0.62

Appendix B – Analysis of Body structure less sub-frame

To be consistent with prior studies, Section 2.2.5 considers the body structure as the body-in-white with front sub-frame less doors and including paint, sealer and mastic sound treatments. Here are the results of an analysis without the sub-frame.



The raw body structure mass data is shown in Figure B-1. The basic statistics for each material class appear to be stable.

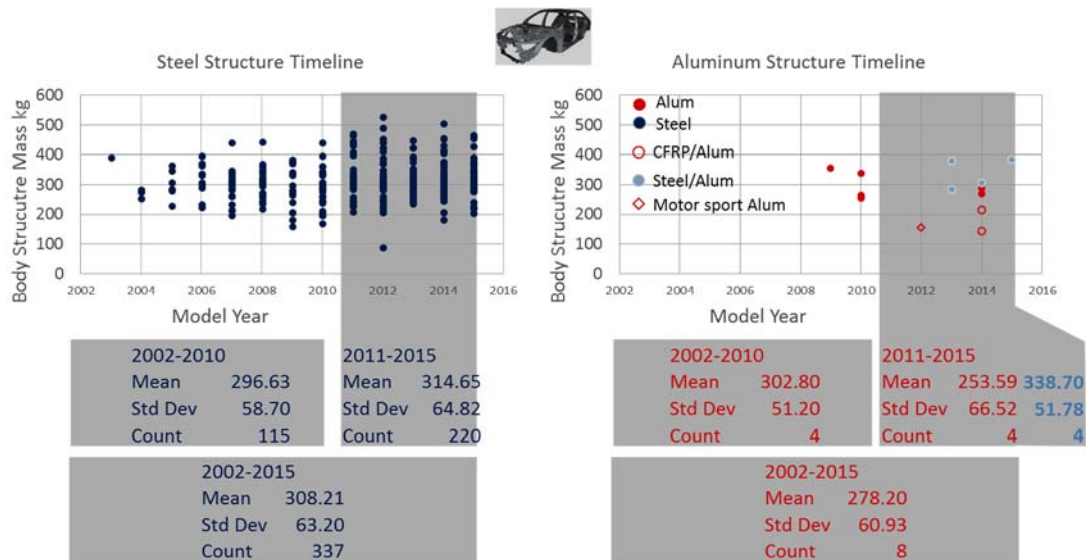


Figure B-1 Body structure without sub-frame
Comparison of unadjusted mass statistics

Figure B-2 shows scatter plots of mass vs. the mass drivers plan view **Area** and gross vehicle mass, **GVM**.

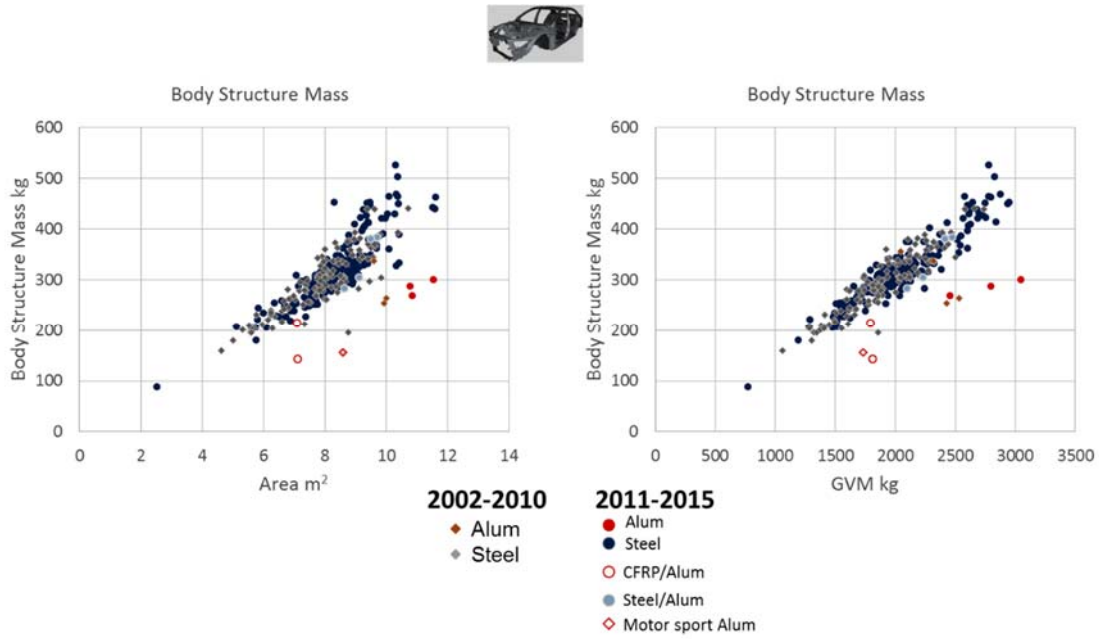


Figure B-2 Body structure without sub-frame
Mass vs mass drivers

Models were then fit using the same mass drivers were used as in the 'with sub-frame' case.

Linear model for structure

$$m_{STRUCT} = -54.19 + 0.126GVW + 14.07AREA + \begin{bmatrix} -162.46 \text{ Alum} \\ -26.37 \text{ St.Al} \\ 0 \text{ Steel} \end{bmatrix}, R^2 = 0.89, \sigma = 20.15$$

Power model for structure

$$m_{STRUCT} = 0.429(GVW)^{0.750}(AREA)^{0.421} \begin{bmatrix} 0.637 \text{ Alum} \\ 0.924 \text{ St.Al} \\ 1.000 \text{ Steel} \end{bmatrix}, R^2 = 0.91, r = 1.061$$

Figure B-3 shows the mass data with the power equation line for mass efficient designs superimposed.

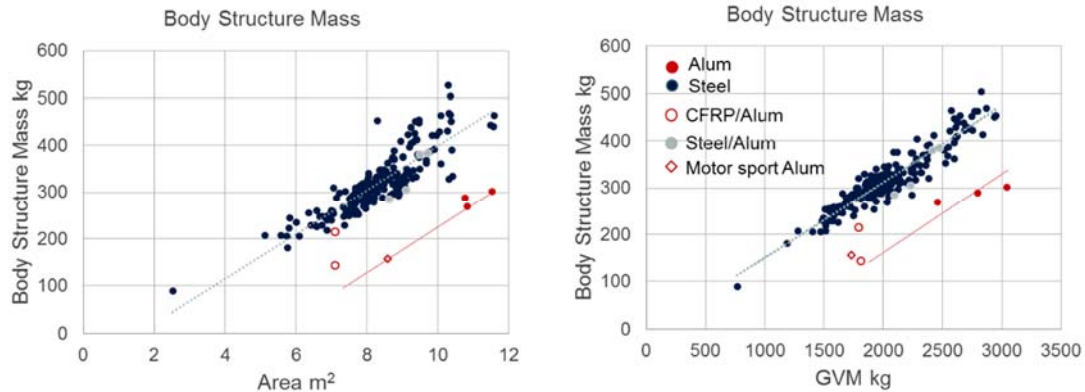


Figure B-3 Body structure without sub-frame
Structure mass with power model for mass efficient Body structures

Comparison of studies

Because the prior studies did not consider the case of without sub-frame, no comparisons of equations can be made. Table B-1 compares the material mass ratio for the **with sub-frame** and **without sub-frame** cases.

Table B-1 Body structure
Comparison of material mass ratio

$\frac{m_{ALUM}}{m_{STEEL}}$	
Nominal designs	Efficient designs
0.652	0.769
0.637	0.761



All body structures were ranked by the difference between actual mass and expected mass. This is shown graphically in the parity plot of Figure B-4 where increasing mass efficiency is the downward distance from the 45° line where actual mass equals expected mass.

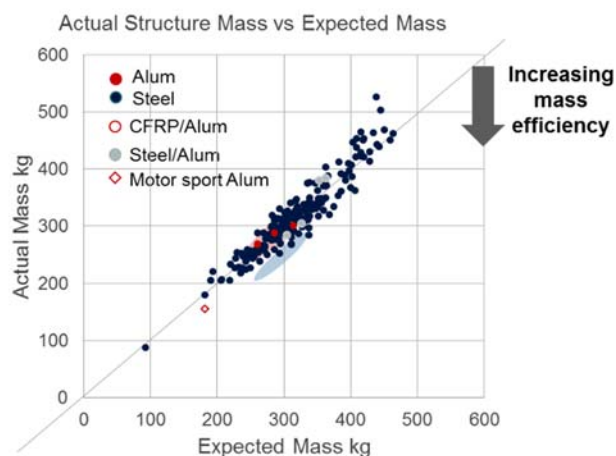


Figure B-4 Body structure without sub-frame
Parity plot to evaluate mass efficiency

Appendix C- 2014 study vehicle types [2]

As of July, 2012 the A2Mac1 European database contained 172 vehicles and the North American database contains 24 vehicles. Data for additional 110 vehicles from A2Mac1 for production years 2005 to 2012 was added to the existing 130 vehicles which were for production years 2000 to 2008. The number of vehicles per production year is shown in Figure C.1. The types of vehicles and vehicle drive configuration in the total data sample are shown in Figures C.2 and C.3, respectively.

For the new data set, the vehicle destination market was determined to be 42 to North/South America, 64 to Europe/United Kingdom, and 4 to Pacific Rim/Asia. These destination market figures do not reflect the distribution of vehicle production locations. The combined A2Mac1 database contains a broad representation of global automotive manufacturers.

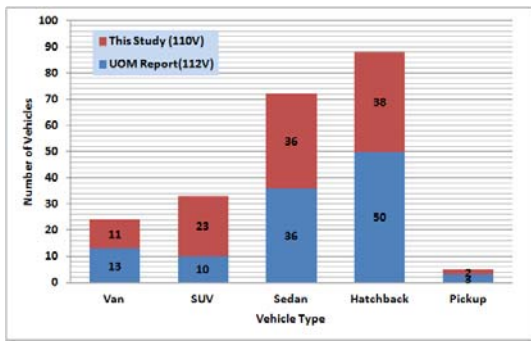


Figure C.1 Number of vehicles per production year

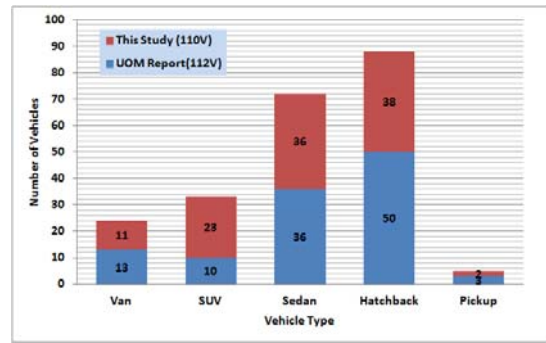


Figure C.2 Types of vehicles

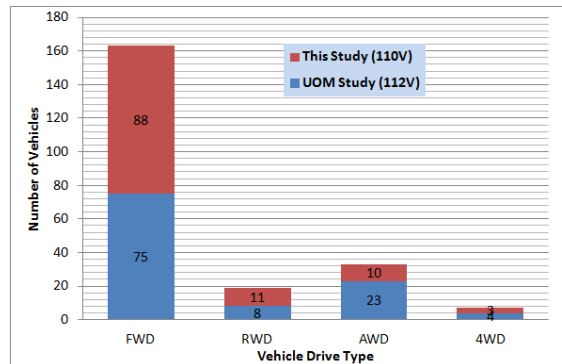


Figure C.3 Vehicle drive type

